

VŠB – Technical University of Ostrava  
Faculty of Electrical Engineering and Computer Science  
Department of Telecommunications

# **Hybrid Access Network xPON/xDSL**

## **Hybridní přístupová síť xPON/xDSL**

# Diploma Thesis Assignment

Student: **Bc. Michal Tkáčik**

Study Programme: N2647 Information and Communication Technology

Study Branch: 2601T013 Telecommunication Technology

Title: Hybrid Access Network xPON/xDSL  
Hybridní přístupová síť xPON/xDSL

The thesis language: English

## Description:

This work will be dealing with actual topic in the field of ICT internet connection providers that are solving problems with metallic and optical networks convergence. The aim of this work is to build up experimental xPON network with xDSL technology included to create hybrid xPON/xDSL access network. In this network student will be performing basic optical measurements (attenuation, dispersion, power level, attenuation budget).

Similar measurements will be performed also in the xDSL metallic part.

Following part of this work will be devoted to simulations in Optiwave or Matlab.

1. Description of access and hybrid xPON networks.
2. xDSL technology description.
3. Building up of the experimental workplace containing xPON network with xDSL technology to obtain xPON/xDSL hybrid access network.
4. Design a simulation model of the created experimental network in Optiwave or Matlab software.
5. Evaluate measured and simulated results with corresponding comments.

## References:

- [1] KAZOVSKY, Leonid G., et al.; *Broadband Optical Access Networks*. Canada: Wiley, 2011. 283 p.. ISBN 978-0-470-18235-2.
- [2] MA, Maode. *Current Research Progress of Optical Networks*. 1st Edition. [s.l.]: Springer, 2009. 282 p. ISBN 978-1402098888
- [3] LAM, Cedric. *Passive Optical Networks: Principles and practice*. Oxford: Elsevier Onc., 2007. 324 p. ISBN 978-0-12-373853-0
- [4] DHAINI, Ahmad R. *Next-Generation Passive Optical Networks*. Saarbrücken: VDM Verlag, 2008. 132 p. ISBN 978-3836435062
- [5] GORALSKI, Walter. *ADSL and DSL technologies*. New York: McGraw-Hill, c1998, xxxii, 379 p. ISBN 00-702-4679-3.

Extent and terms of a thesis are specified in directions for its elaboration that are opened to the public on the web sites of the faculty.

Supervisor: **Ing. Jan Látal**

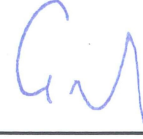
Date of issue: 01.09.2015

Date of submission: 29.04.2016



---

doc. Ing. Miroslav Vozňák, Ph.D.  
*Head of Department*



---

prof. RNDr. Václav Snášel, CSc.  
*Dean of Faculty*

I hereby declare that this master's thesis was written by myself. I have quoted all the references I have drawn upon.

Ostrava, 29th April 2016

A handwritten signature in blue ink, consisting of stylized letters and a flourish, positioned above a dotted line.

.....



I would like to thank my supervisor, Ing. Jan Látal, for methodical guidance and important advices during processing this thesis. Special thank belongs to Ing. Tomáš Hlavinka, Ing. Aleš Vanderka, Ing. Lukáš Hájek, Bc. Zdeněk Wilček, and Bc. Jan Vožický, for help with realizing the laboratory interconnection.

## **Abstract**

The aim of this master thesis is to build up experimental hybrid xPON/xDSL, specifically hybrid EPON/ADSL and EPON/VDSL network, together with deployment of the semiconductor optical amplifiers. The first chapter of the theoretical part is focused to describe access networks in consideration of the used transmission medium. The explanation of the transmission channel and transmission techniques applied in DSL technology are discussed in the second chapter. Following chapter compares the main standards of DSL technology. Data transmission and principle of operation is discussed in single chapter aimed to EPON network. Principles of amplification, basic parameters, and properties of the semiconductor optical amplifiers are explained in a separate chapter.

Thesis continues with the practical part, where are included the results of all realized measurements. Basic optical measurements (attenuation, dispersion, power level) were performed on the created topologies. The semiconductors optical amplifiers were applied to the EPON network to achieve the gain characteristics of amplifiers and to find out advantages or disadvantages of their use. Then the formed hybrid networks were verified by RFC2544 and ITU-T Y.1564 testing standards to investigate quality of services depending on the fiber and metallic line lengths. Created EPON topology with deployment of the semiconductor optical amplifiers was also designed in OptiSystem software to compare the measured and simulated results.

## **Key Words:**

Passive optical network, EPON, hybrid EPON/ADSL2+ network, hybrid EPON/VDSL2 network, semiconductor optical amplifier, gain, RFC2544, ITU-T Y.1564 EtherSAM, OLT, ONU, DSLAM, modem, optical fiber, metallic wire.

# Contents

<b>List of symbols and abbreviations</b>	<b>10</b>
<b>List of Figures</b>	<b>12</b>
<b>List of Tables</b>	<b>17</b>
<b>1 Introduction</b>	<b>18</b>
<b>2 Access Networks</b>	<b>19</b>
2.1 Metallic Line Transmission . . . . .	19
2.2 Wireless Access Technologies . . . . .	21
<b>3 xDSL Transmission Channel Characterization</b>	<b>29</b>
3.1 Transmission Channel and Impairments . . . . .	29
3.2 DSL Transmission Techniques . . . . .	34
<b>4 xDSL Standards</b>	<b>39</b>
4.1 ISDN . . . . .	39
4.2 HDSL . . . . .	39
4.3 SHDSL . . . . .	41
4.4 ADSL . . . . .	41
4.5 ADSL2 and ADSL2+ . . . . .	45
4.6 VDSL . . . . .	45
<b>5 Ethernet Passive Optical Network</b>	<b>47</b>
5.1 Fundamental Parts of PON . . . . .	47
5.2 Definition . . . . .	48
5.3 Transport Convergence Layer . . . . .	48
5.4 Ethernet Layering Architecture and EPON . . . . .	50
5.5 Multiple Point Control Protocol (MPCP) . . . . .	52
<b>6 Hybrid xPON Networks</b>	<b>56</b>
6.1 TDM-WDM PON . . . . .	56
6.2 OFDM-WDM PON . . . . .	56
6.3 OCDM-WDM PON . . . . .	57
6.4 PON/xDSL . . . . .	57

<b>7</b>	<b>Semiconductor Optical Amplifiers</b>	<b>58</b>
7.1	Principles of Amplification . . . . .	58
7.2	Semiconductor Materials . . . . .	60
7.3	Optical Gain . . . . .	61
7.4	Dielectric Waveguide . . . . .	63
7.5	Amplifier Noise . . . . .	63
7.6	Types of SOAs . . . . .	64
7.7	Applications . . . . .	65
<b>8</b>	<b>Used Devices and Components</b>	<b>67</b>
8.1	Network Components . . . . .	67
8.2	Measurement Devices . . . . .	70
8.3	Passive Components . . . . .	73
<b>9</b>	<b>Laboratory Interconnection</b>	<b>74</b>
<b>10</b>	<b>Building up Hybrid Access Network</b>	<b>77</b>
10.1	Optical Fiber Traces . . . . .	77
10.2	Optical Fiber Loss Measurement . . . . .	77
10.3	Semiconductor Optical Amplifiers Testing . . . . .	81
10.4	Metallic Wires . . . . .	87
10.5	ADSL2+ and VDSL2 Link Rates . . . . .	90
<b>11</b>	<b>EPON Testing</b>	<b>94</b>
11.1	Semiconductor Optical Amplifiers deployment . . . . .	95
11.2	Comparison of optical signals depending on topology . . . . .	99
11.3	Summary . . . . .	102
<b>12</b>	<b>Hybrid EPON/xDSL Performance Testing</b>	<b>104</b>
12.1	RFC2544 . . . . .	104
12.2	ITU-T Y.1564 EtherSAM . . . . .	105
12.3	Hybrid EPON/ADLS2+ network – RFC2544 . . . . .	107
12.4	Hybrid EPON/VDSL2 network – RFC2544 . . . . .	113
12.5	RFC2544 – Summary . . . . .	120
12.6	Hybrid EPON/ADSL2+ network – ITU-T Y.1564 EtherSAM . . . . .	120
12.7	Hybrid EPON/VDSL2 network – ITU-T Y.1564 EtherSAM . . . . .	123
12.8	ITU-T Y.1564 EtherSAM - Summary . . . . .	127
<b>13</b>	<b>Simulation of EPON network in Optiwave Software</b>	<b>128</b>
13.1	Optical Network Design . . . . .	128
13.2	Downstream Results . . . . .	130

13.3 Upstream Results . . . . .	132
13.4 Summary . . . . .	135
<b>14 Conclusion</b>	<b>136</b>
<b>References</b>	<b>138</b>
<b>Appendix</b>	<b>142</b>
<b>A Building drawings with marked traces - The second floor</b>	<b>143</b>
<b>B Building drawings with marked traces - The third floor</b>	<b>144</b>
<b>C Results of ITU-T Y.1564 EtherSAM test - EPON/ADSL2+</b>	<b>145</b>
<b>D Results of ITU-T Y.1564 EtherSAM test - EPON/VDSL2</b>	<b>147</b>

## List of symbols and abbreviations

2B1Q	– Two-binary One-quaternary
ASE	– Amplified Spontaneous Emission
C	– Capacitance
CAP	– Carrierless Amplitude and Phase Modulation
CATV	– Cable Television or Community Access Television
CB	– Conduction Band
CD	– Chromatic Dispersion
CDMA	– Code Division Multiple Access
CO	– Central Office
DMT	– Discrete Multitone
DSL	– Digital Subscriber Line
DSLAM	– DSL Access Multiplexer
ECH	– Echo Cancelled Hybrid
EPON	– Ethernet Passive Optical Network
FDD	– Frequency Division Duplex
FEXT	– Far-end Crosstalk
FDM	– Frequency-Division Multiplexing
FSO	– Free Space Optics
G	– Conductance
IEEE	– Institute of Electrical and Electronics Engineers
ISDN	– Integrated Services Digital Network
ISI	– Inter-Symbol Interference
ITU	– International Telecommunications Union
L	– Inductance
LED	– Light-Emitting Diode
LPF	– Low Pass Filter
NEXT	– Near-end Crosstalk
MAC	– Media Access Control
O-band	– Original-Band
ODN	– Optical Distribution Network
OFDM	– Orthogonal Frequency Division Multiplexing
OLT	– Optical Line Termination
ONU	– Optical Network Unit
OTDR	– Optical Time Domain Reflectometer
POTS	– Plain Old Telephone Service
PLC	– Power Line Communications

PMD	– Polarization Mode Dispersion
QAM	– Quadrature amplitude modulation
QoS	– Quality of Services
R	– Resistance
RF	– Radio Frequency
RTT	– Round Trip Time
S-band	– Short-Band
SOA	– Semiconductor Optical Amplifier
SNR	– Signal-to-Noise Ration
TCM	– Time Compression Multiplexing
TDD	– Time Division Duplexing
TDM	– Time Division Multiplexing
TDMA	– Time Division Multiple Access
UMTS	– Universal Mobile Telecommunication System
VB	– Valence Band
WCDMA	– Wideband Code Division Multiple Access
WDM	– Wavelength-Division Multiplexing
Wi-Fi	– Wireless-Fidelity

## List of Figures

1	Connection to a data network with xDSL (b) in comparison with ISDN (a)[1]. . .	20
2	Electrical power transmission and distribution [3] . . . . .	21
3	Wi-Fi channel overlapping . . . . .	23
4	Cellular network architecture. MSC, mobile switching center; BSC, base station controller; HLR, home location register [3] . . . . .	25
5	Simple setup with using lens for free-space optical communications . . . . .	27
6	Relationship between the bit rate and network coverage for fiber optics and free space optics [9] . . . . .	28
7	Attenuation for frequencies up to 18 MHz for twisted pair wires 100, 500, and 2000 m long with core diameter 0.4 mm [5] . . . . .	30
8	Intersymbol interference (ISI) [5] . . . . .	31
9	Near-end crosstalk path [5] [1] . . . . .	32
10	Far-end crosstalk path [5] [1] . . . . .	33
11	RS codeword structure[5] . . . . .	37
12	DSL system reference model [5] . . . . .	38
13	(A) Single-duplex HDSL; (B) Dual-simplex HDSL; (C) Dual-duplex HDSL [11] .	40
14	ADSL reference model [11] . . . . .	42
15	Limitation to lower frequencies by two-way transmission [11] . . . . .	42
16	FDM ADSL [11] . . . . .	43
17	ECH ADSL [11] . . . . .	43
18	Downstream sub-channels generated by an ADSL transmitter [14] . . . . .	44
19	Sub-channels generated by an upstream transmitter for (a) ADSL1 over POTS and (b) ADSL1 over ISDN [14] . . . . .	45
20	Passive Optical Network . . . . .	47
21	EPON TDM . . . . .	49
22	EPON TDMA . . . . .	49
23	Ethernet frame structure [19] . . . . .	49
24	P2P Ethernet and P2MP EPON layering architecture [20] . . . . .	51
25	EPON ranging process [3] . . . . .	52
26	EPON Gate operation [20] . . . . .	53
27	EPON Report operation [20] . . . . .	53
28	Generic format of MPCPDU [20] . . . . .	54
29	Autodiscovery process [20] . . . . .	55
30	Schematic drawing of semiconductor optical amplifier [29] . . . . .	58
31	Two-level system of semiconductor material [29] . . . . .	59
32	Simplified energy vs. wave-vector band structure diagram of a direct-band-gap semiconductor [29] . . . . .	61



33	Semiconductor material systems [31]	61
34	Dielectric waveguide of semiconductor [31]	63
35	TW-SOA and FP-SOA [35]	64
36	Four Wave Mixing	65
37	Schematic configuration for single-pump FWM [37]	66
38	Schematic configuration for single-pump FWM [38]	66
39	Listing of command <show onu>	68
40	Adding the profile	69
41	Assignment of profile to port	69
42	WDM splitter wavelength division	73
43	Topology for method C measurement	75
44	Topology for OTDR measurement	75
45	Reflectogram of measured optical trace EB316 → EB211; $\lambda = 1310$ nm	75
46	Graphic representation of measured insertion loss	76
47	Reflectogram of measured optical trace = 15.03 km	78
48	Topology to measure insertion loss of optical splitters	79
49	Topology for PMD measurement	79
50	Interferogram from PMD analyzer	80
51	Topology for CD measurement	81
52	Result from CD analyzer - dispersion depending on wavelength	81
53	Topology to obtain gain spectrum of the O-band SOA	82
54	O band amplifier's gain spectrum	83
55	Gap between the SOA and adapter	84
56	Gap filling	84
57	Topology to obtain S band SOA's gain in dependence on input power	84
58	Downstream optical spectrum before passes the SOA	85
59	Downstream optical spectrum after passes the SOA	85
60	Optical spectrum before and after passes SOA - A = 0 dB	86
61	Optical spectrum before and after passes SOA - A = 11 dB	86
62	Optical spectrum before and after passes SOA - A = 20 dB	87
63	S band SOA's gain saturation	87
64	Open termination (A) and the short termination (B).	88
65	Characteristic impedance and attenuation coefficient for SYKY metallic wire	90
66	Transmitted bits - wire length 0 km (left) and 2 km (right)	91
67	Link rate depending on wire length - ADSL2+	91
68	Main Menu - VDSL2 modem	92
69	System Maintenance - VDSL2 modem	92
70	List of command <vdsl status> - VDSL2 modem	93
71	Link rate depending on wire length - VDSL2	93

72	Reference (original) topology to SOA testing . . . . .	94
73	Upstream optical spectrum - optical trace 5 and 25 km - reference topology . . .	95
74	Downstream optical spectrum - optical trace 5 and 25 km - reference topology .	95
75	Topology A - SOA deployment . . . . .	96
76	Upstream optical spectrum - optical trace 5 and 25 km - Topology A . . . . .	97
77	Downstream optical spectrum - optical trace 5 and 25 km - Topology A . . . . .	97
78	Topology B - SOA deployment . . . . .	98
79	Upstream optical spectrum - optical trace 5 and 25 km - Topology B . . . . .	98
80	Downstream optical spectrum - optical trace 5 and 25 km - Topology B . . . . .	99
81	Comparison of upstream signals depending on topology - 5 km . . . . .	99
82	Comparison of upstream signals depending on topology - 25 km . . . . .	100
83	Upstream optical signal - 20 km - Topology B . . . . .	101
84	Comparison of downstream signals depending on topology - 5 km . . . . .	101
85	Comparison of downstream signals depending on topology - 25 km . . . . .	102
86	Base topology of hybrid xPON/xDSL network . . . . .	104
87	Traffic Classes [42] . . . . .	106
88	Topology for test hybrid EPON/ADSL2+ network (RFC2544) . . . . .	108
89	Topology for test hybrid EPON/ADSL2+ network (RFC2544) - SOA deployment	108
90	RFC2544 - EPON/ADSL2+ - Throughput - Upstream . . . . .	109
91	RFC2544 - EPON/ADSL2+ - Throughput - Downstream . . . . .	110
92	RFC2544 - EPON/ADSL2+ - Back-to-Back - Upstream . . . . .	110
93	RFC2544 - EPON/ADSL2+ - Back-to-Back - Downstream . . . . .	111
94	RFC2544 - EPON/ADSL2+ - Frame Loss - Upstream . . . . .	111
95	RFC2544 - EPON/ADSL2+ - Frame Loss - Downstream . . . . .	112
96	RFC2544 - EPON/ADSL2+ - Latency . . . . .	112
97	Topology for test hybrid EPON/VDSL2 network (RFC2544) . . . . .	113
98	Topology for test hybrid EPON/VDSL2 network (RFC2544) - SOA deployment .	113
99	RFC2544 - EPON/VDSL2 - Throughput - Upstream - profile A . . . . .	114
100	RFC2544 - EPON/VDSL2 - Throughput - Upstream - profile B . . . . .	114
101	RFC2544 - EPON/VDSL2 - Throughput - Downstream - profile A . . . . .	115
102	RFC2544 - EPON/VDSL2 - Throughput - Downstream - profile A . . . . .	115
103	RFC2544 - EPON/VDSL2 - Back-to-Back - Upstream - profile A . . . . .	116
104	RFC2544 - EPON/VDSL2 - Back-to-Back - Upstream - profile B . . . . .	116
105	RFC2544 - EPON/VDSL2 - Back-to-Back - Downstream - profile A . . . . .	116
106	RFC2544 - EPON/VDSL2 - Back-to-Back - Downstream - profile B . . . . .	117
107	RFC2544 - EPON/VDSL2 - Frame Loss - Upstream - profile A . . . . .	117
108	RFC2544 - EPON/VDSL2 - Frame Loss - Upstream - profile B . . . . .	118
109	RFC2544 - EPON/VDSL2 - Frame Loss - Downstream - profile A . . . . .	118
110	RFC2544 - EPON/VDSL2 - Frame Loss - Downstream - profile B . . . . .	118

111	RFC2544 - EPON/VDSL2 - Latency - profile A . . . . .	119
112	RFC2544 - EPON/VDSL2 - Latency - profile B . . . . .	119
113	Topology to test hybrid EPON/ADSL2+ network (EtherSAM) . . . . .	121
114	Topology to test hybrid EPON/ADSL2+ network (EtherSAM) - SOA deployment	121
115	EtherSAM - EPON/ADSL2+ - Average Throughput . . . . .	122
116	EtherSAM - EPON/ADSL2+ - Maximum Jitter . . . . .	122
117	EtherSAM - EPON/ADSL2+ - Frame Loss . . . . .	123
118	EtherSAM - EPON/ADSL2+ - Round-trip Latency . . . . .	123
119	Topology to test hybrid EPON/VDSL2 network (EtherSAM) . . . . .	124
120	Topology to test hybrid EPON/VDSL2 network (EtherSAM) - SOA deployment	124
121	EtherSAM - EPON/VDSL2 - Average Throughput - profile A . . . . .	125
122	EtherSAM - EPON/VDSL2 - Maximum Jitter - profile A . . . . .	126
123	EtherSAM - EPON/VDSL2 - Frame Loss - profile A . . . . .	126
124	EtherSAM - EPON/VDSL2 - Round-trip Latency - profile A . . . . .	127
125	OLT in OptiSystem . . . . .	128
126	ONU in OptiSystem . . . . .	129
127	ODN in OptiSystem . . . . .	129
128	Downstream - BER depending on fiber length . . . . .	130
129	Opt.Spectrum (DS) - MZM output . . . . .	131
130	Opt.Spectrum (DS) - SOA input . . . . .	131
131	Opt.Spectrum (DS) - SOA output . . . . .	131
132	Opt.Spectrum (DS) - PIN input . . . . .	131
133	Eye diagram (DS) - 0 km . . . . .	132
134	Eye diagram (DS) - 40 km . . . . .	132
135	Eye diagram (DS) - 41 km . . . . .	132
136	Eye diagram (DS) - 56 km . . . . .	132
137	Upstream - BER depending on fiber length . . . . .	133
138	Opt.Spectrum (US) - MZM output . . . . .	133
139	Opt.Spectrum (US) - SOA input . . . . .	133
140	Opt.Spectrum (US) - SOA output . . . . .	134
141	Opt.Spectrum (US) - PIN input . . . . .	134
142	Eye diagram (US) - 0 km . . . . .	134
143	Eye diagram (US) - 30 km . . . . .	134
144	Eye diagram (US) - 31 km . . . . .	135
145	Eye diagram (US) - 43 km . . . . .	135
146	Eye diagram (US) - 52 km . . . . .	135
147	Second floor drawing . . . . .	143
148	Third floor drawing . . . . .	144
149	Legend for EPON/ADSL2+ . . . . .	145

150	EtherSAM - EPON/ADSL2+ - Average Throughput - Full results . . . . .	145
151	EtherSAM - EPON/ADSL2+ - Maximum Jitter - Full results . . . . .	145
152	EtherSAM - EPON/ADSL2+ - Frame Loss - Full results . . . . .	146
153	EtherSAM - EPON/ADSL2+ - Round-trip Latency - Full results . . . . .	146
154	Legend for EPON/VDSL2 . . . . .	147
155	EtherSAM - EPON/VDSL2 - Average Throughput - Full results - profile A . . .	147
156	EtherSAM - EPON/VDSL2 - Average Throughput - Full results - profile B . . .	147
157	EtherSAM - EPON/VDSL2 - Maximum Jitter - Full results - profile A . . . . .	148
158	EtherSAM - EPON/VDSL2 - Maximum Jitter - Full results - profile B . . . . .	148
159	EtherSAM - EPON/VDSL2 - Frame Loss - Full results - profile A . . . . .	148
160	EtherSAM - EPON/VDSL2 - Frame Loss - Full results - profile B . . . . .	149
161	EtherSAM - EPON/VDSL2 - Round-trip Latency - Full results - profile A . . . .	149
162	EtherSAM - EPON/VDSL2 - Round-trip Latency - Full results - profile B . . . .	149

## List of Tables

2	Wi-Fi standards [4] . . . . .	22
3	WiMAX standards [3] . . . . .	24
4	2B1Q . . . . .	35
5	SHDSL frequencies and bit rates [5] . . . . .	41
6	VDSL2 profiles [5] . . . . .	46
7	EPON PMD options [3] . . . . .	51
8	Properties of the SFP module . . . . .	67
9	Properties of ONU unit . . . . .	68
10	Insertion loss of WDM splitter . . . . .	73
11	Measured insertion loss on fiber 1 EB316 -> EB211 . . . . .	76
12	Measured insertion loss of optical traces . . . . .	77
13	Measured insertion loss between the branches . . . . .	78
14	Measured PMD coefficients and Differential Group Delay . . . . .	80
15	Properties of used semiconductor optical amplifiers . . . . .	82
16	Measured values of gain depending on wavelength . . . . .	83
17	Measured values of gain depending on input power . . . . .	84
18	Measured resistance and capacitance . . . . .	88
19	Measured ADSL2+ Link rates . . . . .	91
20	Measured VDSL2 Link rates . . . . .	93
21	Measured values of power - reference topology . . . . .	94
22	Measured values of power - calculated gain - topology A . . . . .	96
23	Measured values of power - calculated gain - topology B . . . . .	98
24	Comparison of peak gain and noise gain - upstream - 5 km . . . . .	100
25	Comparison of peak gain and noise gain - upstream - 25 km . . . . .	100
26	Comparison of peak gain and noise gain - downstream - 5 km . . . . .	102
27	Comparison of peak gain and noise gain - downstream - 25 km . . . . .	102
28	Resulting attenuation . . . . .	103
29	QoS requirements [43] . . . . .	107
30	Set profile to test EtherSAM ITU-T Y.1564 - EPON/ADSL2+ . . . . .	120
31	Set profile to test EtherSAM ITU-T Y.1564 - EPON/VDSL2 . . . . .	124

# 1 Introduction

In present days, one of the main issue that is solving by providers is a network convergence between fiber optics network and metallic network. They are trying to find out the way to reduce access networks costs and hybrid PON/DSL is one of the possible solutions, where passive components and shared fiber used in passive optical networks are inexpensive possibilities. In these hybrid fiber/copper access networks is fiber deployed near to DSLAMs, where the optical signal is converted to electrical signal by the ONU unit, then is processed by the DSLAM and transmitted to subscribers over existing telephone lines. Also, there are devices so called drop-point devices, which implements the ONU unit and DSLAM to one single device to even more cost reduces.

Another issue occurs with optical network coverage. The distance, which is able to overcome by optical systems is mainly limited by attenuation caused by fibers and components used within the network such as splitters, couplers, circulators, etc. To reduce these losses were used regenerators, where optical signal was converted to electrical, repaired and subsequently again converted to an optical signal by using the lasers. These devices were quite expensive and difficult, therefore, the full optical amplifiers began to develop and use. The main advantage of using optical amplifiers against using regenerators is that the optical amplifiers are not sensitive to bit-rate changes, therefore, the optical systems can be easily updated without the need to replace the components used in network.

This thesis deals with the both issues. Chapter 2 is focused to show the fundamental access networks. Chapters 3 and 4 are aimed to discuss xDSL networks with description of transmission parameters associated with DSL networks and also xDSL standards. Chapter 5 describes the passive optical network EPON, which is used to build up hybrid access network. In following chapter are mentioned the hybrid networks, which are the most discussed in present days. Chapter 7 is focused to describe principles of amplification in an optical amplifiers, specifically semiconductor optical amplifiers. In practical part of this thesis are illustrated results from testing semiconductor optical amplifiers within the EPON network. To test hybrid networks were performed tests according to standards RFC2544 and ITU-T Y.1564 and results are also included in practical part together with corresponding comments. The last section of practical part is aimed to design network in simulation software OptiSystem according to measured results.

## 2 Access Networks

Access networks bridges a customer's equipment like computers and other communication devices to service providers through different types of physical medium. The most common used mediums are twist pairs (phone line), coaxial cables, optical fibers and air. Each of these access technologies has its strengths and weaknesses. Nowadays, we can have fast connection, low cost and everywhere, but we can't have it all at the same time. In next few sections I describe most often used access technologies, where each of mentioned technologies have advantages in terms of geography, applications and political domain.

Access network has to conform these system functions:

- Transport signal between a large number of user end devices and network nodes of service providers.
- Multiplex signals to effective using transmission medium and resources and to flexible adjust traffic capacity by requirements of customers and services.
- Sorting traffic load enabling to route associated signals in access network to relevant interfaces of service providers.
- Adaptation of user interface to access network behaviour.
- Adaptation of provider's network interface to access network behaviour [1].

### 2.1 Metallic Line Transmission

#### 2.1.1 Digital subscriber line (xDSL)

Digital subscriber line (also called digital subscriber loop) is family of access technologies which operates over copper line (phone line) at frequencies beyond the voiceband, sending digital data directly from the subscriber, and thus avoiding the need for an analog to digital conversion, to provide broadband access services. The first broadband DSL standard was the integrated services digital network system (ISDN), which was developed in the 1980s by CCITT (predecessor of ITU-T). The ISDN includes two 64 kbps (2B) channels for data and voice and one 16 kbps (1D) digital channel. The result was 144 kbps data rate in both directions. The main difference between ISDN and xDSL connections is that xDSL has a character of permanently data circuit, which is on alert for all the time, when end device is active, in contrast ISDN has a character of temporary data circuit, where communication starts with dialling service provider number (dial-up). Figure 1 shows different connections to Internet Service Provider, when ISDN has to use circuit switched network. More about DSL technology will be described in Chapter 2 and 3.

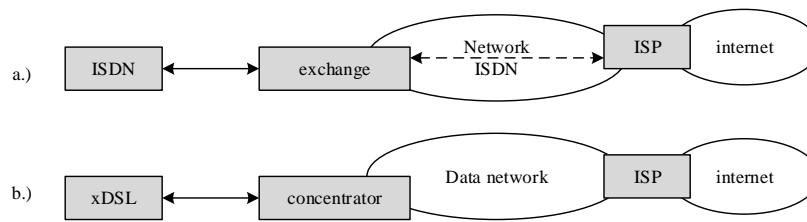


Figure 1: Connection to a data network with xDSL (b) in comparison with ISDN (a)[1].

### 2.1.2 CATV

CATV networks were one-way broadcast systems. They use metallic physical line which consist asymmetric pairs - coaxial cable. Programs of CATV are transmitted as analog signals with using amplitude modulation-vestigial side band (AM-VSB) format. Each of CATV channels takes 6 MHz using frequency division multiplexed (FDM) frequency slot in the North American National Television System Committee standard (NTSC). In other parts of world is used 8 MHz slot in the phase alternative line standard (PAL). For TV signals is used 50 MHz to 500 MHz or 750 MHz frequency band.

In the mid-1990s, North America service providers decided to upgrade their traditional one-way analog broadcast systems by putting in bidirectional RF amplifiers, so they can provide broadcast data services through cable modems.

Nowadays, are coaxial networks used for Digital Video Broadcasting over cable (DVB-C). Cable modem can be integrated to “Set Top Box”, which allow to receive digital signals on current television receiver. There is used FDM to split downstream and upstream channels. For downstream is used frequency band 65 MHz to 850 MHz (8 MHz for channel) in Europe, 42 MHz to 850 MHz (6 MHz for channel) in America. Then for upstream is used frequency band 5 MHz to 65 MHz in Europe and 5 MHz to 42 MHz in America [2].

### 2.1.3 PLC

It is possible to use distribution physical lines of high voltage, which are serving for energy distribution to almost every object. The advantage of using electric powerlines as the data transmission medium is that every building and home are already equipped with the powerline and connected to the power grid. These transmission systems are called Power Line Communications. The three phase power generated at a power plant enters a transmission substation, where the three-phase power is converted to extremely high voltage (155 to 765 kV) for long-distance transmission over the grid. Powerline substations convert high voltage down to distribution voltages (less than 10 kV), and this medium voltage electricity is sent through a bus that can divide the power to different directions. Along the distribution bus, there are regulator banks



that regulate voltage on the line to avoid overvoltage and undervoltage, and taps that send electricity down the street. At each building or house is a transformer drum attached to the electricity pole, reducing the medium voltage (typically 7.2 kV) to household voltage (110 or 240 V). Figure 2 shows, how are used medium-voltage power line to transmit data to and from each house. Typically, repeaters are installed along the power lines for long distance data transmission, and some bypass devices allow RF signals to bypass transformers. Transmission to the house by powerlines is not the only way how to transport data. There can be use some alternative techniques such a Wi-Fi or the other wireless technology for last-mile connection [3].

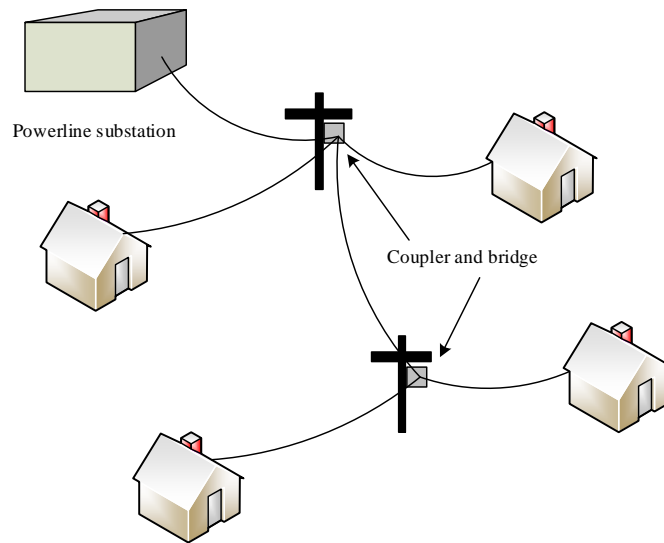


Figure 2: Electrical power transmission and distribution [3]

### 2.1.3.1 Broadband Powerline Modem

A BPL modem is sending and receiving data through a powerline, and is plugged into a power socket on the wall. They use Ethernet cables to connect computers or other networks. In some cases, a wireless router can be integrated into the BPL modem. BPL modems transmit at medium to high frequencies from few MHz to tens of MHz. BPL modem data rates can be from hundred kbps to a few of Mbps. There are used various modulation schemes for Power Line Communications, including the older ASK (Amplitude Shift Keying), FSK (Frequency Shift Keying) modulation and newer DMT (Discrete Multitone), DSSS (direct sequence spread spectrum) and OFDM (Orthogonal Frequency Division Multiplexing) technologies [3].

## 2.2 Wireless Access Technologies

The three types of technologies that are most popular for providing broadband access today are the IEEE 802.11, also known as “Wi-Fi”, the third and fourth generations of cellular technology and WiMAX. These technologies uses radio frequency. Another type of wireless broadband

technology is optical free-space link. A little of these access networks will be discussed in following sections.

### 2.2.1 Wi-Fi

The standard IEEE 802.11 was developed in the 1990s. The standard use unlicensed spectrum with restrictions on the transmit power, therefore, is mostly used as wireless local area network. Because of its flexibility and low cost deployment, has become popular option that is used in households and in the industrial world. The technology is designed to use a simple architecture that is easy to configure and install. Current Wi-Fi networks are based on point-to-multipoint topology, which consist of access-point providing broadband connectivity to several end users with laptops, mobile phones, PDA-s and so on. The wireless links among access points establish wireless links among themselves to enable automatic topology discovery and dynamic routing configuration. In Table 2 is comparison of few most popular standards [4].

Table 2: Wi-Fi standards [4]

802.11 protocol	Frequency [GHz]	Bandwidth [MHz]	Min-Max data rate [Mbps]	Modulation Technique	Approx. Range	
					Indoor [m]	Outdoor [m]
802.11	2.4	22	1 - 2	DSSS, FHSS	20	100
a	5	20	6 - 54	OFDM	35	120
	3.7				-	5k
b	2.4	22	1 - 11	DSSS	35	140
g	2.4	20	6 - 54	OFDM, DSSS	38	140
n	2.4/5	20	7.2 - 72.2	OFDM	70	250
		40	15 - 150		70	250
ac	5	20	7.2 - 96.3	OFDM	35	
		40	15 - 200		35	
		80	32.5 433.3		35	
		160	65 - 866.7		35	

The IEEE has released multiple set of standards for various operating frequency, and ranges specification. The first release was IEEE 802.11 original standard that was defined 1997 and clarified 1999. Some of these old standards are now obsolete, and some are still active. One would be interest in investigation in details the available standards to determine a suitable standard for the intended application of the WLAN network.

The original standard supports data rates of 1 to 2 Mbps using FHSS (frequency hopping direct sequence) with GFSK modulation or DSSS (direct sequence spread centrum) with DBPSK (differential binary-phase shift keying) or DQPSK (differential quadrature-phase shift keying) modulation. The 802.11b support 5.5 and 11 Mbps data rates in addition to the original 1 - 2 Mbps rates. The 802.11b uses eight-chip DSSS with a CCK (complementary code keying) modulation scheme at the 2.4 GHz band. The unlicensed spectrum is divided into 14 channels, the first operational channel has central frequency at 2.412 GHz, each channel central frequency has 5 MHz gap, the fourteenth channel is supported only in Japan. This channel overlapping is

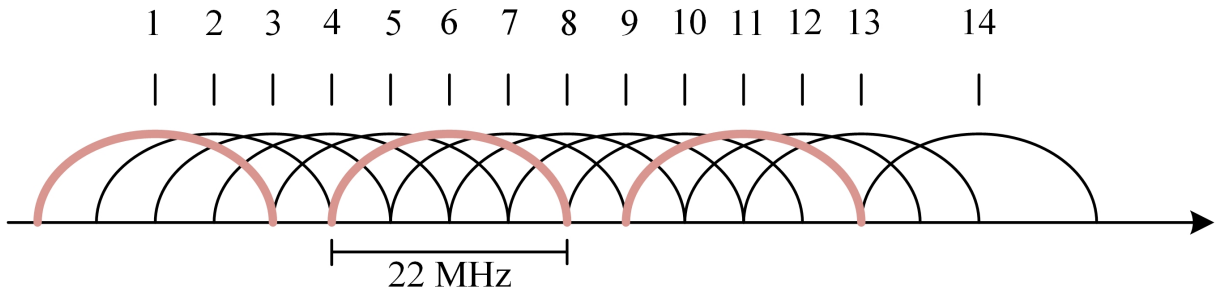


Figure 3: Wi-Fi channel overlapping

shown in Figure 3. The IEEE 802.11a was developed in 1999 and operates at bit rates up to 54 Mbps using OFDM with BPSK, QPSK, 16-QAM or 64-QAM at the 5 GHz band.

Newer standard 802.11g was developed in 2003. Standard supports ranging is from 6 Mbps to 54 Mbps at a bandwidth of 20 MHz. The actual OFDM signal consists of 52 sub-carriers, where 4 sub-carriers are pilot sub-carriers and 48 are data sub-carriers. The 802.11n supports data rates up to 150 Mbps and operates in 2.4 GHz and 5 GHz bands. In addition, the bandwidth supported was doubled to 40 MHz. 802.11 ac is faster and more scalable version of 802.11n. Bandwidth is increased form a maximum of 40 MHz with 802.11n up to 80 or even 160 MHz. Denser modulation, now using 256-QAM , up from 64-QAM in 802.11n [4].

### 2.2.2 WiMAX

WiMAX access networks, based on IEEE 802.16 standards, can provide wireless broadband Internet access at a relatively low cost. A single base station in WiMAX networks can support data rates up to 75 Mbps to residential or business users. However, since multiple users are served by a single base station, data payload delivered to end users is likely to 1 Mbps for residential subscribers and a few Mbps for business clients. Compared to the transmission distance of a few hundred meters supported by Wi-Fi (802.11a/b/g/n), WiMAX promises wireless access range up to 50 km. Therefore, WiMAX can provide citywide coverage and QoS capabilities, supporting multimedia applications from non-real-time data to real-time voice and video. Furthermore, as an IP-based wireless technology, WiMAX can be integrated seamlessly with other types of wireless or wire-line networks.

The salient features of a number of 802.16 standards ratified by IEEE are shown in Table 3. The original IEEE 802.16 standard defines back-haul point-to-point connections with bit rates up to 134 Mbps using frequencies in the range 10 to 66 GHz, and IEEE 802.16d/e specifies point-to-multipoint wireless access at bit rates up to 75 Mbps. The newest standard, IEEE 802.16m, supports data rates up to 1 Gbps but with a much shorter transmission range.

In WiMAX networks, WiMAX base stations are connected to the wire-line networks (usually, optical metro networks) using optical fiber, cable, and microwave high-speed point-to-point links. Theoretically, a base station can cover up to a 50-km radius, but in practice it is usually limited

Table 3: WiMAX standards [3]

Parameter	802.16	802.16a	802.16e	802.16m
Operating frequency [GHz]	10 - 66	2 - 11	2 - 6	<6
Maximum data rate [Mbps]	134	75	63	1000
Typical cell size [km]	2 - 5	7 - 10	2 - 5	5 - 30

to 10 km. The base station serves a number of subscriber stations (deployed at the locations of residential or business users) using point-to-multipoint links. A WiMAX network can be configured with a star topology or a mesh topology; each has advantages and disadvantages. Whereas star topology can support higher data rates, mesh topology provides a longer reach and faster deployment. The WiMAX MAC layer allocates the uplink and downlink bandwidth to subscribers according to their bandwidth needs. Unlike Wi-Fi networks, WiMAX networks adopt scheduled access using a time-division multiplexing technique, but the time slot assigned to each subscriber can vary in length depending on the bandwidth allocated to the subscriber. Because of the scheduling algorithm, WiMAX networks are more bandwidth efficient than are Wi-Fi networks [3].

### 2.2.3 Cellular Networks

The primary function of cellular network is to carry voice communications for mobile users. Cellular networks are spread all around a world, evolving from first generation (1G) to 2G and 3G and moving toward the fourth generation (4G) systems. Nowadays, with increasing demand for multimedia services such a video or data, is necessary to raise a capacity by migrating from voice to data-centric networks. First generation of cellular networks were analog systems, which supported only voice services. Further that, the quality of the services compared to the fixed telecommunication network, was low. The solution came with second generation. Feature of the 2G networks is using of digital system. Transmission power was decreased and size of cells too. They had a better resistance against errors and the security was also better than in first generation systems. The 2G system continued in voice orientation, but with new systems were introduced new services such a text messaging, which becomes a very popular applications. Digital encoding techniques were based on TDMA (Time Division Multiple Access) and CDMA (Code Division Multiple Access). The most common standard, used worldwide, is GSM, which is based on TDMA. In addition, GPRS (General Packet Radio Switching) adds packet switching in GSM to allow data transmission with data rates up to 172.1 kbps. The EDGE (Enhanced data rates for GSM evolution) improved high-speed data transmission up to 473.6 kbps. The Figure 4 shows the architecture of typical cellular network [3].

### 2.2.4 UMTS

UMTS (Universal Mobile Telecommunication System) system is leader of the third generation

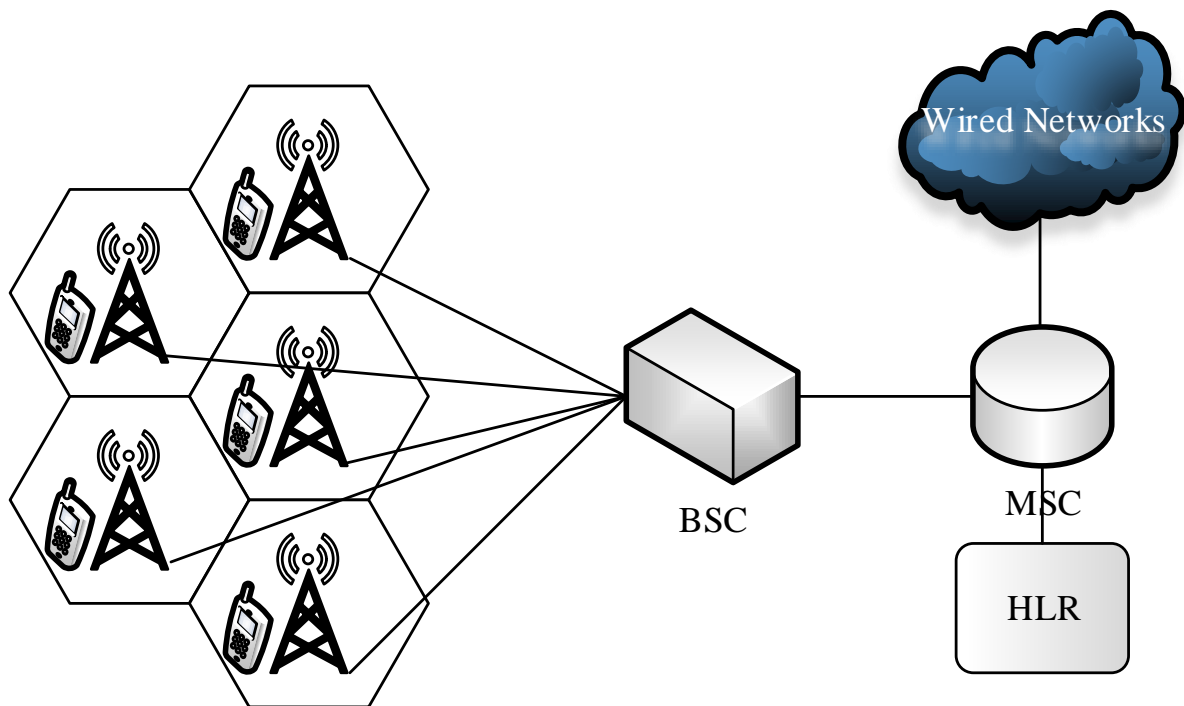


Figure 4: Cellular network architecture. MSC, mobile switching center; BSC, base station controller; HLR, home location register [3]

networks. It is the first cellular technology that could truly provide broadband speeds of several megabits per second (Mbps). System is based on the WCDMA (Wideband-CDMA) air interface and a core network that has evolved from the GSM-based core network for circuit-switched and packet-switched services.

3G systems architecture is more complex than architecture of Wi-Fi. 3G systems have to provide quality voice services, with seamless mobility, over a much greater area. The architecture contains two different part to support the two modes of operation: circuit switched mode for voice and packet switched mode for data. The system is divided into three-subsystems:

- UE (User Equipment) - The mobile device.
- UTRAN (UMTS Terrestrial Radio Access) - Fixed part of infrastructure, which handle access over the air.
- CN (Core Network) - Supports the access network consisting of the UE and UTRAN.

UE consist of hardware, software and SIM (Subscriber Identity Module). SIM is used for authentication and authorization. In hardware and software are included all communication protocols. UTRAN consist of Node B and RNC (Radio Network Controller). Node B comprise of the antennas, the radio unit and the baseband unit. The RNC control several Node Bs (typically hundreds of them). The RNC is responsible for the mobility management and admission control

functions. The CN comprise all the switching and routing functions required for global network connectivity [5].

The UMTS is based on WCDMA (Wideband Code Division Multiple Access) for paired channels using frequency division duplexing (FDD) or TD-CDMA (Time Division - Code Division Multiple Access) for unpaired channels using time division duplexing (TDD). FDD uses two frequency channels, where one is used for downlink, another one for uplink transmission. Therefore, one channel uses 10 MHz band. On the other hand, TDD uses one frequency channel for both uplink and downlink transmission. According that, sufficient band for channel is 5 MHz [6]. For terrestrial access to UMTS is specified 155 MHz wide band, with frequency ranges from 1900 MHz to 1980 MHz, next one is from 2010 MHz to 2025 MHz and from 2110 MHz to 2170 MHz. Satellite access is possible in ranges from 1980 MHz and 2010 MHz and from 2170 MHz to 2200 MHz.

The first specification of UMTS (Release 99) supported 2 Mbps downlink data rate, a peak rate of uplink is 384 kbps. Following release after Release 99 was Release 4, but did not bring any major changes. Major release Release 5 introduced High-Speed Downlink Packet Access (HSDPA). HSDPA brings high download speeds, where peak data rate was 14 Mbps and typical speeds were from 2 Mbps to 3 Mbps. These speeds were achieved by defining new transport and physical channels, adding more functionality to Node Bs and moving some of the control from RNC over to the Node B. Release 6 followed HSDPA development and deployment and brought High-Speed Uplink Packet Access (HSUPA). Release 7 starts to support real-time services such as VoIP and interactive games. Release 8 of UMTS/HSPA also coincides with the first release of LTE (Long Term Evolution).

### **2.2.5 Free Space Optics (FSO)**

Optical data transmission on the world is the most often realized by optical fiber, because this option allow the transmission over a long distances without extremely power loss and is not affected with atmosphere influences. It is also possible to transport data over air (free space). Free space optics, also called free space photonics (FSP), is transmission of modulated visible or infrared (IR) beams through atmosphere to obtain broadband communications. Most frequently are used lasers as source, however, light-emitting diode (LED) or infra-red-emitting diodes (IRED) are applied too [7].

The theory of FSO is almost the same as that for fiber optic transmission. The main difference is that the laser beam is collimated and sent through air from source to the detector. Because of very large loss of power, is necessary to direct the energy of the sender accurately in the form of a well-collimated laser beam. In order to limit the beam divergence, it is essential to organize for a large beam radius from an optical source with high beam quality. Ideally, is to use a diffraction-limited source and a large high-quality optical telescope for collimating a large beam. Also is very useful to have a high directionality on the side of the receiver. Two facts are the most important to accomplish a high transmission capacity. First is to collect as much

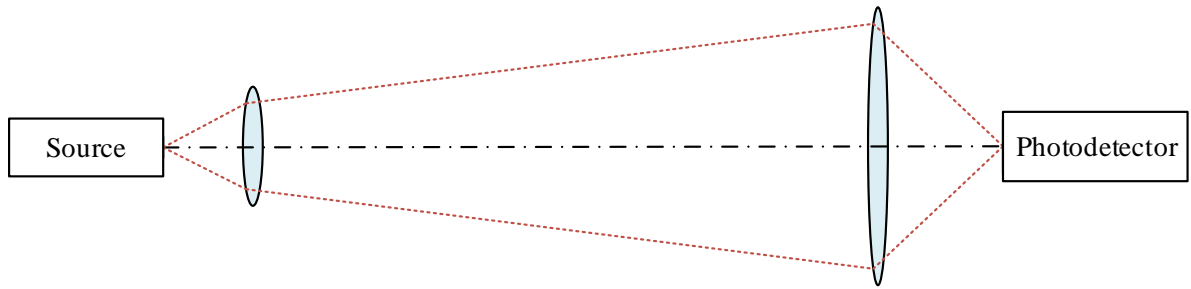


Figure 5: Simple setup with using lens for free-space optical communications

power as is possible and second is to minimize disturbing influences, e.g. from background light, which introduces noise. To achieve high sensitivity and directionality is necessary to use a large telescope at the receiver end. The simple setup for FSO is shown in Figure 5.

An important issue is the power budget, which is characterized by transmitter's power and all power losses. The power gained at the receiver determines possible data transmission rate. This power is also affected by the modulation format, the acceptable bit error rate, and various noise sources, in particular laser noise, amplifier noise, excess noise in the receiver, and background light. These issues can be suppressed with narrow-band optical filters, because the optical bandwidth of the signal is limited and background light is very broadband. To solve inter-symbol interference caused by atmospheric disturbances such as clouds, were developed sophisticated techniques of digital signal processing, which allow for reliable high-capacity optical links even through thick clouds [8].

Optical links, optical fiber links or optical free-space links, are used for high-speed data transmission. In context of free space-optics is obvious, that with increasing distance between source and detector, declines maximum possible data rate. In present, is able to obtain 1.25 Gbps, and in the future, is capable of speeds of 10 Gbps using wavelength division multiplexing (WDM). The Figure 6 show the comparison of free space optics and fiber optics.

Optical free-space links works in horizontal and vertical directions. Horizontal links are the most often installed for distances from hundreds of meters to ones of kilo-meters. These types of links are able to communicate up to ten kilo-meters. Vertical links allows distance tens of kilometres between source and detector [9].

Information transmission is realized by generating a physical signal and varying it through time. This signal is influenced along its channel. Some distortions are deterministically and some are randomly occurring. Several ways exist how to imprint the data onto the laser beam. It is possible to modulate the amplitude, the frequency, the phase and last but not least the polarization. For FSO links dominant methods include on-off-keying (OOK), differential-phase-shift keying (DPSK), phase-shift-keying (PSK), and orthogonal modulation formats such as Mary pulse-position modulation (M-PPM) and frequency-shift-keying (M-FSK). Concerning space or even deep space links, an important point to stress is the resistance of PPM against

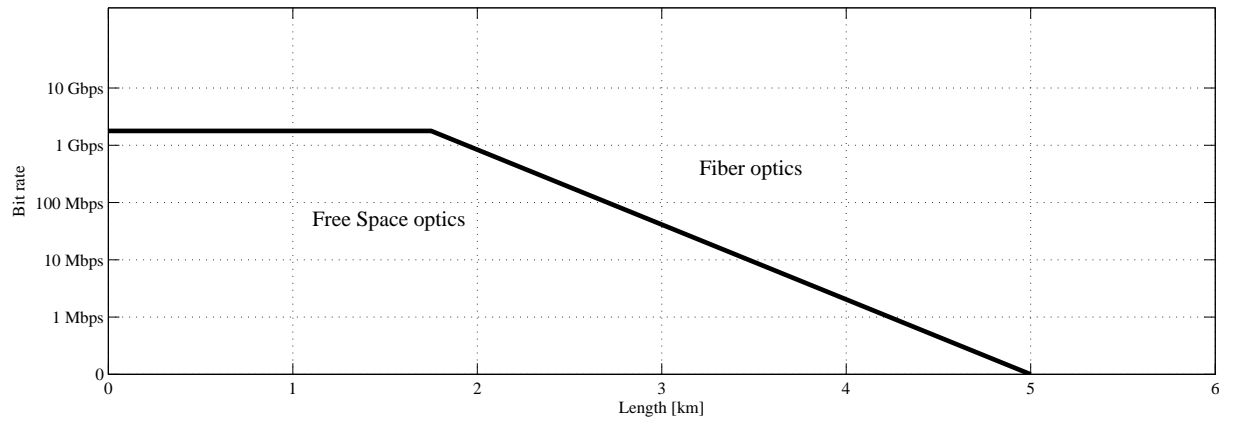


Figure 6: Relationship between the bit rate and network coverage for fiber optics and free space optics [9]

background radiation [10].



### 3 xDSL Transmission Channel Characterization

The term xDSL has also been used in the industry to refer all types of DSLs. As I described at previous chapter, DSL is access technology which operates over telephone subscriber's line. Telephone lines, which were constructed to carry a single voice signal with a 3.4 kHz bandwidth channel, can now transport nearly 100 digitally compressed voice signals, or a video signal with quality similar to broadcast television. High speed transmission over telephone wires requires advanced signal processing to overcome transmission influences due to signal attenuation, crosstalk noise from the signals present on the other wires in the same cable, signal reflections, radio frequency noise, and impulse noise [11]. For the better understanding I describe these impairments in the next section.

#### 3.1 Transmission Channel and Impairments

A telephone line consist of two isolated, solid-copper wires that are twisted together. Main reason, why are the wires twisted, is that twisted wires helps to reduce coupling of signals also known as crosstalk.

##### 3.1.1 Signal Attenuation

Figure 7 shows signal attenuation for frequencies up to 18 MHz for twisted pair wires 100, 500, and 2000 m long with diameter 0.4 mm. Attenuation is shown as negative decibels to illustrate that signals become weaker on longer telephone wires. The line on the top of graph shows that 100 m line has little attenuation and is not increasing rapidly with the frequency. The line which illustrate 500 m long line has a more attenuation, and attenuation grow rapidly with increasing the frequency. The bottom line shows the 2000 m long line with more pronounced increase of attenuation, where the attenuation difference between 100 m and 2000 m long lines is more than 200 dB. Since a wider range of frequencies is needed to transmit higher bit rates, this illustrates why the bit rate capacity is less for longer lines.

DSL modems are able to operate with up to about 65 dB of attenuation at the frequencies used for transmission. The maximum usable frequencies for the following line lengths are:

- 1.5 MHz at 2000 m.
- 5 MHz at 1000 m.
- 18 MHz at 500 m.
- Over 30 MHz at 100m.

Signal attenuation is also affected with diameter of copper wires, especially at lower frequencies. A wire with smaller diameter has a higher attenuation per meter, than a wire with bigger diameter. Next force, which has effect to attenuation is the temperature. High temperature causes more signal attenuation [5].

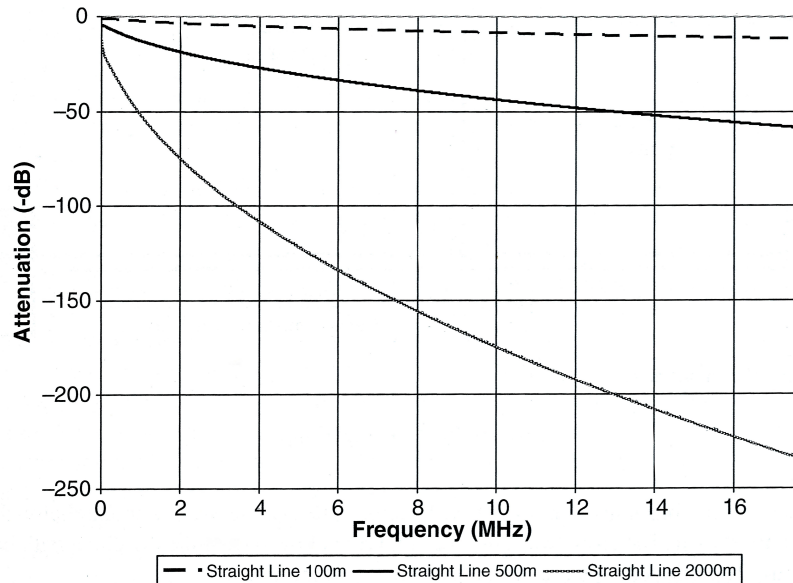


Figure 7: Attenuation for frequencies up to 18 MHz for twisted pair wires 100, 500, and 2000 m long with core diameter 0.4 mm [5]

### 3.1.2 Intersymbol Interference

DSL modems modulate the data to be transmitted into short symbols. The symbols are pulses of precisely adjusted phase, frequency, and amplitude. For ADSL, 4000 symbols are sent each second, and the duration of each symbol is  $250 \mu s$ . Different frequencies propagate at different speeds along a twisted pair line. This causes that some of the frequency components in a symbol arrive later than others causing a portion of the symbol to spread into the next symbol.

ISI is the effect of transmitted symbols spreading into each other, and this is illustrated in Figure 8. ISI effects all lines and is one of the main factors limiting DSL performance and it is particularly prejudicial on long lines and for high symbol rates. To minimize the ISI, DSL modems uses specialized techniques including receiver decision feedback equalization (DFE), transmitter pre-coding, and maximum-likelihood detection (Viterbi algorithm). Also, discrete multi-tone transmission (DMT) inserts a short cyclic prefix to each symbol to reduce ISI. The cyclic prefix is a copy of the last few microseconds of the symbol, and it is placed at the start of thy symbol. As a result, the first and the last few microseconds of the DMT symbol are identical, and it makes the channel look periodic to the receiver [5].

### 3.1.3 Crosstalk Noise

The most serious source of interference in DSLs are transmission systems deployed on the other symmetric pairs in cable. Some of the signal energy from each pair of wires radiates into the other pairs of wires in the cable. The energy electromagnetically coupled into wire pairs appear as noise to the DSL receivers connected to that line. The electric and magnetic fields thereby

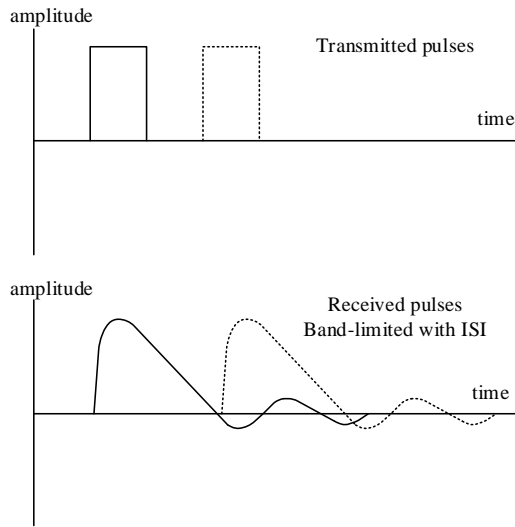


Figure 8: Intersymbol interference (ISI) [5]

create induce currents in neighbouring twisted pairs, leading to an unwanted crosstalk signal on those other pairs.

### 3.1.3.1 Near-end Crosstalk

Near-end Crosstalk (NEXT) is the type of crosstalk that become from signals travelling in opposite directions on two twisted pairs (or from a transmitter into a "near-end" receiver). NEXT coupling between pairs increases with signal frequency, and it is a major factor confining the performance of DSL systems that use the same frequencies for upstream and downstream transmission e.g. SHDSL, and ISDN. ADSL nd VDSL by separating frequency bands i.e. using frequency division multiplexing (FDM), virtually eliminate the effect of NEXT. For FDM-type DSLs, the NEXT appears outside of the frequency band used by the near-end receiver. The standard 99% worst-case model for received NEXT at frequency  $f$  is defined by Equation 1 [5]:

$$NEXT(f, N) = 10^{-13} \cdot \left(\frac{N}{49}\right)^{0.6} \cdot f^{1.5} \cdot S(f) \quad (1)$$

where  $N$  is the number of disturbing wire pairs (for a 50 pair binder group), and  $S(f)$  is the signal power input to one of the disturbing wire pairs at frequency  $f$ . NEXT is independent on length of line. This equation is based on empirical analysis of laboratory measurements of telephone cables. NEXT increases with frequency and with the number of disturbers (line causing crosstalk). The total amount of NEXT produced by two disturbing lines is about 50% greater than the NEXT produced by one disturbing line, but the total amount of NEXT produced by 24 disturbers is only about 10 more than the total NEXT produced by 20 disturbers [5].

NEXT attenuation is defined as ratio of powers, shown in Figure 9. This attenuation is defined by Equation 2 [5]:

$$A_{NEXT} = 10 \cdot \log \frac{P_{1N}}{P_{2N}} \quad (2)$$

where  $P_{1N}$  is an input power of disturbing pair, and  $P_{2N}$  is an output power of disturbed pair on "near-end".

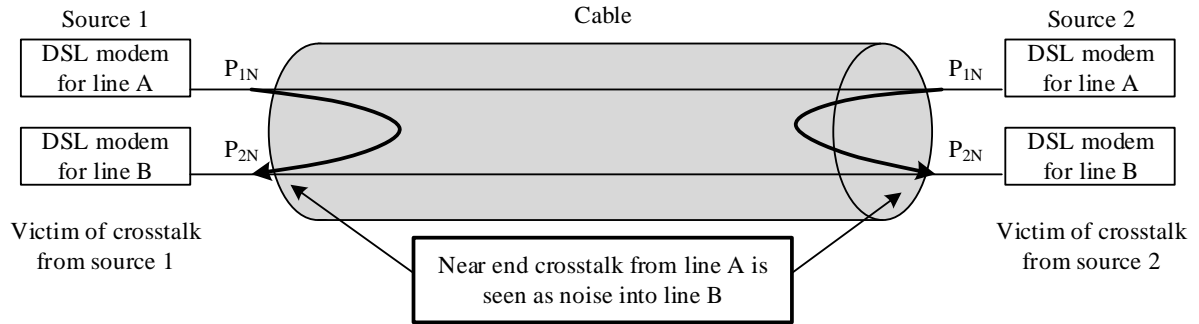


Figure 9: Near-end crosstalk path [5] [1]

### 3.1.3.2 Far-end Crosstalk

Far-end Crosstalk (FEXT) results from signals travelling in the same direction on two-twisted pairs (or from a transmitter into a "far-end" receiver, see Figure 10). FEXT coupling between wire pairs increases with signal frequency to a greater degree than NEXT. FDM in this case provides no benefits against FEXT, because the FEXT noise is located at frequencies used by the victim receiver. FEXT is more significant on shorter lines. The reason is, that shorter lines are able to carry higher frequencies, so DSLs often use higher frequency capacity, and FEXT coupling is much greater at higher frequencies. The second reason is, that the FEXT couples over the all the length of the line, but most of the FEXT coupling exhibits near the transmitter, where the transmitted signal is the strongest. The FEXT noise seen by the victim receiver is defined by Equation 3:

$$FEXT(f, L, N) = 9 \cdot 10^{-20} \cdot \left(\frac{N}{49}\right)^{0.6} \cdot f^2 \cdot L \cdot H(f, L)^2 \cdot S(f). \quad (3)$$

The degree of FEXT is a function of the number of disturbers (N), frequency (f), lengths of line (L), and the power of the disturbing signal source S(f). The "L" represent the length of wire, where is crosstalk coupling. With the increasing length of wire, more FEXT energy is coupled from the disturbing wire to the victim wire pair. The "H(f,L)" factor is the attenuation of FEXT coupled energy on the victim wire pair. The combined effect of these two factors plus the  $f^2$

factor for the frequency results in the FEXT noise seen by the victim receiver being greater than for the short lines, primarily due to higher frequency signals typically present on shorter lines.

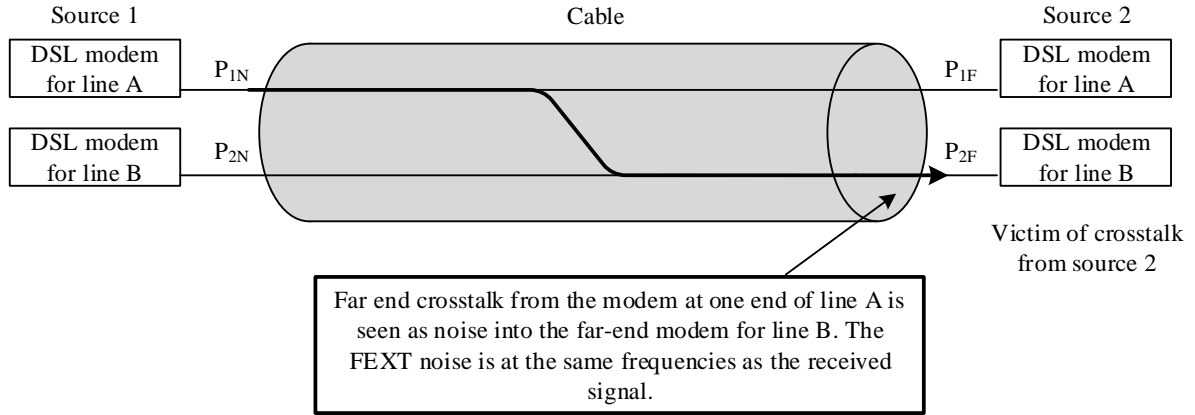


Figure 10: Far-end crosstalk path [5] [1]

FEXT attenuation is defined as ratio of powers, shown in Figure 10. This attenuation is defined by Equation 4 [5]:

$$A_{NEXT} = 10 \cdot \log \frac{P_{1N}}{P_{2F}} \quad (4)$$

where  $P_{1N}$  is an input power of the disturbing pair, and  $P_{2F}$  is an output power of the victims pair on "far-end".

### 3.1.4 Impulse Noise

Impulse noise is non-stationary crosstalk from temporary electromagnetic events near the phone lines. It occurs in relatively short bursts that sometimes have such high amplitude that it overcomes the signal on DSLs operating with high signal-to-noise margin. Often observed types of impulse noise are:

- Prolonged electrical impulse noise (PEIN) - Impulses with duration less than ten milliseconds. They are often correctable by interleaved Reed Solomon forward error control (FEC). PEIN may be caused by analog telephone signalling transients on the same line or an adjacent line.
- Short high amplitude impulse noise event (SHINE) - Impulses with duration of ten milliseconds or more. FEC is not possible to use, but for correction is possible to use packet retransmission. SHINE may be caused by an electrical motor starting and stopping.
- Repetitive electrical impulse noise (REIN) - Periodic impulses with duration less than one millisecond. REIN impulses usually occur every 10 ms in countries with 50 Hz AC power. A REIN impulse is produced by some AC-powered equipment at a certain voltage of the

AC power phase and is usually produced at both the positive and negative portions of the AC cycle [5].

### 3.1.5 Narrowband Noise (Radio Frequency Noise)

Radio noise is the residue of wireless transmission signals on phone lines, where the sources of noise include AM radio broadcasts, amateur radio (HAM), and switching power supplies with faulty radio frequency (RF) noise suppression.

Radio frequency signals impact on twisted-pair phone lines, especially aerial lines. Phone lines, which are made of copper, make relatively good antennas with electromagnetic waves incidents them leading to an induced charge flux with respect to earth ground. The amplitude of the noise can be so high that the DSL system will have no usable transmission capacity within the affected frequencies [11].

The high power of AM broadcast radio can be very damaging, especially if the AM antenna is within two kilo-meters of the DSL equipment. AM radio transmits at frequency bands from 535 kHz to 1.7 MHz. Television transmits at frequencies over 54 MHz, so it doesn't affect DSL [12].

### 3.1.6 Transmission Channel Models

The twisted pair of wires that DSL signals traverse may be represented as a transmission line model where the disturbed characteristics are equivalent to a concentrated electrical circuit. This is called the RLGC transmission line model where R represents the series resistance, L represents the series inductance, G represents the parallel conductance, and C represents the parallel capacitance between the tip and ring wires. The characteristic impedance ( $Z_0$ ) of the cable can be derived from the primary constants R, L, G, and C, as shown in Equation 5:

$$Z_0 = \sqrt{\frac{R + j\omega L}{G + j\omega C}} \quad (5)$$

where:  $j = \sqrt{-1}$ ;  $\omega = 2\pi f$ ;  $f = \text{frequency}$ .

## 3.2 DSL Transmission Techniques

DSL modem is able to outperform the imperfections of twisted line pair. Modulation converts the digital signal to an analog signal which is better suited for transmission over the wires because the signal energy is placed at frequencies with better channel characteristics. The most common used modulation techniques in DSL are 2B1Q, CAP, and DMT.

### 3.2.1 Modulation Techniques

The aim of modulation is to convert stream of DSL input bits into equivalent analog signals that are suitable for the transmission line.

#### 3.2.1.1 2B1Q

Two-binary one-quaternary (2B1Q) line code converts block of two consecutive signals into a single, four - level pulse. The 2B1Q is primarily used in early symmetric DSLs, IDSL, and HDSL. The 2B1Q is assigned to baseband transmission, which means the frequencies near the 0 kHz. Two bits are expressed according the Table 4, where each of the two bits have the different voltage. This line code is used in the U interface of DSL.

Table 4: 2B1Q

Binary	10	11	1	0
Level	+3 V	+1 V	-1 V	-3 V

#### 3.2.1.2 CAP

Carrierless amplitude and phase (CAP) modulation is a single carrier modulation technique that uses frequency ranges. For downstream data is reserved 900 MHz range, 75 MHz for upstream data, and 4 kHz for POTS service [13].

#### 3.2.1.3 DMT

Discrete multi-tone (DMT) modulation is the method by which the frequency range is divided into 256 sub-channels of 4.3125 kHz each. To partition uses an inverse discrete Fourier transform (IDFT). The DMT measures signal-to-noise ratio (SNR) of each sub-channel and assigns data. By dividing the frequency spectrum into multiple channels DMT is able to avoid channels which are degraded by interference. Thereby, maximization of bit rate is possible [13].

### 3.2.2 Duplexing

Duplexing techniques are applied for split the data transmission from the customer (upstream) and to the customer (downstream).

ECH (echo cancelled hybrid) is the duplexing technique used for ISDN, HDSL, and SHDSL systems. With ECH, data is simultaneously transmitted in both directions in the same frequency band. The signals in both directions are superimposed upon the same pair of wires. The receivers at both end recover the desired signal by sub-tracing the portion of the signal sent by the local transmitter. Since the signal sent from the far end is attenuated by the line, the amplitude of the signal from the local transmitter is much greater than the desired signal send from the far end. The near-end signal can be removed with the high precision, because the locally transmitted data pattern is exactly known, and the DSL modem adapts to the reflection characteristics of

the channel. The term training is used to describe the process of the modem learning the channel characteristics.

The advantage of the ECH duplexing method is that the utilized frequency band does not extend as high as would be needed for the FDM technique. Disadvantages are the high levels of the NEXT and the limited precision for cancelling the signal from the local transmitter.

FDM (frequency division multiplexing) is the duplexing method used for ADSL and VDSL systems. With FDM, downstream data is placed in one or more frequency bands that are separate from the frequencies used for upstream transmission. Interference from the local transmitter is simply removed by filtering out the frequencies used by the local transmitter. NEXT is also simply removed by the same filtering, provided that all other lines use the same frequency plane (i.e., all customer-end modems transmit upstream data in the same frequency bands, and all network end-modems transmit downstream data in the same frequency bands).

ADSL and VDSL systems are asymmetric, that is, the downstream frequency bands are larger than the upstream bands. To avoid excessive NEXT, all lines must transmit in the same direction at each frequency. Thus, it is not possible to operate ADSL or VDSL systems with reverse asymmetry (upstream bandwidth greater than downstream).

The advantages of FDM are the simplicity and effectiveness of avoiding NEXT and interference from the local transmitter. The disadvantage of FDM is that it is necessary to use higher frequencies, because frequencies are not reused to send data in both directions.

TCM (Time Compression Multiplexing) also known as TDD (Time Division Duplexing) is a duplexing technique used for some of the basic-rate ISDN systems in Japan. For data transmission are used short one-way bursts in alternating directions, where downstream transmission is 1 ms long and then upstream transmission is accordingly 1 ms long. Between the bursts is used a guard interval to reduce interference from echoes. TCM is an effective method to avoid NEXT and interference from local transmitter. The effectiveness of avoiding NEXT depends on the transmitted bursts from all modems connected to a cable and their precise synchronization. The synchronization is especially difficult when some of the pairs in the same cable are fed from different DSLAMs [5].

### 3.2.3 Coding

When we talk about coding we focus on two aspects: error detection and error correction. A cyclic redundancy block code (CRC) serves to detect errors. CRC checksum is attached to each transmitted block and it's able to detect errors with high reliance, moreover if there are multiple bit errors. In a situation, when CRC checksum indicates an error in received block is called a code violation (CV).

For error correction is used forward error correction (FEC) and automatic repeat request (ARQ). ARQ is generally executed by upper layer protocols such as TCP-IP. The receiver is able to detect an error bits by examining the CRC checksum. If any errors are detected, receiver sends a NAK message to the transmitter. Response from the transmitter is retransmission of



packets. The effectiveness of ARQ is only in cases of correcting large burst of errors, which occur rarely. Packet retransmission increases additional delay also known as jitter.

FEC, which is implemented to a DSL, sends redundant check bits (i.e., additional bits) together with the data. The receiver uses these bits to correct transmission errors. One of the options is to send every block of data three times. If there are received two identical copies, is possible to evaluate these same copies as the correct data. This form of error correction is used for low bit rate operations for some types of DSL. VDSL and ADSL systems with high bit rate payload data use a Reed Solomon (RS) forward error correction code.

The RS codes attaches redundancy data at the end of each block of digital data. After this is formed codeword of  $N = K + R$  bytes for transmission, where  $K$  is bytes of data and  $R$  is bytes of redundancy. The structure of the RS codeword is shown in Figure 11. The data bytes and the appended redundancy bytes are referred as systematic  $(N, K)$  code. After codeword transfer through the channel is possibility that the errors will occur in codeword, which is caused by the noise in transmission channel. The RS decoder examines the received data and redundancy in each of the received codewords and tries to optimize the probability in recovering the original data correctly [5].

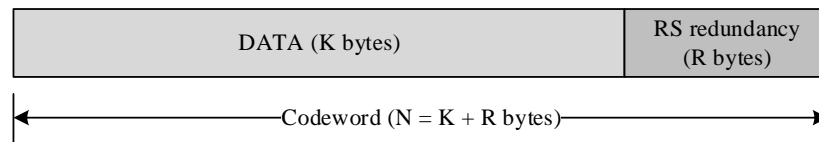


Figure 11: RS codeword structure[5]

The maximum number of bytes for ADSL2 and VDSL2 in RS codeword is 255. With using Reed-Solomon decoder is possible to correct up to  $t = R/2$  bytes that contain errors within a codeword. The number of redundancy bytes inside codeword is ranging from 0 to 16, and the number of bytes  $N$  per codeword ranges from 32 to 255. Therefore, RS code is able to correct up to 8 bytes with errors per codeword. Even if there is only small number of error bits in byte is able to correct the same number of bytes.

The RS code is also useful for correcting bursts of errors. With use of interleaving may be extended the length of correctable error burst. The interleaver shuffles the order of bytes, and then the de-interleaver un-shuffles the bytes to gain the original order of the data. The bytes of consecutive RS codewords may be interleaved to a specified interleave depth of  $D$  codewords before transmitting on the channel. While codewords are transmitting on the line, an impulse noise is affecting. This causes that sequence of interleaved bytes will be corrupted (i.e., cause a burst of errored bytes). The DMT receiver reconstructs the received RS codewords (which may contain errors), the de-interleaving process spreads the location of errored data bytes across the span of the interleave depth  $D$  as it reconstructs the original codewords. It makes that long series of errors are transformed into many shorter series of errors and they are spread out

across of several codewords. Hence, there are not so many byte errors per codeword and the RS decoder can correct errors. Unfortunately, interleaving has two disadvantages. First, it increases transmission latency. Second one, if the number of errors exceeds the capacity of the interleaved RS FEC, it can corrupt several packets. A non-interleaved operation would have had only a single corrupted packet. Figure 12 shows the reference transmission model for DSL system.

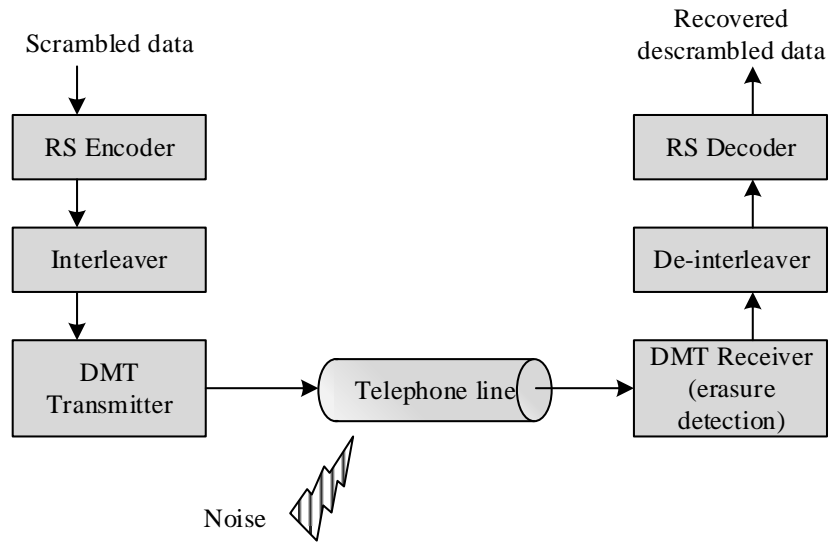


Figure 12: DSL system reference model [5]

## 4 xDSL Standards

This section discusses details of the Integrated Services Digital Network (ISDN), High Bit-Rate DSL (HDSL), Symmetric High Bit-Rate DSL (SHDSL), Asymmetric DSL (ADSL), and Very High Bit-Rate DSL (VDSL) standards.

### 4.1 ISDN

ISDN we can consider as the first of DSL family. The basic rate interface (BRI) and the primary rate interface (PRI) are two basic versions of ISDN. Services based on ISDN are known as basic rate access (BRA) and primary rate access (PRA). The ISDN PRI consists of two 64 kbps carrier channels (“B channels”) for data or voice, and a 16 kbps signalling channel (D channel). In addition, there is an overhead for signalling and framing. The total transmitted bit rate is 160 kbps. ISDN BRA uses for encoding 2B1Q (two binary, one quaternary) line code or 4B3T line code. The 4B3T line code is used in Germany.

The primary rate ISDN channels depend on location in the world. In Japan and North America, the PRI uses 23 B channels (64 kbps per channel), one D channel (64 kbps), and 8 kbps of overhead. The resulting line rate is 1544 kbps. The PRI in Europe and most of the rest of world uses 30 B channels (64 kbps per channel), one D channel (64 kbps) with an additional 64 kbps overhead channel for signalling, framing, and other overhead. The resulting payload is 2048 kbps [14].

An innovation of the ISDN is called ISDN DSL (IDSL), but it is non-ISDN application of BRI transceivers. The ISDN local switch is replaced by a packet router. Most forms of IDSL are able to work with a conventional ISDN Network Terminal at the customer end of line. The BRI symmetric channels (128 kbps or 144 kbps) are coupled to form one channel for transmission of packet data between a router and the customer’s computer [11]. To transport on physical layer is used 2B1Q line code [14].

### 4.2 HDSL

High bit rate digital subscriber line uses mostly the same technology as ISDN-BRI. HDSL supports symmetric 1.544 Mbps or 2.048 Mbps transmission. HDSL splits a 1.544 Mbps signal into two twisted wire pairs which run at 784 kbps, allowing the service to run on longer loops without repeaters, for example, 3.7 km on 0.5 mm wire [15]. The need for HDSL became obvious as T1 and E1 transmission systems ended up to be used for their original application as interoffice trunks and saw rapid growth as private lines from Central Office to customer premises. T1/E1 transmission systems operated over the existing telephone wires, but at a large cost for special engineering, loop conditioning (removal of bridged taps and loading coils), and splicing for units cases to hold the repeaters that were required every 1 to 1.5 km. More than 95% of HDSL lines

have not any repeater. Nevertheless, repeaters are usually used for lines of 2.75 to 3.7 km. With one repeater is able to reach up to 7.3 km, with two repeaters is able to reach up to 11 km.

The 2B1Q line code is used for most of HDSL systems. In some countries of Europe is used discrete multi-tone (DMT) and carrierless CAP. Several transmission techniques were developed for HDSL systems: single duplex, dual simplex, and dual duplex.

Single duplex is requiring only one pair of wires. To separate transmission directions is used frequency division multiplexing (FDM) or echo-cancelled hybrid (ECH) transmission. Single duplex is shown in Figure 13 A.

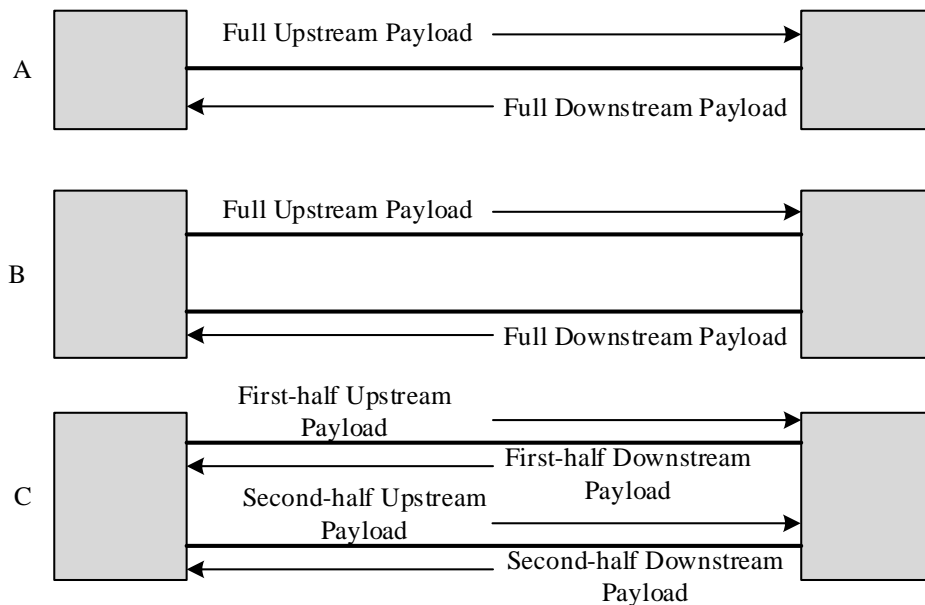


Figure 13: (A) Single-duplex HDSL; (B) Dual-simplex HDSL; (C) Dual-duplex HDSL [11]

Dual simplex transmission (Figure 13 B) operates with two pairs of wires. One of the wire pair is carrying full payload in upstream direction and the second pair is carrying full payload in downstream direction. The drawback of the dual simplex transmission is transmitting a signal with a wide frequency bandwidth, which causes a high loss and crosstalk at the higher frequencies.

Dual duplex transmission (Figure 13 C) operates also with two pairs of wires. This transmission improves the achievable loop reach and spectral compatibility by sending one half of the total information on each wire pair. Moreover, HDSL reduces the bandwidth of transmitted signal by using ECH transmission to send the two directions of transmission in the same frequency band. The dual duplex HDSL transmitted signal power is significantly less for frequencies above 196 kHz. As a result, the signal crosstalk and attenuation is reduced. Another advantage of dual duplex transmission is that using one pair of wires can provide a half rate transmission system [11].

Second generation HDSL technology (HDSL2) provides the same bit rate (1.544 Mbps) and loop reach as HDSL. HDSL2 uses only one pair of wires instead of two. The transmission efficiency was increased by trellis-coded pulse amplitude modulation (TC-PAM) with partially overlapped upstream and downstream frequency bands. Upstream signal uses frequencies from zero to 280 kHz, downstream transmission frequencies are from zero to 400 kHz. Required transmitted power is 3 dB more than HDSL [5].

### 4.3 SHDSL

The official name of the SHDSL is “single pair high speed digital subscriber line”. Although, the SHDSL is often represented as “symmetric high bit rate DSL”. The line code for transmission is also used the TC-PAM like in HDSL2 standard. The SHDSL provides symmetric bit rates from 192 kbps to 5.7 Mbps. Transmission is ensured via one pair of wires. Higher bit rates can be reached by combining multiple pairs of wires to serve a customer [5]. SHDSL does not support the POTS, the frequency band used for digital transmission is extends nearly to 0 Hz. The approximate frequency bands for transmission in both directions are shown in Table 5.

Table 5: SHDSL frequencies and bit rates [5]

<b>SHDSL bit rate</b>	<b>Maximum transmitted frequency</b>
192 kbps	70 kHz
1 Mbps	320 kHz
1.5 Mbps	470 kHz
2.3 Mbps	720 kHz
5.7 Mbps	1.3 MHz

### 4.4 ADSL

Asymmetric digital subscriber line (ADSL) was designed to transmit higher downstream bit rates than upstream. This was reached by allocating most of the frequency band for downstream transmission. Transport is ensured via one wire pair and achieves the following bit rates:

- Downstream - up to about 9 Mbps.
- Upstream - up to 1 Mbps.
- Plain old telephone service (POTS, i.e. analog voice).

Analog voice is transmitted at baseband frequencies and combined with the passband data transmission through a low-pass filter (LPF) also know as a “splitter”. Figure 14 shows reference model of ADSL, where ATU-R means transmission unit at the remote side (customer) and ATU-C means transmission unit at the Central Office side.

The ADSL concept includes two fundamental parts:

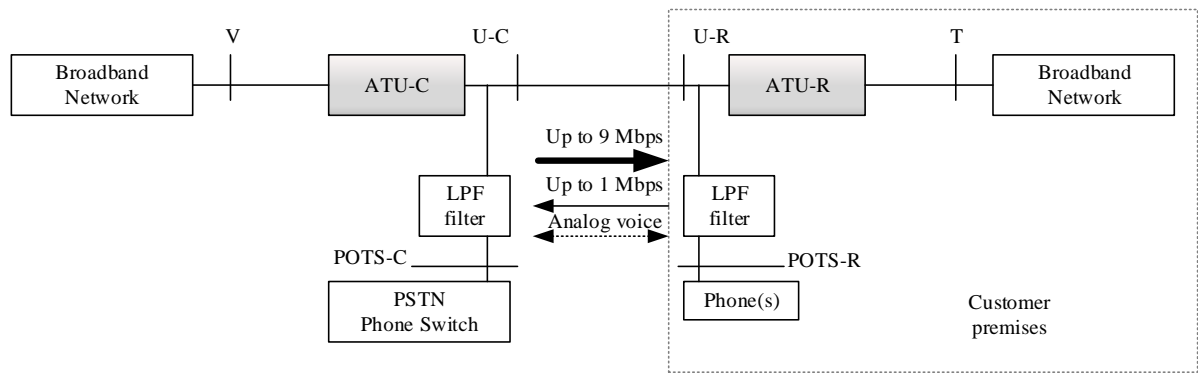


Figure 14: ADSL reference model [11]

- Near-end crosstalk is reduced by having the upstream bandwidth and bit rate much smaller than the downstream bandwidth and bit rate.
- Simultaneous transport of data and POTS by transmitting data in a frequency band above the voice telephony.

Due to the effect of loop loss and crosstalk is rare to see two-way transmission of megabit rates on telephone lines. Figure 15 shows decrease of received signal power with frequency, and increase of crosstalk noise in proportion with frequency. Therefore, two-way transmission is not possible at frequencies where the crosstalk noise overwhelms the received signal.

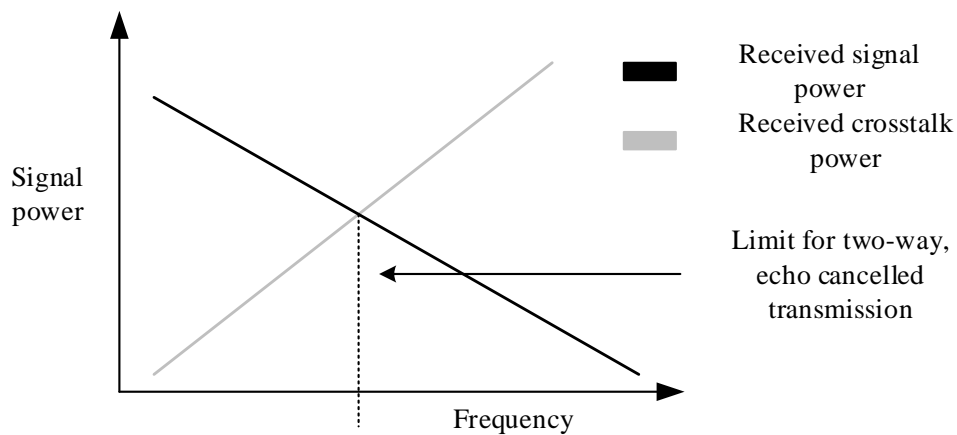


Figure 15: Limitation to lower frequencies by two-way transmission [11]

Two-way transmission in ADSL works beneath the two-way cut-off frequency. The frequencies above the two-way cut-off frequency are suitable only for one-way transmission. This allows much higher downstream rates in comparison with those which are possible in two-way transmission.

Most of ADSL system use for transmission a frequency division multiplex (FDM) technique. This technique separates the upstream transmission band from the downstream transmission

band to prevent self-crosstalk. Also, there is necessary to use guard band which ensures easy segregation of the digital transmission from POTS noise. See figure 16.

Less used transmission technique in ADSL systems is ECH, where the upstream frequency band lies within the downstream frequency band. This overlap reduces the total transmitted bandwidth. However, the ECH is susceptible to self-crosstalk. For the ECH implementation is inevitable to use complex digital signal processing. See Figure 17.

Due to lack of self-crosstalk at the ATU-C, FDM offers much better upstream performance than ECH. The wider downstream bandwidth of ECH provides better downstream performance, particularly for the short loops.

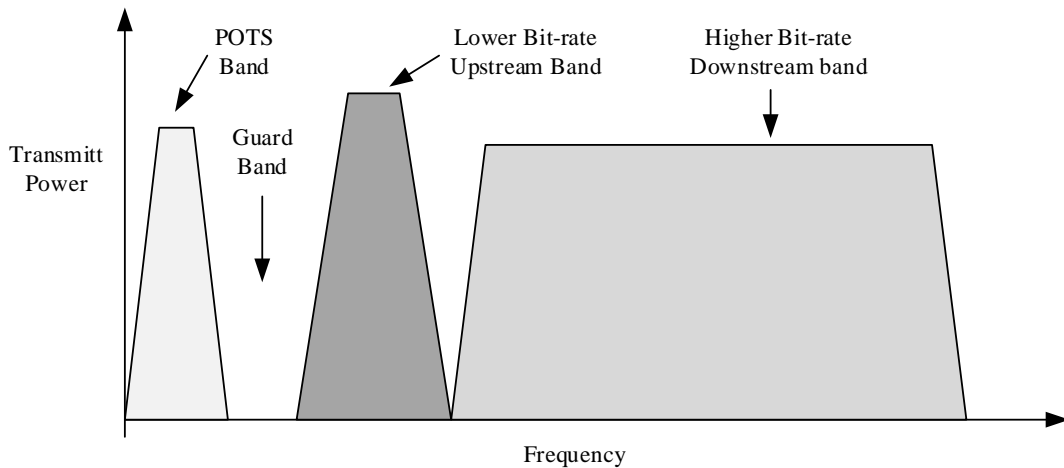


Figure 16: FDM ADSL [11]

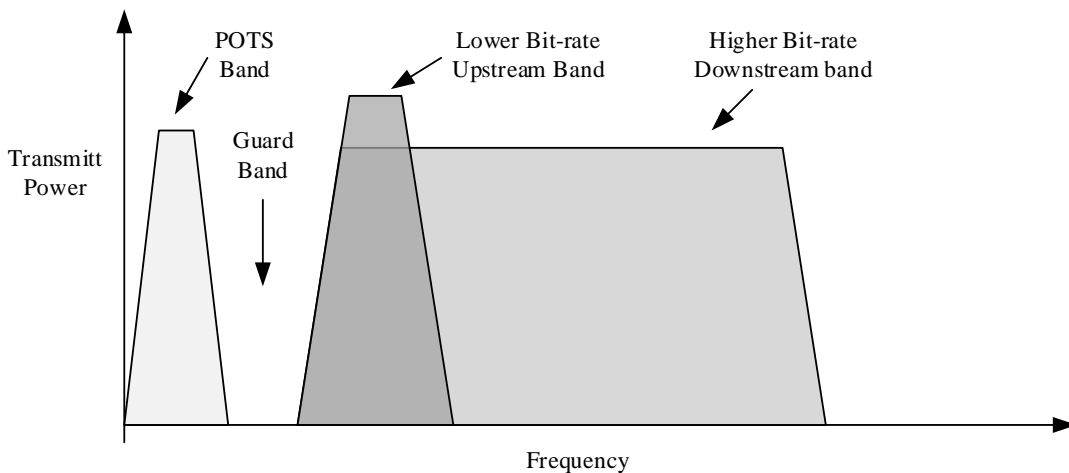


Figure 17: ECH ADSL [11]

Symmetric DSL performance is mostly limited by self NEXT (self-near-end-crosstalk). ADSL eliminates self NEXT at the customer end by reducing the source of the self NEXT. By reducing

the upstream bit rate, the upstream channel may be positioned to minimize crosstalk into the downstream transmission. By placing the upstream channel at lower frequencies is easier to receive signal, because at lower frequencies loss of loop is smaller and crosstalk noise is smaller, too.

The frequency range of ADSL transmitter is dependent according to whether it is upstream or downstream transmission. In addition, the range of frequencies generated by the transmitter in the upstream direction depends on whether ADSL operates on the same physical loop as POTS or ISDN.

The downstream frequency bandwidth is from 0 to 1.104 MHz. This bandwidth is splitted into 257 sub-channels, 255 of them are passband sub-channels with 4.3125 kHz bandwidth, and two of them are baseband sub-channels with 2.15625 kHz bandwidth. The channels are numbered from 0 to 256 with increasing frequency. The passband sub-channels, with indexes 1 through 255, are centered at integer multiples of 4.3125 kHz, which are the sub-carrier frequencies. The sub-channel 0 at 0 Hz and sub-channel 256 at 1.104 MHz are not used in ADSL. Figure 18 illustrates the downstream sub-channels in ADSL.

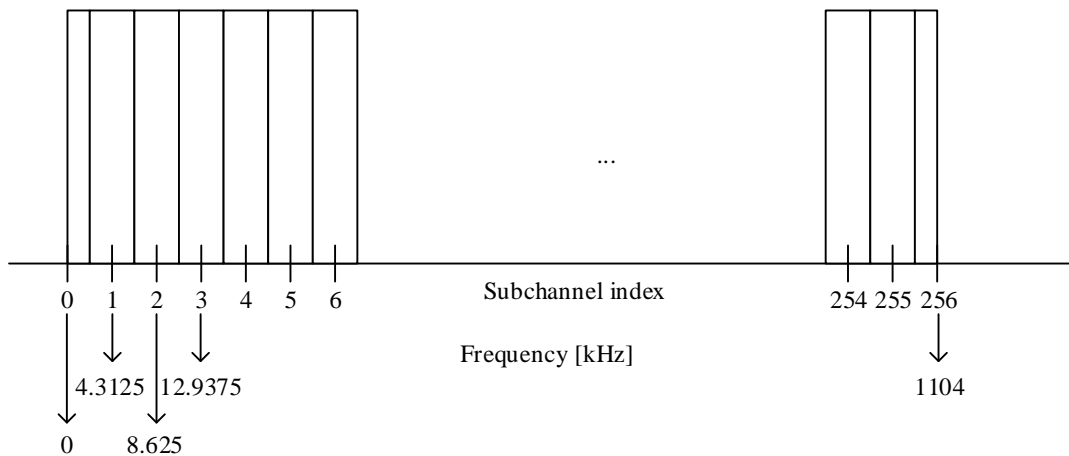


Figure 18: Downstream sub-channels generated by an ADSL transmitter [14]

The range of frequencies in the upstream direction generated by transmitter depends on used operating loop. In the case of ADSL over POTS, there are generated sub-channels from 0 to 138 kHz (sub-channels from 0 through 32) by the upstream transmitter. The first and last channels are not used, and the first several passband sub-channels are not enabled to permit a POTS signal to share the line. Although, inevitable bandwidth for the POTS is only 4 kHz, there have to be sufficiently wide guard band to ensure that ADSL signals will be attenuated in the POTS band. In the case of ADSL over ISDN, the upstream transmitter generates sub-channels from 138 to 276 kHz (sub-channels from 33 to 64). The sub-channels 0 through 32 are generated only with one type of implementation. For either type of transmitter implementation, sub-channels under 138 kHz are not used so an ISDN signal may share the same telephone line. Figure 19 shows the upstream sub-channels in ADSL over POTS (A) and in ADSL over ISDN



(B). The broken lines in B scheme indicates the sub-channels, which are dependent on the type of implementation [14].

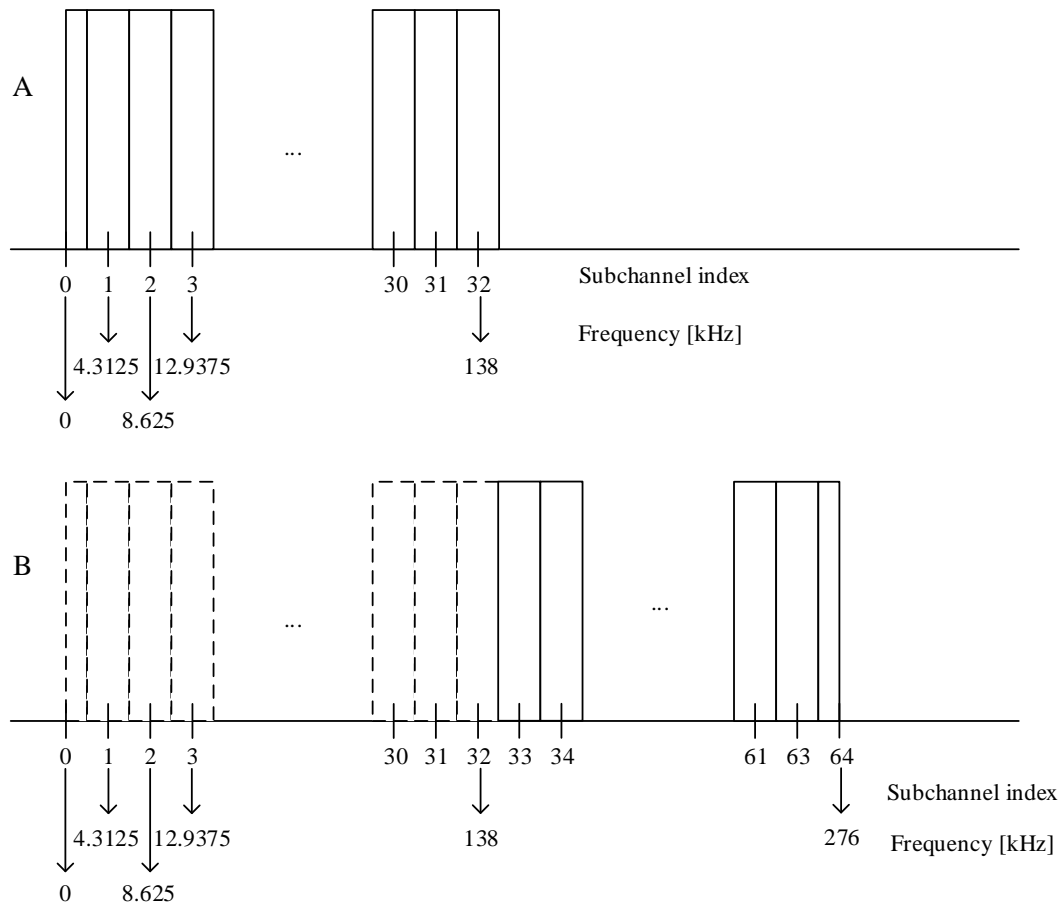


Figure 19: Sub-channels generated by an upstream transmitter for (a) ADSL1 over POTS and (b) ADSL1 over ISDN [14]

#### 4.5 ADSL2 and ADSL2+

ADSL2 is an extension of ADSL, which uses the same bandwidth allocation as ADSL. ADSL2 provides 8 Mbps downstream and 800 kbps upstream.

ADSL2+ has increased the maximum frequency to 2.208 MHz with 512 DMT tones. ADSL2+ provides downstream bit-rate up to 24 Mbps and upstream bit rate more than 1 Mbps. The upstream/downstream frequency boundary is set at 138 kHz.

#### 4.6 VDSL

Very-high-bit-rate digital subscriber line (VDSL) is an improvement of ADSL, which supports higher bit rates than ADSL2plus, up to 52 Mbps for downstream and . VDSL operating

bandwidth is at considerably higher frequencies than in ADSL. However, due to high attenuation at the higher frequencies is VDSL designed to operate on short lines, usually less than 1.5 km. Because of that, VDSL is provided from remote terminals (RTs) with using optical fibers to connect to the Central Office (CO).

The VDSL standards transmits at frequencies up to 12 MHz. Two different FDM frequency plans are specified for VDSL. The VDSL 998 frequency plan is used mostly in North America. Downstream frequencies are from 138 kHz to 3.75 MHz and from 5.2 to 8.5 MHz. For upstream transmission are reserved frequencies from 3.75 to 5.2 MHz and from 8.5 to 12 MHz. The VDSL 997 frequency plan is in use in some parts of Europe. For downstream transmission are reserved frequency bands from 138 kHz to 3.25 MHz and from 5.1 to 8.1 MHz. Upstream transmission uses frequencies from 3.25 to 5.1 MHz and from 8.1 to 12 MHz.

The VDSL2 uses frequencies up to 30 MHz. The distance between sub-carriers is 4.3125 kHz, but the 8.6125 kHz can be also used. Depending on the band plan can be used up to 4096 sub-carriers [5]. The several VDSL2 profiles and their rates is shown in Table 6.

Table 6: VDSL2 profiles [5]

<b>Profiles</b>	<b>Highest Frequency [MHz]</b>	<b>Maximum Downstream bit rate [Mbps]</b>	<b>Maximum Upstream bit rate [Mbps]</b>
8a, 8b, 8c, 8d	8.5	48	10
12a, 12b	12	48	30
17a	17	60	30
30a	30	120	100

## 5 Ethernet Passive Optical Network

Over the past decade several PON architectures have been developed by the International Telecommunications Union (ITU) and the Institute of Electrical and Electronic Engineers (IEEE). The four main PON variations developed by the ITU and IEEE can be categorized into two groups. The first kind of architecture is based on Asynchronous Transfer Mode (ATM) and includes ATM PON (APON), Broadband PON (BPON) and Gigabit PON (GPON) and the second group consists of Ethernet PON (EPON). EPON and GPON are the most popular PON variations found in use today [16].

In this chapter I will describe EPON network. EPON is base network for build up hybrid access network in the practical part.

Ethernet passive optical network is Point-to-Multipoint network, where one fiber is shared for many end users. It serves generally for the cost reduction, because is not necessary to use a large amount of optical fibers. Passive in context of passive optical network mean that no electronic components, such a regenerators and amplifiers, are placed between the OLT (Optical Line Terminal) and the ONU (Optical Network Unit). For the fiber distribution to more end users is used passive optical splitter. Optical signal after crossing the splitter is not amplified or modified, the signal is just splitted to several branches. The principle of passive optical network is shown in Figure 20.

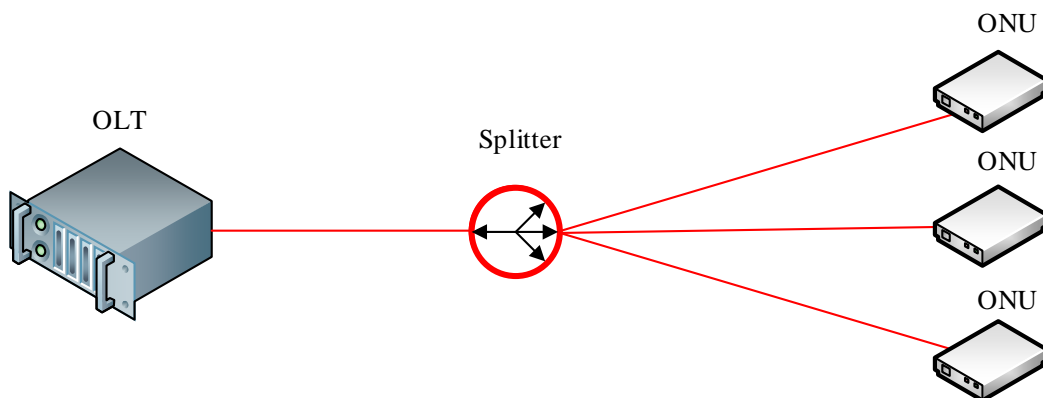


Figure 20: Passive Optical Network

### 5.1 Fundamental Parts of PON

- Optical Line Terminal (OLT) - active component situated in the Central Office (CO). Component serves as network interface between communication service network and access network. Also manages traffic in ODN.
- Optical Distribution Network (ODN) - set of transmission facilities situated between the OLT and the ONU.

- Optical Network Unit (ONU) - active component serves as interface between optical and metallic part of access network. This device is generally placed in the cabinet, which is situated in the building or somewhere near.

## 5.2 Definition

Ethernet passive optical networks are access networks that provides a low-cost technology of optical lines between an OLT and customer site. EPON is build on the International Telecommunications Union (ITU-T) standard G.983 for ATM passive optical networks. EPON is able to transmitt data, video, and voice over a single optical access network, also known as Full Service Access Network (FSAN)[17].

The Institute of Electrical and Electronics Engineers (IEEE) developed their own concept with standardization 802.3ah, through the Ethernet in the First Mile (EFM) study group. The aim was to create a standardization with high-speed access based on Ethernet interface.

EPON solves many demerits of APON networks, specifically low bandwidth, and complexity. Also solves issue with conversion among the ATM and IP protocols.

## 5.3 Transport Convergence Layer

The EPON transport protocol is based on the standard Ethernet frame structure. For communication applies Time Division Multiplexing (TDM) technique (Figure 21) in the downstream transmission and Time Division Multiple Access (TDMA) technique (Figure 22) in the upstream. EPON transmission speed is symmetrical 1 Gbps with 8B10B line coding, resulting in 1.25 Gbps line rate. There are no limits to the maximum logical distance between the OLT and the ONUs. However, the limits are set by the physical characteristics of the optical transmitters which are defined in the PMD sublayer. The data are carried in Ethernet frames and each ONU receives only the frames addressed to it. In the upstream direction, each ONU has a reserved time slot when the ONU can transmit. The identification of ONU is ensured by a 2 byte long tag, called Logical Link ID (LLID) [18].

EPON is single fiber network, where the upstream transmission operates at the wavelength of 1310 nm and the downstream transmission operates at the wavelength of 1490 nm. The 1550 nm wavelength window is open for additional services such as Community Antenna television (CATV) networks [18].

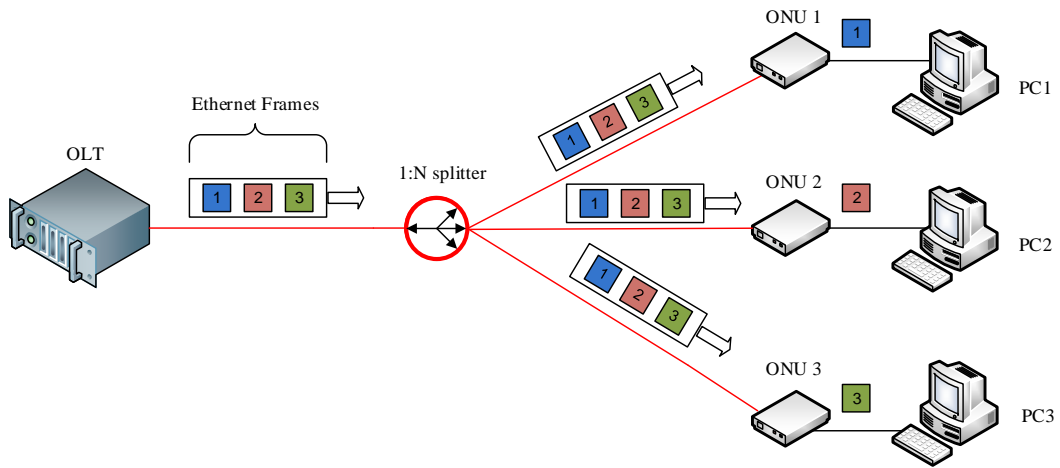


Figure 21: EPON TDM

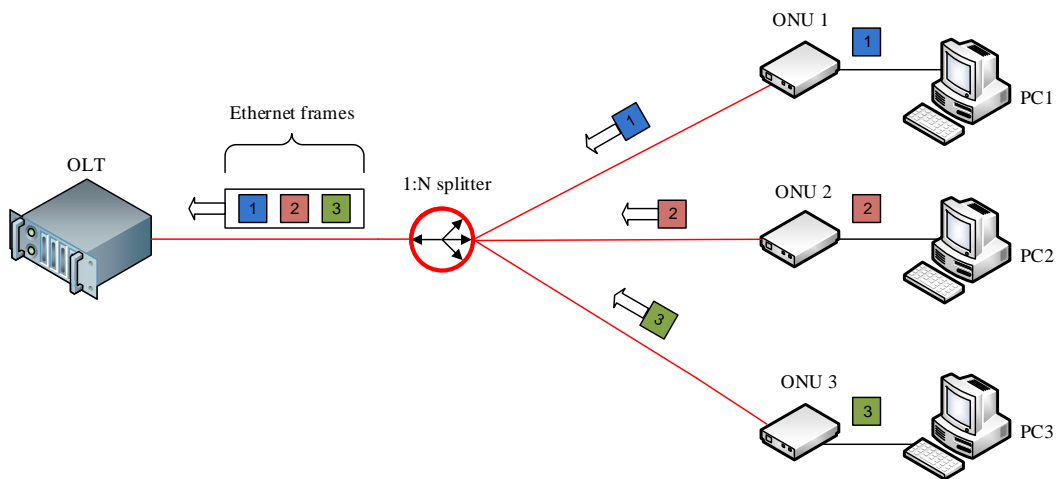


Figure 22: EPON TDMA

### 5.3.1 Ethernet Frame Format

The transmission in EPON networks is ensured by Ethernet frame that is defined by standard IEEE 802.3. The Ethernet frame structure is shown in Figure 23.

Preamble	SFD	Destination Address	Source Address	Length	802.2 Header + Data	FCS
7 bytes	1 byte	6 bytes	6 bytes	2 bytes	46– 1500 bytes	4 bytes

Figure 23: Ethernet frame structure [19]

A description of the each of the fields:

- Preamble - serves to synchronization with the receiver's clock,
- Start of Frame Delimiter (SFD) - the field contains a byte sequence 10101011 to initialization the start of frame,
- Destination Address - Media Access Control (MAC) address of the destination network interface with a length of 48 bits; it can be unicast, broadcast or multicast address,
- Source Address - Media Access Control (MAC) address of the source network interface with a length of 48 bits,
- Length - specifies the number of bytes in the data field,
- Data - contains data; minimum size 46 bytes is necessary to detect a collision within a segment,
- Frame Checksum (FCS) - 32-bit hash code of the data; by cyclic redundancy checksum (CRC) is realized error detection caused due to noise on the cable [19].

#### 5.4 Ethernet Layering Architecture and EPON

Figure 24 shows the differences between the Point-to-Point (P2P) Ethernet and Point-to-Multipoint (P2MP) EPON architecture. From the figure is obvious that Ethernet operates over the physical layer and datalink layer of the open system interconnect (OSI) reference model.

The EPON layering is similar to that of P2P Ethernet. Datalink and physical layer is divided into multiple sublayers by the Ethernet standard. The physical layer is connected to datalink layer by interface MII or GMII.

The MAC sublayer from P2P Ethernet is in EPON replaced by MPMC sublayer. To coordinate the access to the shared PON medium among EPON ONUs is running multipoint control protocol (MPCP) at MPMC sublayer [20].

##### 5.4.1 Physical Medium-Dependent Sublayer (PMD)

The PMD sublayer defines the physical characteristics of the optical transmitters. The 1000BASE-PX10-U/D define the OLT and ONU characteristics for a 10-km reach. The 1000BASE-PX20-U/D define the OLT and ONU characteristics for a 20-km reach. The difference between these two specifications repose primarily in the OLT transceivers, where 1000BASE-PX20 uses better transmitter and APD receiver. The specifications of ONU transmitters are very similar so that the same type of ONU can support both -PX10 and -PX20 systems. Table 7 summarizes the EPON PMD options [20] [3].

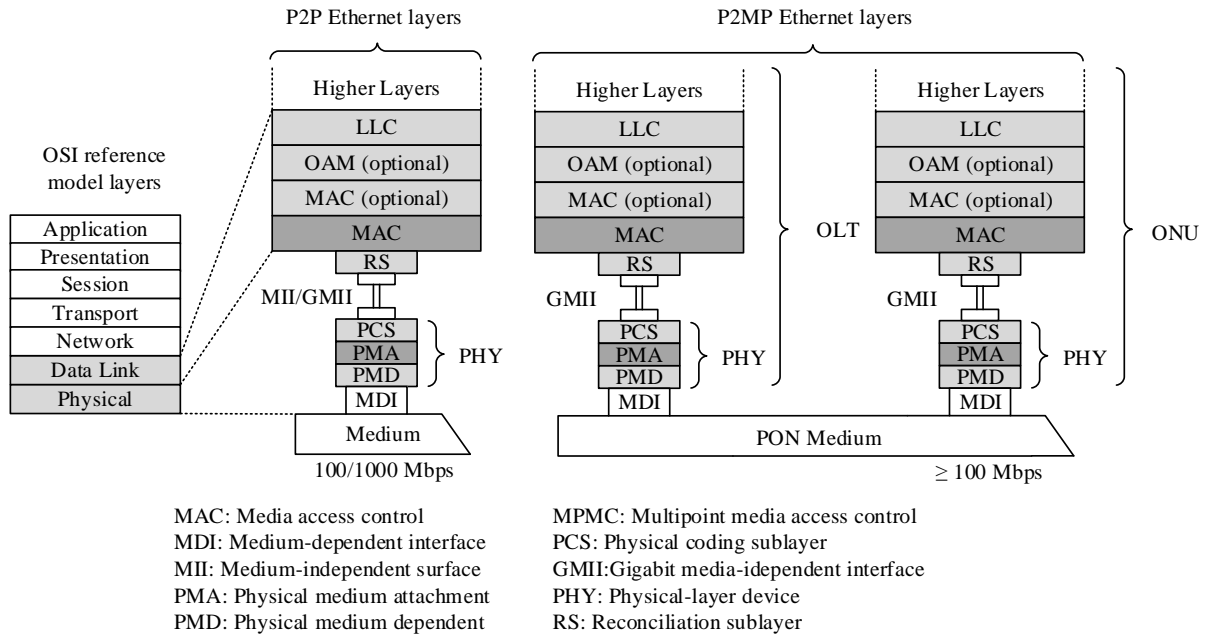


Figure 24: P2P Ethernet and P2MP EPON layering architecture [20]

Table 7: EPON PMD options [3]

Parameter	1000BASE-PX10-U/D	1000BASE-PX20-U/D
Distance [km]	10	20
Data Rate [Gbps]	1	1
Minimum channel insertion loss [dB]	5.0/5.0	10.0/10.0
Minimum channel insertion loss [dB]	30.0/19.5	24.0/23.5
Maximum split ratio	16 (without FEC)	16 (without FEC)
	32 (with FEC)	32 (with FEC)

#### 5.4.2 Physical Coding Sublayer (PCS) and Forward Error Correction

EPON specifies a symmetric data rate 1 Gbps in both directions and 8b/10b line coding. An 8b/10 line code produces a sufficient number of zero-one and one-zero transitions and DC balanced output to ensure easy clock recovery. However, this increases the baud transmission rate to 1.25 Gbaudps. Moreover, the PCS defines a data detection function to control the laser-on/off function. The data detection function could be seen as a delay line that turns the laser on or off at the correspondent time after detecting waiting or completion of data from MAC.

The application of FEC in EPON is optional. The EPON standard defines RS (255,239) cyclic code in the EPON PCS layer. At the end of the each frame are attached parity bits. Since the clock rate does not change when FEC parities are appended, the data throughput is decreased when FEC is used. The block code does not change the information bits. This allows ONUs which do not support FEC to coexist with ONUs supporting FEC coded frames. The parity bits will be ignored by ONUs with no FEC support [20] [3].

## 5.5 Multiple Point Control Protocol (MPCP)

The MPCP in the MPMC sub-layer uses multipoint control protocol data unit (MPCPDU) to perform ONU discovery and ranging functions. The MPCP also performs bandwidth arbitration mechanism for upstream medium access control among multiple ONUs. The MPCPDU has a fixed 64B frame size.

### 5.5.1 Ranging

All ONUs are synchronized to the OLT clock based on a loop-timing mechanism. The process of ranging measures the Round Trip Time (RTT) between an OLT and ONU. On the basis of this the OLT can properly divide the time slots granted to ONUs to avoid the upstream collision. It is realized by using GATE and REPORT control messages. The OLT sends a GATE message with time stamp  $T_0$ . The ONU receives the GATE message and responds with the REPORT message after some delay,  $T_R$ . The time stamp on the REPORT message  $T_1$  represents exactly  $T_0 + T_R$  because the ONU has precise loop timing obtained from the OLT. The OLT receives REPORT message at  $T_2$ , then OLT can use the information  $T_2 - T_1$  to determine the RTT [3]. The ranging process is shown in Figure 25.

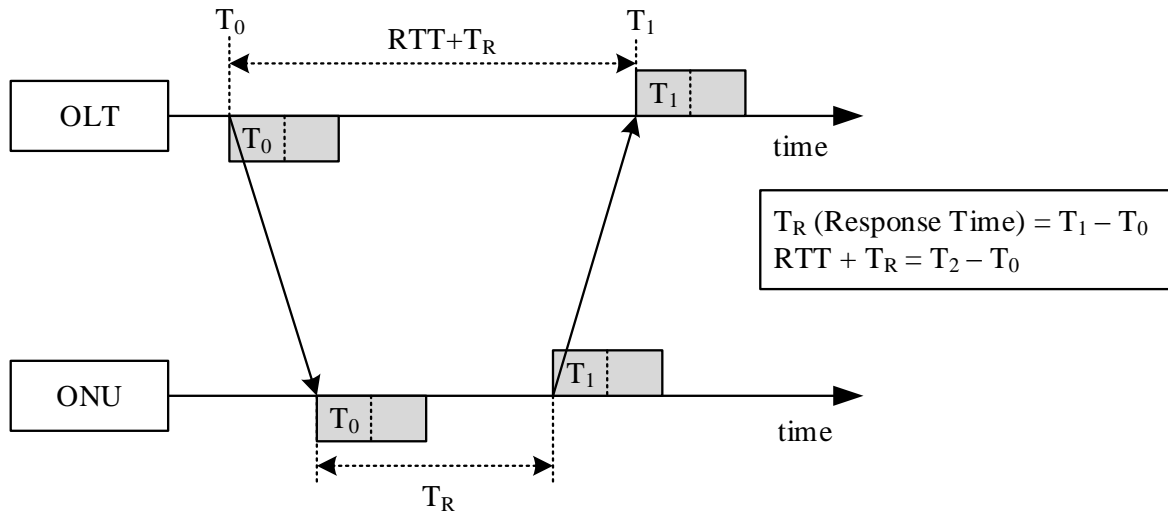


Figure 25: EPON ranging process [3]

### 5.5.2 Gate and Report Operation

By the Gate operation are specified the time slots when the ONUs can transmit. The operation specifies the start time and length of time slots in increments of 16 ns. In the Gate MPCPDU is included time stamp, the start time, and length of upstream transmission. Time stamp register, slot-start register- and slot-length register is updated until the ONU receives the Gate message [20]. EPON Gate operation is shown in Figure 26.



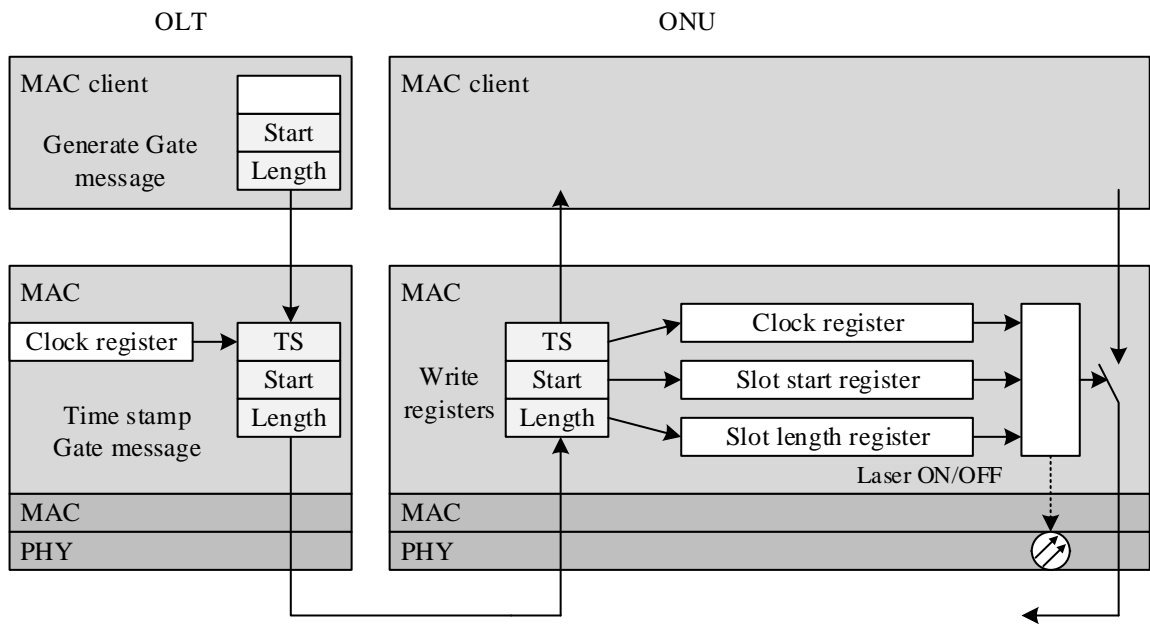


Figure 26: EPON Gate operation [20]

In the Report operation, an ONU informs the OLT with its queue lengths and provides the timing information to calculate RTT by sending the Report MPCPDU. Upon receiving the Report MPCPDU, the OLT updates ONU queue length registers and RTT register as shown in Figure 27.

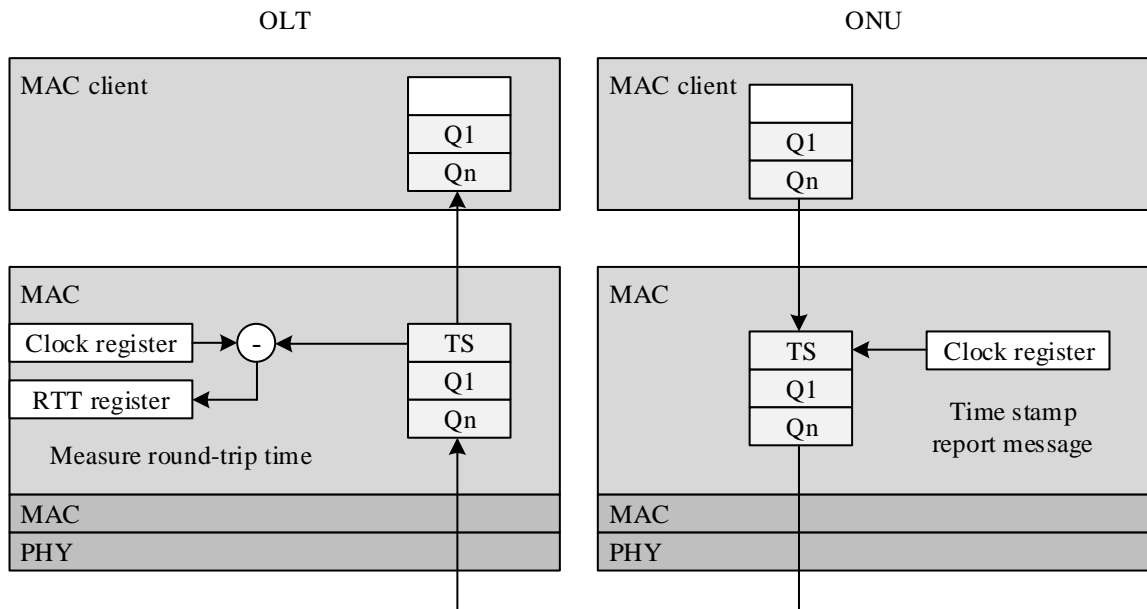


Figure 27: EPON Report operation [20]

### 5.5.3 Multiple Point Control Protocol Data Unit

MPCPDUs are 64-byte long MAC frames. To recognition of MPCPDU serves the length type field that includes MAC frame type 0x88-08. The 2-bytes long op-code field identifies the type of MPCPDU message. The possible control messages included in op-code are: GATE, REPORT, REGISTER\_REQUEST, REGISTER, and REGISTER\_ACK. For continuously update between the OLT and ONUs is in every MPCPDU message Time Stamp field. The data/pad portion of the MPCPDU contains the MAC parameters used in MPCP and the necessary zero padding to maintain the 64-byte frame size [20]. The generic format of MPCPDU is shown in Figure 28.

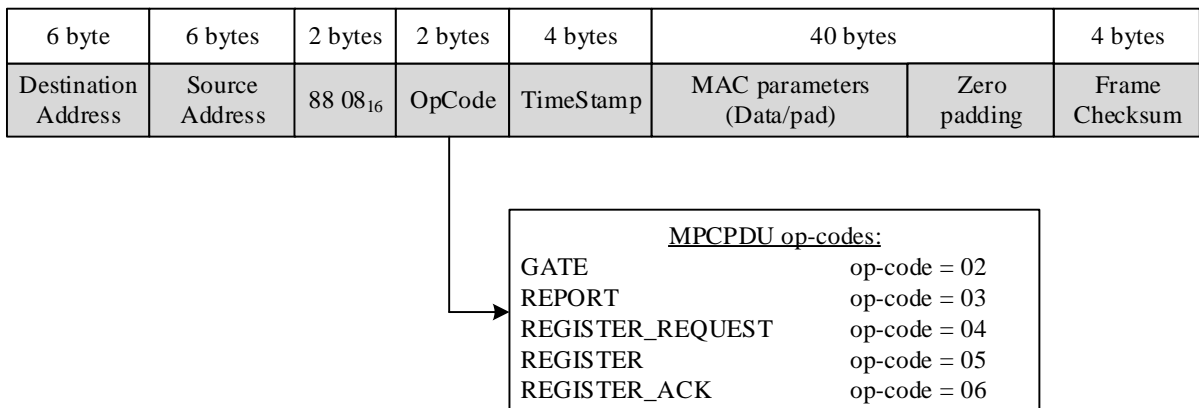


Figure 28: Generic format of MPCPDU [20]

### 5.5.4 Autodiscovery of EPON ONU

An EPON autodiscovery process allows an ONU to register and join or rejoin the system after powering up. The An EPON OLT broadcasts periodically to open up a discovery window for all initialized ONUs to respond. For point-to-point emulation the OLT allocates the virtual MAC and assigns LLIDs to ONUs.

During autodiscovery are exchanged capabilities such as synchronization time of the OLT burst mode receiver between OLT and ONU. Synchronization time is the time required by the OLT, after receiving a burst of data, to lock itself to the ONU transmitter clock and adjust its decision threshold to account for the differences in received power levels from different ONUs. The discovery Gate frames are periodically broadcasted by the OLT. This is when autodiscovery process starts. A reserved discovery window is granted by the discovery Gate. The burst mode synchronization time is also transmitted by the OLT within the discovery Gate. Based on synchronization time received from the OLT, ONUs know to consolidate the upstream signal with idle symbols during the initial burst synchronization time. An ONU after receiving the discovery Gate is waiting for a random delay. After that the ONU sends a Register Request. The

OLT after receiving the Register Request is able to allocate the ONU with the specific LLID. For the grant upstream time slot for the ONU, the OLT sends another Gate frame. The Gate frame contains newly allocated LLID. The last step is that ONU sends Register Acknowledgement frame, which represents the end of the registration process.

The random delay before an ONU sends the Register frame serves as a prevention before collisions, when several ONUs may attempt to register at the same time [20]. Autodiscovery process is illustrated in Figure 29.

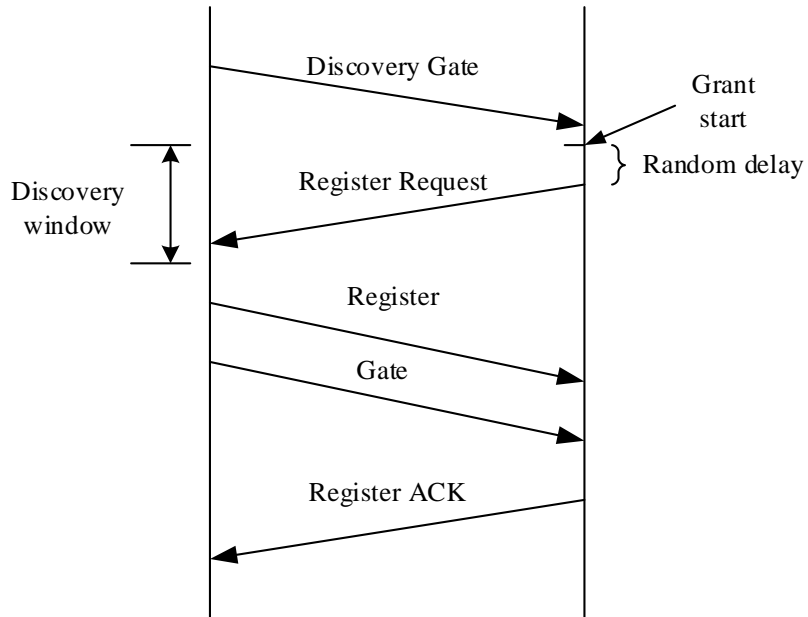


Figure 29: Autodiscovery process [20]

## 6 Hybrid xPON Networks

In present days, the hybrid xPON networks are not the first choice of the providers, but we can expect that in the near future they will want to exploit the potential of the optical fibers to maximum. The demand on the bandwidth is growing and it is a matter of time, when the providers decide to choose this option. At the moment, not so much literature is aimed to describe hybrid PON networks.

### 6.1 TDM-WDM PON

Hybrid TDM-WDM PON is a combination of TDM and WDM PON. The base principle is that the set of wavelength are shared over time by different ONUs. The wavelengths are not dedicated to one ONU as in case of WDM-PON. This architecture improves the efficiency of the network resources, and provides a more flexible and cost-effective access network. In case of pre-configured ONUs into a group to share wavelength, the network is called static WDM-TDM PON. In other case, when ONUs can be dynamically configured into a group to share a wavelength in responding to traffic load changes, the network is called hybrid WDM-TDM PON.

To create a dynamic hybrid WDM-TDM PON several issues have to be solved. Architecture of WDM-TDM PON should allow dynamic assignment of wavelengths to different ONUs. Receivers and transmitters have to be tuned to newly assigned wavelengths in time for packet sending and receiving. Also, traffic scheduling algorithms have to allocate wavelengths and also timeslots to the ONUs based on traffic condition and available resources, i.e., performing dynamic wavelength and bandwidth allocation. More about this issues is discussed in [21]. A TDM-WDM PON with capacity of 8192 ONUS, symmetric traffic of 320 Gbps and links of 135.1 km are described in [22].

In [23] is introduced hybrid PON network configurator, which simulates the TDM and WDM convergence, based on various specific network parameters. With this configurator can be calculated a total network capacity, average network capacity, and possible network extensions with adding WDM nodes.

### 6.2 OFDM-WDM PON

OFDM is a multiplexing scheme that offers a major spectral efficiency due to use of orthogonal frequencies for data transmission. The advantage of OFDM-WDM PON is it, that is more efficient due to the guard bands between channels are eliminated.

OFDM channel can be modulated by amplitude, phase, polarization and intensity. Depending on used modulation format can be obtained different reception schemes.

OFDM offers higher capacity for the optical fiber systems through a multiple variations for the implementation of optical OFDM. OFDM-PON is the simplest form to transmission of multiple dedicated optical sub-carriers over the PON. TDM-OFDMA PON provides multiple

access by sharing the sub-carriers as needed, where sub-carriers are allocated to different users in different time slots. OFDMA-WDM PON transmits sub-carriers over a dedicated wavelengths and offer the highest capacity for the future optical networks. In [24] is demonstrated record of 1.92 Tbps over 40 wavelengths and transmission capacity 48 Gbps per wavelength. Transmission speed was accomplished over 100 km and standard single mode fiber was used. The optical sub-carriers were separated by a 50 GHz band for the uplink and downlink. The used wavelength range for the both, downstream and upstream is 1532.29 – 1563.45 nm.

In [25] was demonstrated DWDM-OFDMA PON with symmetric 1.2 Tbps data rate over a standard single mode fiber with a 1:32 passive splitter. The presented system supports 800 connected ONUs.

### 6.3 OCDM-WDM PON

OCDM-WDM PON is a combination of the OCDM (Optical Code Division Multiplexing) and WDM over passive optical network. With using OCDMA each ONU has a code word to distinguish their optical transmission. Before transmission each bit has to be encoded by optical operation. OCDMA supports higher amount of users than TDMA and eliminates network overhead required for TDMA synchronization.

Experimental OCDMA-PON is described in [26] was introduced multi-port device encoder and decoder with ability to generate and process calculations with multiple codes on multiple wavelengths. A maximum achieved maximum speed is 2.56 Tbps over a 50 km fiber [27].

### 6.4 PON/xDSL

In [28] is introduced drop-point device, where is bridged PON and xDSL network. The drop-point device combines optical network unit and DSL access multiplexer. These drop-point devices uses a reverse power feed from a subscriber's power source and therefore consume as little power as possible.

## 7 Semiconductor Optical Amplifiers

The transmission distance of fiber-optic communication systems is mostly limited by fiber losses, which are caused by scattering and absorption mechanism in an optical fiber. To overcome fiber losses in long-haul systems are used optoelectronic repeaters, which firstly convert the signal into an electric current and subsequently regenerated signal is transmitted by laser. For wavelength-division multiplexed systems is using of repeaters complicated and expensive. An alternative is to use optical amplifiers, which amplifies the signal directly without any conversion. Thus optical amplifiers have become requisite components in high-performance optical communication links.

There are three fundamental types of optical amplifiers. The semiconductor optical amplifier (SOA), doped fiber amplifier (DFA), and Raman amplifier. SOA operates on the same principles as laser diodes. DFAs and Raman amplifiers uses the fiber as the gain mechanism. While the DFAs uses the fiber with special earth-dopants as amplification medium, a Raman amplifier makes use of the transmission fiber itself. Because the deployment of semiconductor optical amplifier is crucial in Master's thesis, this chapter is devoted to Semiconductor Optical Amplifier.

### 7.1 Principles of Amplification

SOA is very similar to a laser, but it has no reflecting facets. A typical long of amplifier chip is  $\sim 0.6$  to 2 mm. It consists of a p-cladding layer, a n-cladding layer and a gain region. The schematic drawing of semiconductor optical amplifier chip is show in Figure 30. The facets of amplifier have the anti-reflection coating to the maximum reduction of the reflections. The amplifier has a p-n junction which is forward biased during operation. The gain is produced by injection current in the gain region.

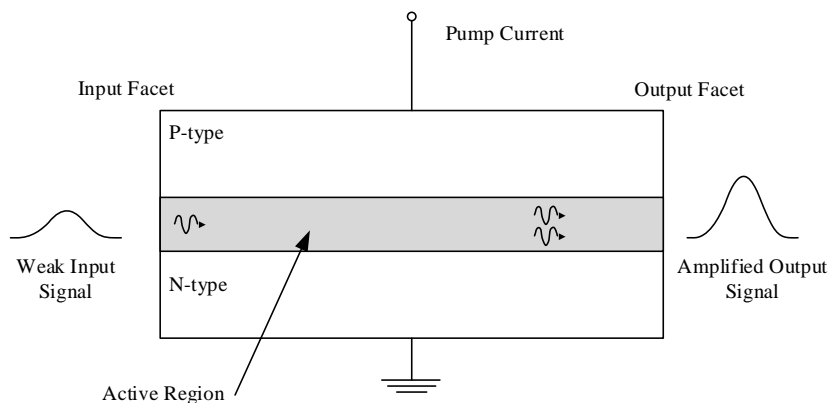


Figure 30: Schematic drawing of semiconductor optical amplifier [29]

### 7.1.1 Recombination Processes in Semiconductors

The holes in the p-cladding layer and the electrons in the n-cladding are the majority carries. An amplification is achieved by the emission of photons, whereby there have to occur the recombination of electron-hole pair. Electron-hole pair recombination occurs when excited electrons residing in the higher energy Conduction Band (CB) fall and in the process recombine with the holes that reside in the lower energy Valance Band (VB). During this process is released energy in the form of a photon. A typical two-level system of semiconductor material is shown in Figure 31. The higher energy band CB is represented as energy level  $E_2$  and the lower energy band CB is represented as energy level  $E_1$ . They are separated by an energy gap.

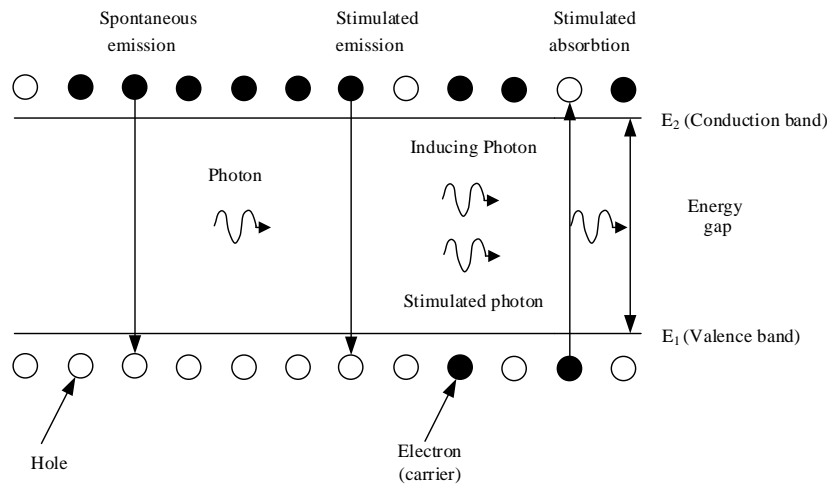


Figure 31: Two-level system of semiconductor material [29]

Current source injects into the SOA active region high energy electrons (also knowns as carries). The carries will move to occupy the CB whereby the holes are created in the VB. The result is the creation of electron-holes pairs. The transition of electrons between the CB and VB is defined by three fundamental processes: stimulated absorbption, stimulated emission, and spontaneous emission.

Stimulated absorption occurs when an incident photon with sufficient energy can stimulate a high-energy electron residing in the VB to move to the CB. This is a loss process because the incident photon is eliminated. The difference arises when a photon of suitable energy arrives. Such a photon can stimulate a carrier residing in the CB to recombine with a hole in the VB. The incident photon is not eliminated and continues through the active region. During this recombination, the carrier moving from the CB to the VB loses energy in the form of a coherent photon. That photon has the same phase, frequency and direction as the incident photon. The both photons, the incident and the stimulated one, will continue through the active medium to support more stimulated transitions. If there is enough of injected current to create population inversion, where the population of the carriers in the CB significantly exceeds that of the VB, the probability of the stimulated emission is much higher than the probability of the stimulated

absorption and that is manifested as optical gain of the SOA. In the case of absence of current (carriers and holes), the semiconductor would absorb the incident photons. A certain minimum number density of carriers are required to achieve optical gain or amplification.

However, the spontaneous emission also occurs in the gain medium of the SOA. The spontaneous emission occurs when the carrier from the CB spontaneously recombine with the hole in the VB. The result is a photon with random phase, frequency and direction. By this undesirable process is added noise to the amplified signal. Moreover, the population inversion is reduced, resulting in less optical gain. This process is known as amplified spontaneous emission (ASE) noise. This is a natural behaviour of semiconductors and it can not be avoided. The spontaneous emission is independent of the intensity of the inducing signal. Unfortunately, stimulated emission is dependent on the intensity of the incident light [31] [30].

A simplified energy vs. wave-vector band structure diagram of a direct-band-gap semiconductor is shown in Figure 32. Near the band edges, it obeys a parabolic band model of the type [32]:

$$E_{c(k)} = E_{c,min} + \frac{\hbar^2 k^2}{2m_c} \quad (6)$$

$$E_{v(k)} = E_{v,max} - \frac{\hbar^2 k^2}{2m_v} \quad (7)$$

where  $E_c$  is the energy of electrons in the CB and  $E_v$  is the energy of electrons in the VB.  $E_{c,min}$ ,  $m_c$  are the minimum energy and effective mass of the electrons in the CB and  $E_{v,max}$ ,  $m_v$  are the maximum energy and effective mass of the holes in the VB.  $k$  is the magnitude of the wave-vector, which is related to the carrier momentum  $p$  as  $k = p/\hbar$  and  $\hbar$  is the Planck's constant. When the minimum energy of the CB is situated at the same wave vector as the maximum energy of the VB, the semiconductor is classified as the direct-band-gap semiconductor [29].

## 7.2 Semiconductor Materials

The choice of materials for semiconductor optical amplifiers which will be used as the gain medium depends on probability of radiative recombination. The probability of radiative recombination has to be enough high to produce gain at low current. The "direct gap" semiconductors satisfies this condition. The several semiconductor material systems with their corresponding emission ranges are shown in Figure 33. The lines represents the range of band gaps that can be obtained by mixing of the constituting elements. The optical gain in semiconductor optical amplifiers occurs at the wavelengths close to the band gap. Therefore, to achieve optical gain at specified wavelength is necessary to use appropriate set of materials [31].



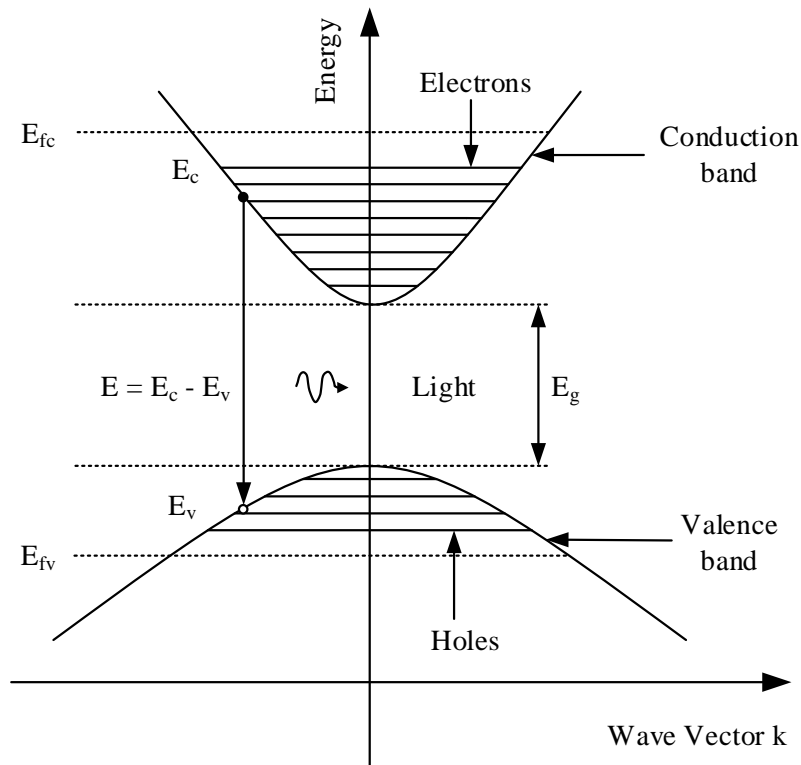


Figure 32: Simplified energy vs. wave-vector band structure diagram of a direct-band-gap semiconductor [29]

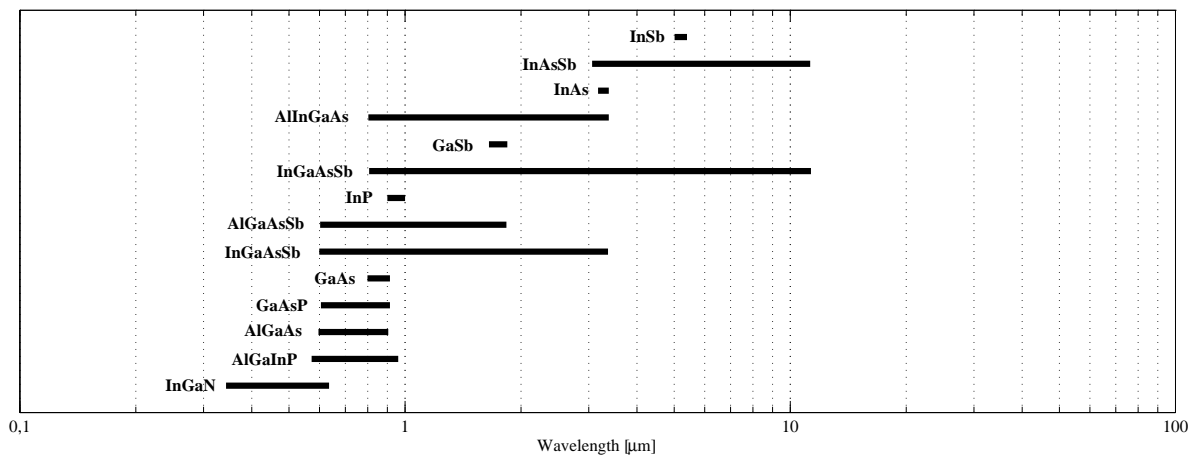


Figure 33: Semiconductor material systems [31]

### 7.3 Optical Gain

The gain of the optical amplifier depends on the wavelength of the incident signals and also on the local intensity of the signal. The gain medium may be modeled as homogeneously

broadened two-level system. Such a medium has the gain coefficient written as:

$$g(\omega) = \frac{g_0}{1 + (\omega - \omega_0)^2 T_2^2 + P/S} \quad (8)$$

where  $g_0$  is the maximum (peak) value of the gain,  $\omega$  is the optical frequency of the incident signal,  $\omega_0$  is the atomic transition frequency,  $P$  is the optical power of the signal being amplified, and  $P_S$  is the saturation power of the gain medium. The saturation power is dependent on the parameters of the gain medium such as radiative recombination time and transitions cross section. The  $T_2$  parameter means the dipole relaxation time with its typical values in the 0.1 to 1 ps range [31].

### 7.3.1 Gain Spectrum and Bandwidth

Following equation is valid for low powers (i.e.  $P/P_S \ll 1$ ), the gain coefficient is given by

$$g(\omega) = \frac{g_0}{1 + (\omega - \omega_0)^2 T_2^2}. \quad (9)$$

From the equation is resulting that the maximum gain is achieved when the incident frequency  $\omega = \omega_0$ . The gain spectrum spectrum is given by a Lorentzian profile that is characteristic of a two-level system. The gain bandwidth is specified as the full width at half maximum (FWHM) of the gain spectrum  $g(\omega)$ . For the spectrum of the gain bandwidth,  $\Delta\omega_g$  is given by  $\Delta\omega_g = 2/T_2$  or equivalently by  $\Delta v_g = \Delta\omega_g/2\pi = 1/\pi T_2$ , where  $\Delta v_g$  is the bandwidth of the gain spectrum.

The gain bandwidth is able to determine when the amplifier is a single element. The gain  $G$  is defined as

$$G = \frac{P_{out}}{P_{in}} \quad (10)$$

where  $P_{in}$  is the optical input and  $P_{out}$  is the optical output power of the amplifier. The gain is dependent on the length of amplifier medium [31].

### 7.3.2 Output Saturation Power

When the input signal power injected to the SOA is increased, or when amplified spontaneous emission increases with the gain, the carriers in the active region used for amplification are depleted, results in decrease of the gain. The output saturation power  $P_{sout}$  is defined as the output power at the point at which the gain is reduced by 3 dB (half of its unsaturated value, i.e. the value of  $P_{out}$  for which  $G=G_0/2$  [31], [?]). The  $P_{sout}$  is given by:

$$P_{sout} = \frac{G_0 \ln(2)}{G_0 - 2} \cdot P_S. \quad (11)$$

$P_S$  is larger than  $P_{sout}$ . For a typical SOA with gain 30 dB ( $G_0=1000$ ) is  $P_{sout}$  approximately  $0.69 \cdot P_S$ .

#### 7.4 Dielectric Waveguide

From previous sections we know that stimulated emission in a semiconductor optical amplifier is due to electron-hole recombination in the active region. The light created in the active region is bounded and leaded by a dielectric waveguide. A dielectric waveguide is formed by three layers: the p-cladding, the n-cladding, and the active region. The p- and n-type cladding have a bit lower refractive index than the active region. In the Figure 34 is shown the dielectric waveguide of the semiconductor amplifier. Also, in the figure is sketched the energy distribution of the essential mode of the waveguide.

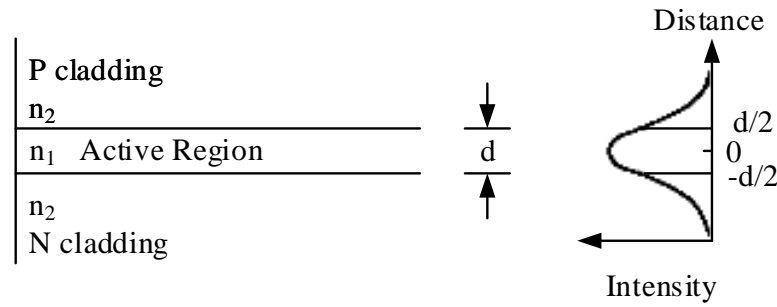


Figure 34: Dielectric waveguide of semiconductor [31]

#### 7.5 Amplifier Noise

An amplified signal is degraded due to additive noise. This is caused by undesirable process of spontaneous emission. The process of spontaneous emission adds fluctuations to the signal which adds noise to the detector photocurrent. The noise is defined in the optical and electronic domains by the noise figure  $F$ . The  $F$  is specified as the degradation of the signal-to-noise ratio (SNR) of the electrical power generated when the signal is converted to current by a photodetector. Noise figure is defined as

$$F = \frac{(SNR)_{in}}{(SNR)_{out}} \quad (12)$$

where SNR refers to the signal-to-noise ratio of the electrical power generated by photodetector

in process of converting the optical signal to the current. The photodetector SNR is assigned to the two types of noises: the thermal noise and the shot noise [31].

## 7.6 Types of SOAs

We distinguish the three main types of semiconductor optical amplifiers: Fabry-Perot (FP-SOA), travelling wave (TW-SOA), and R-SOA. In FP-SOA, the signal reflects between the input and output faces, thereby the signal makes many passes through the amplifier. The facets are partially reflective end mirrors. The reflectivity of these facets is about 32%. An optical signal in the cavity of amplifier, reflects between facets until it is emitted at a higher intensity. Fabrication of FP-SOA is simple, but the optical gain is very sensitive to variations in amplifier temperature and input optical frequency. Thus, very precise temperature stabilization and injection current stabilization is required.

Traveling-wave amplifier has the same structure as an FP-SOA except that the TW-SOA facets are anti-reflection coated to avoid the internal reflection. The optical signal is amplified only once during the single pass through the TW-SOA. Using of these types of amplifiers is more often than the FP-SOAs because of their large optical bandwidth, high saturation power, and low polarization sensitivity. TW-SOAs is choice for networking application [34]. Schematic of FP-SOA and TW-SOA is shown in Figure 35. Also, the gain spectrum of both types is illustrated [35].

The R-SOAs have a high reflective coating on one facet and an ultra low reflectivity coating on the other. Input facet is angled and the gain region is curved close to the centre of the chip. To reduce facet reflectivity and improve coupling, the device output far field is reduced through the linear tapering of the active region [36].

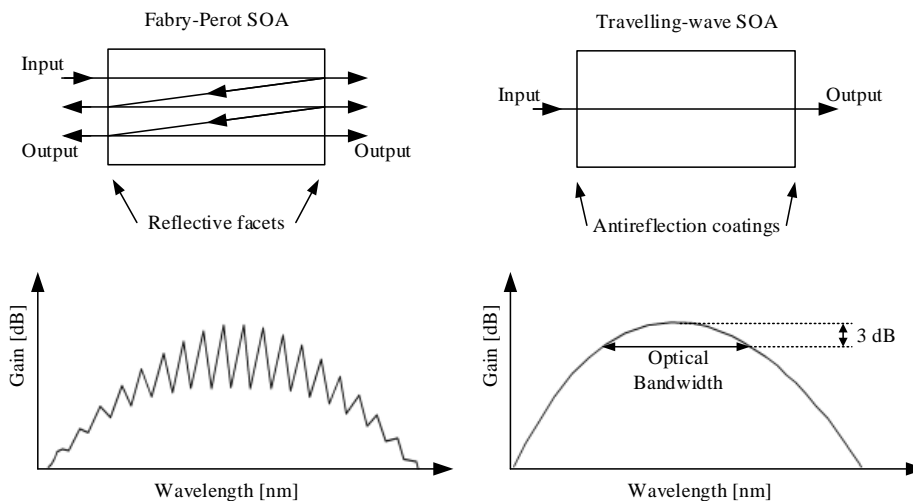


Figure 35: TW-SOA and FP-SOA [35]

## 7.7 Applications

Semiconductor optical amplifiers have a wide enforcement in the field of optical telecommunications. The deployment is possible in the access, core and metropolitan networks. They are useful for all-optical signal processing task at very high bit rates that cannot be handled by electronics. Their applications include a wavelength conversion for all optical networks, signal regeneration, optical demultiplexing, optical switching, and other applications such as clock recovery for optical time division multiplexed (OTDM) transmission. To implement these processes are used nonlinearities. Four-wave mixing (FWM), cross gain modulation (XGM), and cross phase modulation.

### 7.7.1 Four Wave Mixing

Four Wave mixing is a process where interaction of two waves with high power at frequencies  $\omega_1$  and  $\omega_2$  produce a downshifted (Stokes) wave at frequency  $\omega_3$  and an upshifted (anti-Stokes) wave at frequency  $\omega_4$ . The frequencies have equal spacing, that is,  $\omega_1 - \omega_3 = \omega_2 - \omega_1 = \omega_4 - \omega_2$ . Frequency diagram for four-wave mixing is shown in Figure 36.

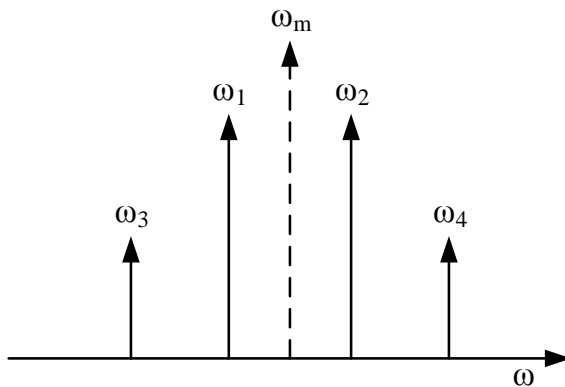


Figure 36: Four Wave Mixing

In SOAs is FWM used for wavelength conversion due to good efficiency of conversion and high speed response for wavelength division multiplexing (WDM) networks [31]. Two copolarized waves are injected into the SOA, referred as pump and probe beams. The pump wave with frequency  $\omega_p$  has typically higher power than the probe signal with frequency  $\omega_q$ . The pump and probe signals are mixed inside the SOA. Propagation through the SOA results in the generation of two additional signals with frequencies  $\omega_{cs} = 2\omega_p - \omega_q$  and  $\omega_{cs'} = 2\omega_q - \omega_{1p}$ . The signal at frequency  $\omega_{cs}$  has higher power if the power of the pump signal is higher than the power of the probe signal. The intensity at frequencies  $\omega_{cs}$  and  $\omega_{cs'}$  is measured using a spectrometer. If  $I_p$  and  $I_q$  are the signal intensities at frequencies  $\omega_p$  and  $\omega_q$ , the intensities of the signals at frequencies  $\omega_{cs}$  and  $\omega_{cs'}$  are proportional to  $I_p^2 I_q$  and  $I_p I_q^2$  respectively. Schematic configuration for single-pump FWM is shown in Figure 37.

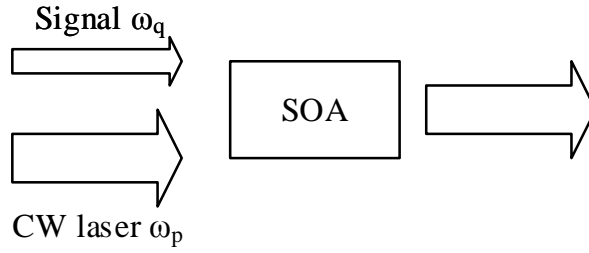


Figure 37: Schematic configuration for single-pump FWM [37]

### 7.7.2 Cross Gain Modulation

Cross gain modulation (XGM) is caused by saturation gain in SOA. A pump and probe waves on different wavelength are injected into SOA. When operated under gain saturation conditions, the optical gain is divided between the two signals and depends on their relative photon densities. If the pump power level changes, the probe power level changes inversely against the power level of the pump signal. This is resulting to data transfer to another wavelength. When the pump power level is modulated with data, the probe gain is also modulated, so the probe output power is modulated. Thus the data are transferred from pump to probe. This results in wavelength conversion [31].

### 7.7.3 Cross Phase Modulation

The cross phase modulation (XPM) uses interferometer configuration to convert the phase modulation to an amplitude modulation. This configuration is used for wavelength conversion, optical demultiplexing, optical switching, and for clock recovery. The efficiency and signal to noise ratio in this configuration is high[31].The schematic of the Mach-Zehnder Interferometer using SOA is shown in Figure 38 To upper arm of the interferometer structure is injected the input signal beam and the control signal is injected into the lower arm. The continuous signal is coupled through the each of interferometer arms. A phase shift in the data signal and control signal is caused by the continuous signal. In the upper arm of interferometer is a  $\pi$  phase shift according to the strength of the signal. These signals are then aggregated and interfered at an output junction [38].

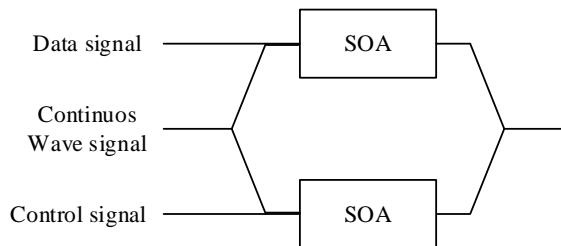


Figure 38: Schematic configuration for single-pump FWM [38]

## 8 Used Devices and Components

For build up and test a hybrid access network, several fundamental components and measurement devices were used. This chapter is aimed to short introduce a most of them.

### 8.1 Network Components

#### 8.1.1 MiniMAP 9102

MiniMAP 9102 is an integrated Multiservice Access Platform made by Allied Telesis. It provides a broad range of access technologies such as Ethernet, xDSL, FTTH, CES, EPON and many more.

The platform used to our needs contains 4 pluggable modules: ADSL24B-ADSL, FX20BX-20, and EPON2. The fourth, CFC12, is a control module. In our case the EPON2 card serves as a Optical Line Termination (OLT) of the EPON. The EPON 2 card has two ports for SFP modules. Used SFP module is FTM-9712S-SL20 with following parameters (see Table 8):

Table 8: Properties of the SFP module

Transmitter			Receiver		
Wavelength range [nm]	1480 - 1500		Wavelength range [nm]	1260 - 1360	
Optical Power [dBm]	Max.	2	Detector sensitivity [dBm]	Max.	-10
	Min.	-30		Min.	-30

##### 8.1.1.1 MiniMAP configuration

To configure the OLT unit was used reduction from RJ-45 ethernet connector to USB connector. This USB was connected to console port of the OLT. To access CLI of the EPON was used PuTTY terminal emulator. Following parameters was set to access:

- Serial line to connect: COM3
- Speed: 9600 baud
- Data bits:8
- Stop bits: 1
- Parity: None
- Flow control: XON/XOFF

After accessing to the CLI, verification was required. The login was „officer“ and the same was password. After verification was necessary to register the ONU units. This was obtained by command: `create onu <onu name> onuid <1-15> interface=2.0 MAC=<ONU MAC address>`

With command <show onu> is able to achieve states of actually registered ONUs, their IDs, and MAC addresses. The list of this command is shown in Figure 39

```
officer SEC>> sh onu

--- ONU Interfaces ---

Interface      State EPON  ID MAC Address
-----
ONU1           UP-DN  2.0 1  00:15:77:43:98:68
ONU2           UP-DN  2.0 2  00:15:77:43:A5:60
ONU3           UP-UP  2.0 3  00:15:77:43:A5:50
ONU4           UP-DN  2.0 4  00:15:77:43:A5:58
ONU5           UP-DN  2.0 5  00:A5:77:43:98:58
```

Figure 39: Listing of command <show onu>

### 8.1.2 AT ON-1000

AT ON-1000 is an Optical Network Unit (ONU) of the EPON network. The ONU has two ports: 1 Gbps optical WAN port and 10/100/1000 Mbps LAN port. The parameters of optical port are shown in Table 9.

Table 9: Properties of ONU unit

Transmitter			Receiver		
Wavelength [nm]	1310		Wavelength [nm]	1490	
Optical Power [dBm]	Max.	4	Detector sensitivity [dBm]	Max.	-3
	Min.	1		Min.	-26

### 8.1.3 ZyXEL IES-1000

IES-1000 is an IP-base multi-service access node. It has two slots for various combinations of DSL and VoIP line cards to provide ADSL2+ and VoIP services to customers. IP DSLAM technology significantly makes easier conversion between data formats, solves troubles with network overloading by introduction of high-speed Ethernet switching. The DSLAM used to testing hybrid access network has ADSL2+ module with 12 ports. This module supports data rates from 128 kbps to 24 Mbps with maximum distance 6 km.

#### 8.1.3.1 Configuration

Because the DSLAM was configured as switch, no difficult configuration was required. The DSLAM works with IP addresses 10.0.0.0/8, so the only condition is that devices to test have to be within this subnet. To configure ADSL links was used web configuration interface. The Figure 40 shows the setup to add a profile. Then Figure 41 shows assignment the profile to port.



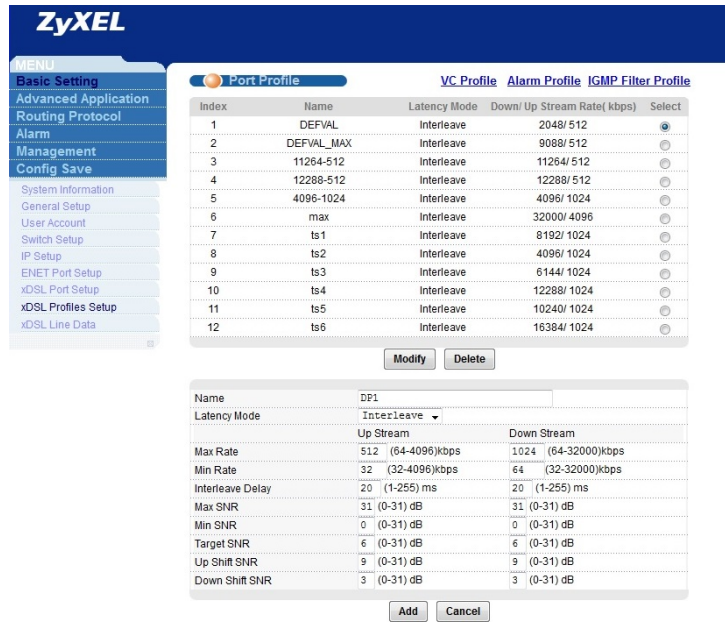


Figure 40: Adding the profile

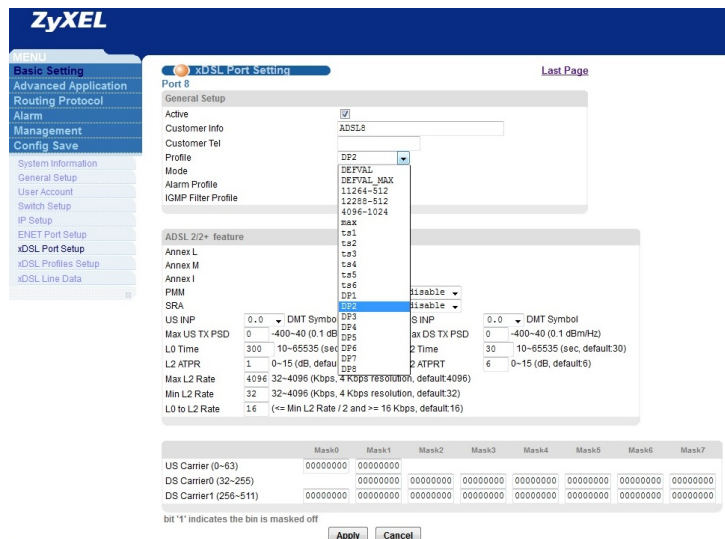


Figure 41: Assignment of profile to port

### 8.1.4 ZyXEL IES-5005

The IES-5005 is a chassis-based system that facilitates Telco/ISP delivering high degree of quality of experience to today's demanding residential and business customers, and achieving its infrastructure provisioning criteria of reliability, flexibility and scalability. The IES-5005 is equipped with the VLC1224G-41 VDSL line card.

#### **8.1.4.1 VLC1224G-41 VDSL2 line card**

The VDSL2 line card contains 24 ports with the maximum transmission rate up to 65 Mbps/35 Mbps. The line card supports VDSL2 profiles 8a, 8b, 8c, 8d, and 12a. The line card also supports frequency allocation band-plan 998 and 997.

#### **8.1.5 ZyXEL Prestige 660RU-T3 ADSL2+ modem**

ZyXEL Prestige 660RU-T3 is an ADSL router. It supports ADSL, ADSL2, and ADSL2+ standards with maximum downstream rate 24 Mbps. Web configuration interface is included.

#### **8.1.6 ZyXEL P-870MH VDSL2 Modem**

ZyXEL P-870MH is a VDSL2 modem, which supports downstream rates up to 65 Mbps and upstream rate up to 35 Mbps. Also supports frequency band plans 997 and 998. The modem is equipped with one VDSL RJ-11 or RJ-45 port and 4 LAN ports.

## **8.2 Measurement Devices**

### **8.2.1 EXFO FTB-1/FTB-860 Net Blazer**

Net Blazer is a compact device which supports complete network verification. It offers network testing through standards RFC2544 and ITU-T Y.156 (EtherSAM), BERT test, multi-stream traffic generation and others. Net Blazer is equipped with two Ethernet ports 10/100/1000 BASE-TX and two SFP ports 100/1000 BASE-FX. The RFC2544 and EtherSAM ITU-T Y.1564 tests were performed with this device.

#### **8.2.1.1 Configuration**

The device was used for two tests. In first case was connected to iMAP port 4.0 and served as remote unit to execute RFC2544 Dual Test. In second case was connected to DSL modems to execute EtherSAM tests.

RFC2544 Dual Test configuration:

- Interface:
  - Electrical
- Network:
  - DHCP: Disabled
  - IP address: 10.0.0.17
  - Subnet Mask: 255.0.0.0
  - Default Gateway: Disabled

- RFC2544
  - Dual Test: Local

Loopback configuration:

- Interface:
  - Electrical
- Network:
  - DHCP: Disabled
  - IP address: 10.0.0.17
  - Subnet Mask: 255.0.0.0
  - Default Gateway: Disabled

### 8.2.2 EXFO FTB-500

FTB-500 is an universal platform which supports broad range of modules from OTDR module to 100G Multiservice Test Module.

For measurements were used modules:

- FTB-5240B (Optical Spectrum Analyzer)
  - Wavelength spectrum range: 1250 - 1650 nm,
  - Dynamic range: -80 - +23 dBm
  - Resolution Bandwidth: 0.033 nm
- FTB-7200D (Optical Time Domain Reflectometer) ,
  - Measurements of optical fibers are performed at wavelengths 850 nm and 1300 nm for multimode fibers, 1310 and 1550 nm for single-mode fibers
  - Dynamic range: 27 dB for multi-mode fibers and 36 dB for single-mode fibers
  - Identifying dead zone: 1m
- FTB-5500B (Polarization Mode Dispersion Analyzer)
  - Wavelength range: 1260 - 1675 nm
  - Responsivity: -45 dBm
- FTB-5800B (Chromatic Dispersion Analyzer)
  - Wavelength range: 1530 - 1625 nm, 1200 - 1700 nm
  - Dynamic range: - 42 dB
  - Accuracy: 0.1 nm

### **8.2.3 FLS-5800A**

FLS-5800A is a high power, wideband LED source for chromatic (CD) and polarization mode (PMD) dispersion measurement. FLS-5800A is often used in configuration with FTB-5500B and FTB-5800B modules. In this configuration was also used to measurement of chromatic and polarization mode dispersion.

### **8.2.4 EXFO PPM-350B-EG**

PPM-350B-EG is device for measurement optical power in EPON and GPON networks. It contains two optical ports: OLT and ONT. With these two ports is able to measure both, downstream and upstream optical power at the same time. Measured wavelengths are: 1310 nm, 1490 nm, and 1550 nm.

### **8.2.5 EXFO AXS-200/350**

AXS-200/350 is an optical loss test set (OLTS). The OLTS is the ideal tool for network-link characterization. The OLTS supports measurements at wavelengths 1310 and 1550 nm for singlemode and 850, 1300 nm for multimode. It contains the Ge photodetector with dynamic range 26 dBm.

### **8.2.6 Yenista Tunics-T100S-HP/O**

Yenista Tunics-T100S-HP/O is a high power tunable laser source. Output peak power is more than +13 dBm. The wavelength spectrum range is from 1260 to 1360 nm. Absolute wavelength accuracy is +- 30 pm and tuning speed speed is 1 s (100 nm). Spectral width (FWHM) for this tunable laser is more than 100 MHz.

### **8.2.7 Yenista OSA20**

OSA20 is an spectrum analyzer manufactured by Yenista Optics. It provides high performance spectrum measurements and it is the fastest diffraction-grating based instrument operating from 1250 to 1700 nm. A maximum sweep speed is 2000 nm/s. A fixed sampling resolution is 2 pm for all scans. Absolute wavelength accuracy is +- 25 pm over 1250-1700 nm. OSA20 also supports measurements in burst mode. The burst sensitivity as adapted to burst signal and dedicated to GPON measurements.

### **8.2.8 VeEX VePAL BX100V**

VePAL BX100V is an industry's tester which can serve as ADSL2+ modem emulator. It is able to pre-qualify broadband links. This device displays link-up results: upstream/downstream data rates, noise margin, latency, attenuation, training time. It also displays graphical and tabular representation of bits per tone.

### 8.2.9 Lini-T UT70A

Digital multimeter which provides measurements of following articles: DC voltage, AC voltage, DC current, AC current, Resistance, Capacitance, Inductance, and Temperature.

## 8.3 Passive Components

### 8.3.1 Wavelength Splitters

In builded topologies were used wavelength splitters (also called WDM splitters) to split the optical signal according to wavelength. The used WDM splitters splits the wavelength bands S, C, and L (1460 – 1620 nm) to one branch and the O wavelength band (1260 – 1360 nm) to other branch. Figure 42 shows the wavelength division of used WDM splitter.

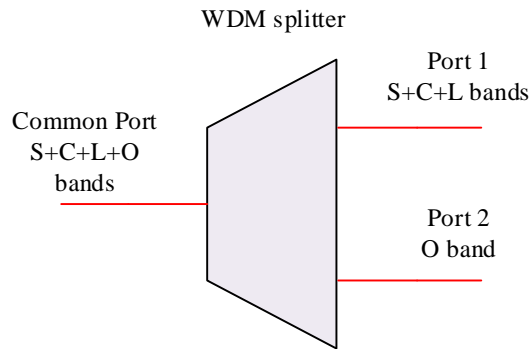


Figure 42: WDM splitter wavelength division

In topologies were used 2 pieces of these WDM splitters. Table 10 shows the insertion loss between the common port and the ports 1 and 2. The values of insertion loss are obtained from the datasheets.

Table 10: Insertion loss of WDM splitter

Port	Insertion Loss [dB]	
	Splitter 1	Splitter 2
1	0,53	0,44
2	0,69	0,58

## 9 Laboratory Interconnection

First step to build up hybrid xPON/xDSL network was interconnection between the laboratories EB316 and EB315, EB215, and EB211 situated in the building of Faculty of Electrical Engineering and Computer Science. The devices and components included in the laboratories are shown in following list:

- EB316 - EPON Optical Line Termination and all optical fiber components
- EB315 - Long optical fiber traces.
- EB215 - ADSL DSLAM, VDSL DSLAM, modems.
- EB211 - ADSL DSLAM, wireline simulator, modems.

For the interconnection was used optical cable with the 24 optical fibers and two UTP cables. The optical fibers within the cable are the ITU-T G.652.D single mode fibers. The drawing of the realized connections is a part of the Appendix A and B.

The interconnection consisted from following parts:

- Splicing the ends of optical fibers to Splice-Ready fiber connectors.
- Storage to the optical patch panel
- Optical Fiber Loss measurements.

Fiber loss measurements were accomplished by the Optical Time Domain Reflectometer (OTDR) method and insertion loss testing with the three reference cables (i.e., method C). The principle of method C is shown in Figure 43, then the schematic of OTDR measurement is shown in Figure 44. Firstly, reference has to be done with a short optical fiber. After that is the short reference optical fiber removed and replaced with a measured optical fiber.

There was connected only eight fibers from the total amount of 24. It is a sufficient amount of fibers for these purposes, the rest of fibers can be used in the future. Each of these fibers were tested from the both sides with the both methods. The method C was used five times per fiber to perform measurement. Table11 shows measured attenuation of fiber 1 between the laboratories EB316 and EB211. Figure 45 shows the output from the OTDR at wavelength 1310 nm from the laboratory EB316 to the EB211. The all measured values from method C and outputs from the OTDR are attached on the DVD.

Launch fiber is represented from the beginning to the event No.2. The length of the launch fiber is 236 meters. Event No.2 represents connection between the launch fiber and measured fiber. Because of use angled-polished connector with high return loss, no backscatter is visible. However, the attenuation of this connection event is 0.826 dB. The measured fiber between events No.2 and No.3 is 75 meters long with attenuation 0.104 dB.

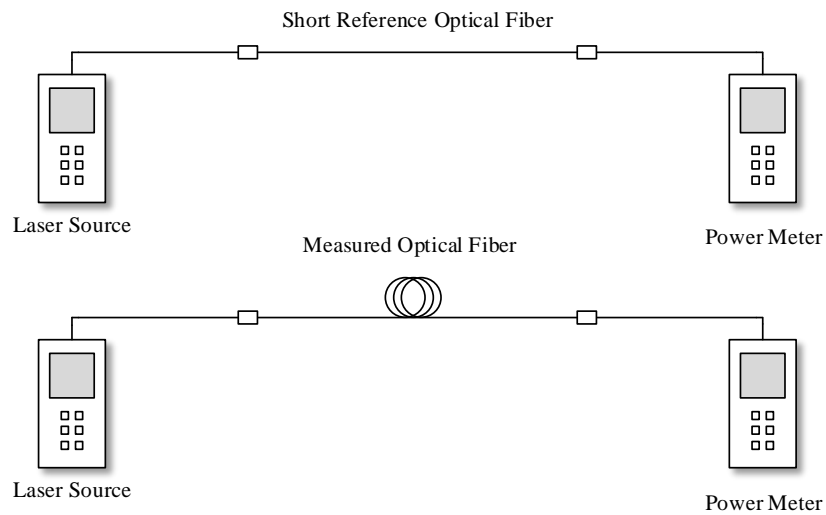


Figure 43: Topology for method C measurement



Figure 44: Topology for OTDR measurement

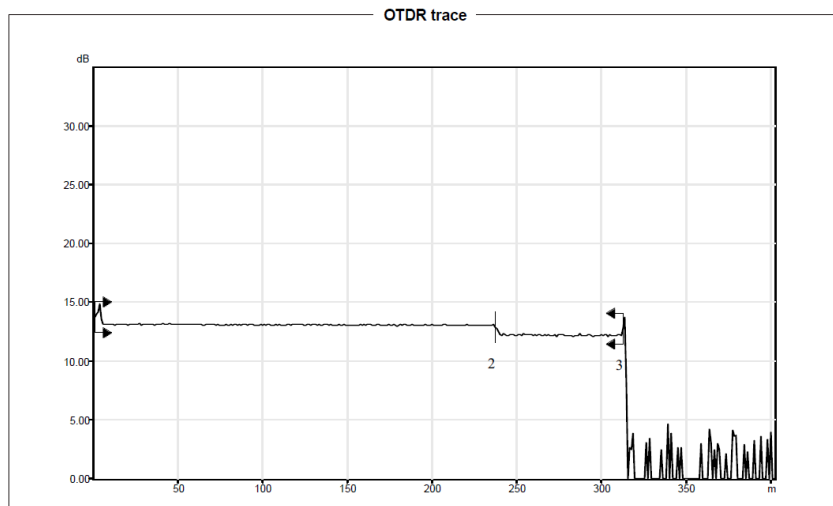


Figure 45: Reflectogram of measured optical trace EB316 -> EB211;  $\lambda = 1310$  nm

For better imagination are values from table shown in Figure 46. Is obvious that the fiber has higher attenuation at wavelength 1310 nm than at the 1550 nm. It is caused by the spectral attenuation, where the higher number of OH-ions is at wavelength of 1310 nm than at the 1550 nm.

Table 11: Measured insertion loss on fiber 1 EB316 → EB211

Fiber 1		
Measurement	$\lambda$ [nm]	
	1310	1550
	IL [dB]	
1	0,76	0,61
2	0,77	0,63
3	0,78	0,62
4	0,89	0,64
5	0,88	0,64
Average	0,816	0,628

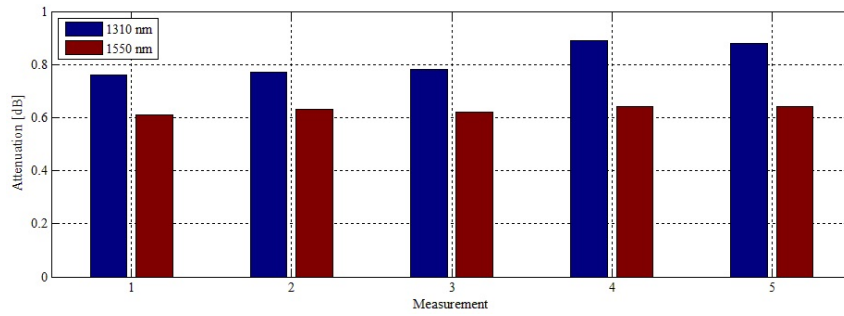


Figure 46: Graphic representation of measured insertion loss



## 10 Building up Hybrid Access Network

Hybrid access network consists of two general parts: the EPON network and consecutive connection with ADSL2+ or VDSL2 technology. First step was to test each of these technologies independently. Both technologies were tested to find out the maximum distance that they are able to overcome. In case of the EPON network, measurements of the whole optical traces used in hybrid network were accomplished. These measurements involves measurements of the optical losses, polarization mode dispersion, and chromatic dispersion. Also, the spectral analysis of the EPON network with deployment of semiconductor optical amplifiers was done. On the metallic lines were executed basic measurements of the resistance and the capacitance to calculate approximate attenuation.

### 10.1 Optical Fiber Traces

### 10.2 Optical Fiber Loss Measurement

Measurements of optical losses were executed the same way as in previous chapter with using the Optical time domain reflectometer (EXFO FTB-7200D) and the method C (EXFO FTB 200/350). The used optical fiber is G.562A. Optical traces are put together with optical fibers with a length of about 5 kilometers. These optical traces are placed in server room, the ends of fibers are placed in optical patch panel in the laboratory EB215. For our purposes, these optical traces were interconnected with the laboratory EB316 through the interconnections mentioned in previous section. Table 12 shows the measured attenuation of the optical traces. These values were measured by method C and the lengths of the traces are obtained from the OTDR. The figure 47 shows the output of the OTDR (wavelength 1310 nm) where the length of optical trace is 15.03 km.

Table 12: Measured insertion loss of optical traces

l [km]	$\lambda$ [nm]			
	1310		1550	
	IL [dB]	$\alpha$ [dB/km]	IL [dB]	$\alpha$ [dB/km]
5,04	3,09	0,61	2,54	0,50
9,76	5,65	0,58	5,28	0,54
15,03	7,38	0,49	8,02	0,53
19,81	10,58	0,53	7,27	0,37

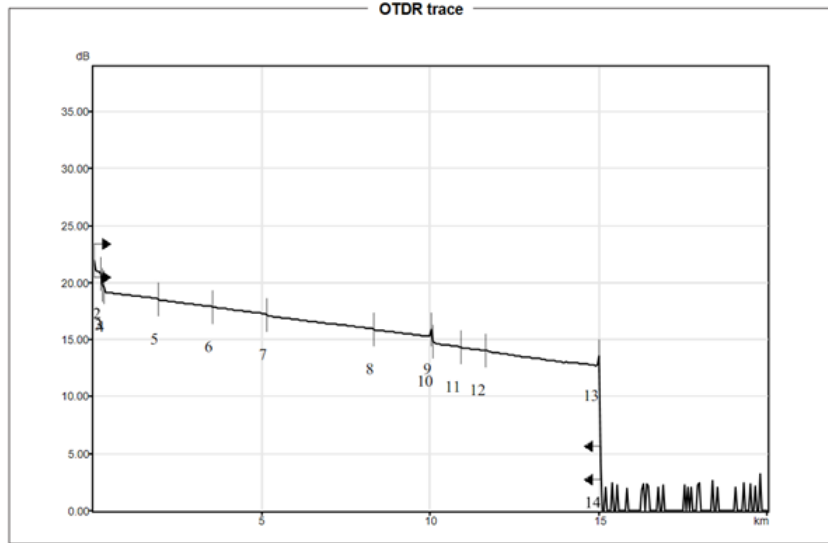


Figure 47: Reflectogram of measured optical trace = 15.03 km

From figure can be seen several attenuation and reflective events. Events No.2, No.3, and No.4 are linked with the launch fiber at the beginning to eliminate dead zone. Events No.5, No.6, No.7, No.8, No.11, No.12 are splices of fibers. Events No.9, and No.10 represents connector reflectance and connector loss. Event No.13 is connector reflectance at the end of fiber. Overall attenuation of measured fiber is 8.437 dB. All of the OTDR outputs are attached on the DVD.

### 10.2.1 Splitter Insertion Loss Measurement

To obtain attenuation of the splitter 1:2 was used method C. Two branches have a split ratio 90:10, where the 90% of the optical power travels to one branch and the 10% of the optical power travels to the second one. The Figure 48 shows the topology for insertion loss measurements, where both devices, power meter and laser source is the same device (AXS-200/350). Table 13 shows the average values of the attenuation between the individual ports.

Table 13: Measured insertion loss between the branches

$\lambda$ [nm]	Insertion Loss [dB]			
	Splitter 1		Splitter 2	
	1 ->2	1 ->3	1 ->2	1 ->3
1310	0,88	10,50	0,82	10,73
1550	0,99	10,51	0,89	10,62

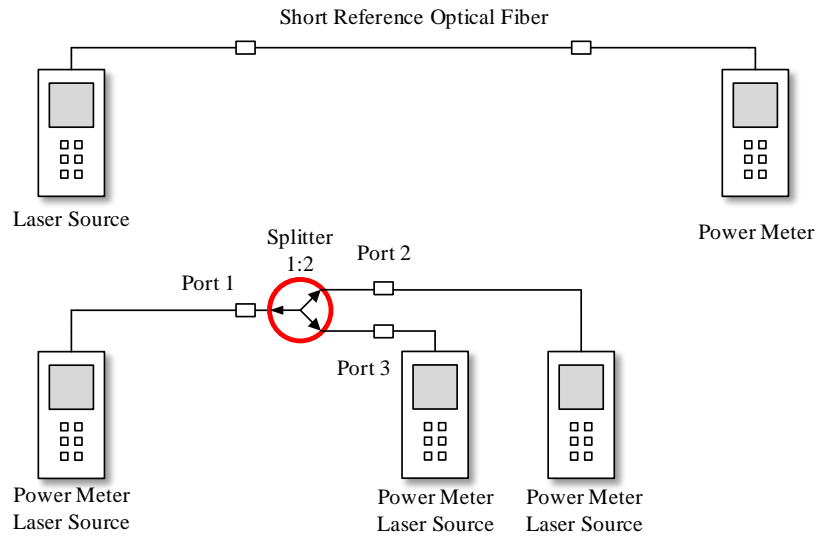


Figure 48: Topology to measure insertion loss of optical splitters

### 10.2.2 Polarization-Mode Dispersion Measurement

Polarization-mode dispersion is an undesirable effect that spreads pulse of the optical signal. PMD is caused by the birefringence of the fiber. There are two kinds of the birefringence: material and waveguide. Material birefringence is caused due to stress on the fiber. Waveguide birefringence is caused by geometrical variations in the fiber. The magnitude of PMD in a fiber is expressed as differential group delay (DGD), delay between the electric field vector and the magnetic field vector of the light. Then the PMD coefficient is an average of the DGD [39].

The PMD was measured at the optical traces mentioned above. For measurement were used the PMD module (FTB-5500B) and the wideband light source (FLS-5800A). The topology for PMD measurement is shown in Figure 49.

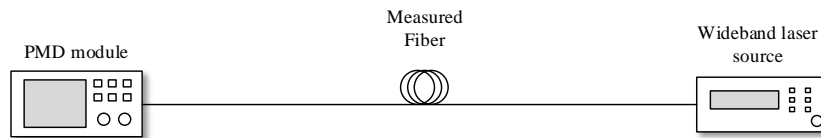


Figure 49: Topology for PMD measurement

For every single optical trace has to be set the length of fiber. The lengths were obtained from the OTDR reports. Table 14 shows the PMD coefficient and DGD of each optical trace.

From table can be seen that values of the PMD coefficient are mostly high. This is because the fibers are about 20 years old and it is possible that are under the stress. Also the large number of splices on the measured fiber is a significant factor for PMD. The guaranteed maximum

Table 14: Measured PMD coefficients and Differential Group Delay

length [km]	PMD coefficient [ps/km <sup>1/2</sup> ]	DGD [ps]
5.04	0.6352	1.426
9.76	0.1047	0.327
15.03	0.7073	2.742
19.81	0.9312	4.145

value (for the most of standard fibers) for PMD is 0.5 ps/km<sup>1/2</sup>. It can be quite limiting for high data-rate systems (more than 10 Gbps) and for multiple wavelength systems. In this case is not limiting, because the EPON uses only two wavelengths with maximum data-rate 1.25 Gbps. The Figure 50 shows the interferogram from the PMD analyzer for the fiber length of 15.03 km. All reports from measurements are attached on the DVD.

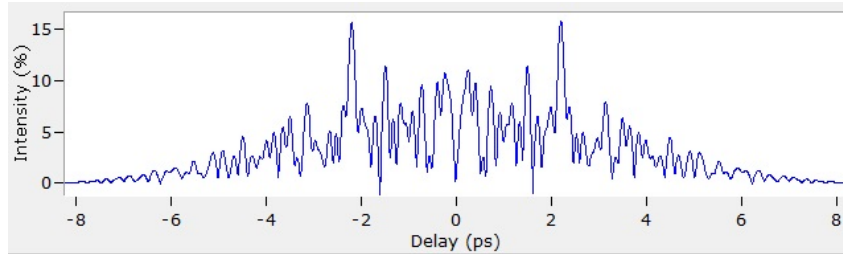


Figure 50: Interferogram from PMD analyzer

### 10.2.3 Chromatic Dispersion Measurement

Chromatic dispersion (CD) is the spreading of a light pulse in an optical fibre caused by different the group velocities of the different wavelengths composing the source spectrum. Group delay is the time required for a light pulse to travel a unit length of fiber. The group delay is expressed in ps/km and it is a function of wavelength marked as  $\tau(\lambda)$ . Chromatic dispersion coefficient is the change of the group delay of a light pulse for a unit fiber length caused by a unit wavelength change. The chromatic dispersion coefficient is given by equation [40] :

$$D(\lambda) = \frac{d\tau(\lambda)}{d(\lambda)} [ps/(nm \cdot km)]. \quad (13)$$

The chromatic dispersion consists of two components: waveguide dispersion and material dispersion. The waveguide dispersion is dependent on the core radius and the index difference in fiber. The material dispersion is the dominant contribution. It occurs because of refractive index of silica changes with the wavelength. The CD was also measured at optical traces mentioned above. The topology for CD measurement is the same as with the PMD measurement except the used module was CD (FTB-5800B). The wideband source is the same. The topology for CD

measurement is shown in Figure 51. This measurement of the CD is a phase shift method, and this method is recommended as reference method to chromatic dispersion measurement.

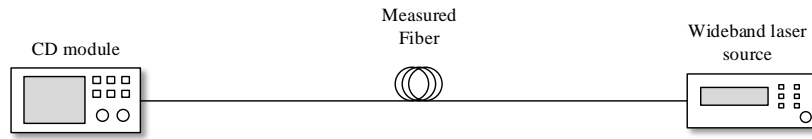


Figure 51: Topology for CD measurement

As in PMD measurement, the length of the fiber had to be set. The Figure 52 shows the curve of chromatic dispersion coefficient (D) and relative group delay (RGD) in dependence on wavelength.

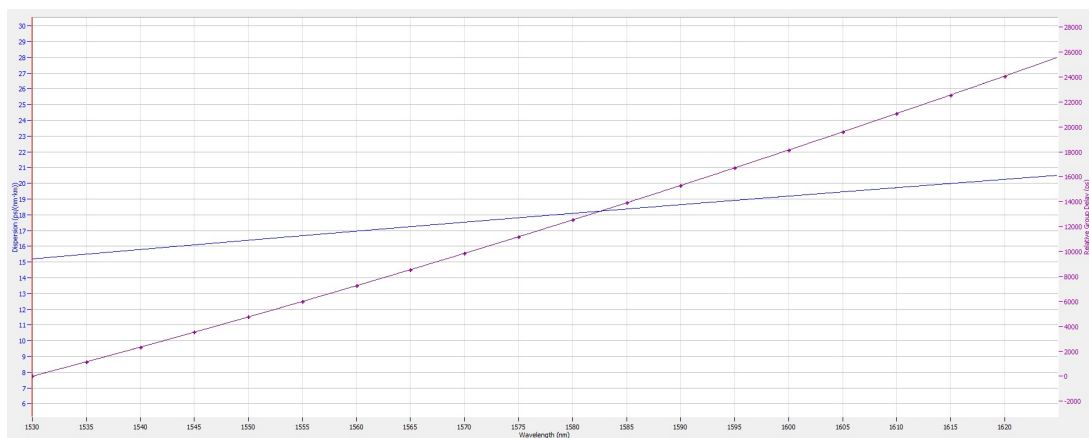


Figure 52: Result from CD analyzer - dispersion depending on wavelength

With method of phase shift was measured the chromatic dispersion coefficient  $D(\lambda)$  16.38 ps/(nm.km) at wavelength 1550 nm. It is a common value for a conventional single-mode fibers.

### 10.3 Semiconductor Optical Amplifiers Testing

To increase the EPON network coverage were used semiconductor optical amplifiers. Before they were deployed to the network several tests were executed. There were applied two types: the O-band SOA to amplify upstream and the S-band SOA to amplify downstream direction. The O-band SOA is manufactured by Thorlabs with part number BOA1017S. The S-band SOA is manufactured by Aeon with part number SASH 24P151. The both types of SOAs are a butterfly-type amplifiers and both are used together with the adapters manufactured by Thorlabs. Fundamental properties of the SOAs achieved from datasheets are shown in Table 15.

Table 15: Properties of used semiconductor optical amplifiers

SOA type	Operating current [mA]	Central Wavelength [nm]	3 dB Bandwidth [nm]	Saturation Output Power [dBm]	Peak Gain [dB]	Average Noise Figure [dB]
BOA 1017S	600	1319.1	79.5	16.9	30.3	6.5
SASH 24P151	390	1470.0	64.5	11.6	29.4	7.0

### 10.3.1 BOA 1017S

The analysis was focused to obtain gain spectrum of semiconductor optical amplifier. For this purpose was available tunable laser source Yenista Optics TUNICS T100S-HP. The wavelength range of this laser source is from 1260 to 1360 nm with minimum step size 1 nm. The laser source output power was set to -3 dBm. An amplified signal was analyzed by optical spectrum analyzer (EXFO FTB-5240B). Behind the optical amplifier was deployed optical attenuator with attenuation of 21 dB to prevent spectral analyzer damage. Injected current to the optical amplifier was 600 mA. Figure 53 shows circuit diagram to obtain the gain spectrum of the SOA.

Table 16 shows the resulting gain in dependence on wavelength.  $P_{IN}$  means the values measured by the spectral analyzer.  $P_{IN+A}$  means values increased by the value of the optical attenuator (i.e., output power from the amplifier). The resultant gain is calculated as:

$$G = P_{IN+A} - (-3) = -1.4 + 3 = 1.6dB$$

where -3 is the amplifier input power. From table and also from Figure 54 is evident that the peak wavelength do not correspond with the peak wavelength indicated by the manufacturer. Also the amplifier gain is not as high as expected. The gain indicated by manufacturer is measured as a power of the full amplifier bandwidth, whereas here was measured as a peak power, also for EPON network is important only peak gain. The maximum gain is 10.34 dB.

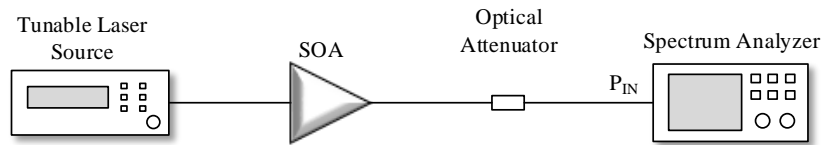


Figure 53: Topology to obtain gain spectrum of the O-band SOA

Table 16: Measured values of gain depending on wavelength

$\lambda$ [nm]	$P_{IN}$ [dBm]	$P_{IN+A}$ [dBm]	$G$ [dB]
1260	-24.47	-3.47	-0.47
1270	-22.40	-1.40	1.60
1280	-19.68	1.32	4.32
1290	-17.70	3.30	6.30
1300	-16.45	4.55	7.55
1310	-15.32	5.68	8.68
1320	-14.59	6.41	9.41
1330	-14.12	6.88	9.88
1340	-13.66	7.34	10.34
1350	-14.38	6.62	9.62
1360	-15.38	5.62	8.62

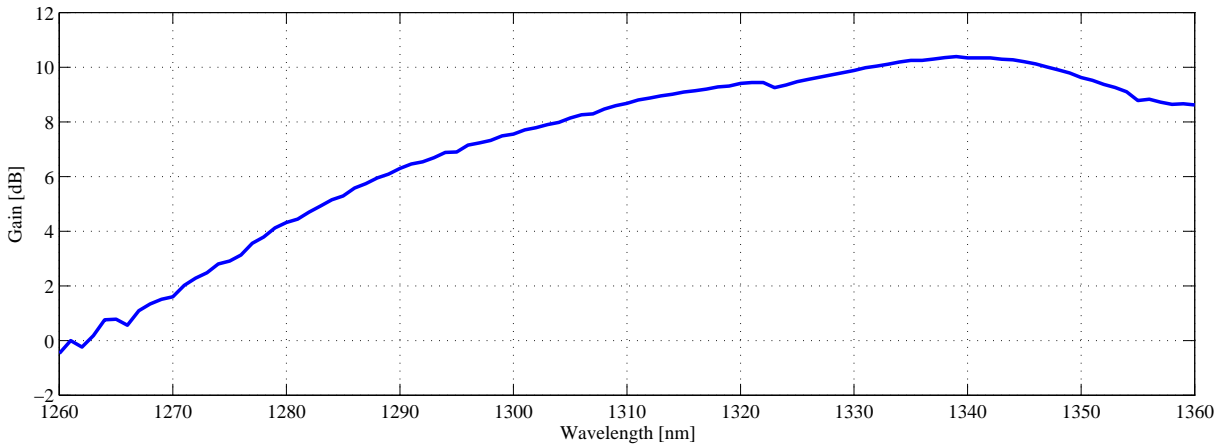


Figure 54: O band amplifier's gain spectrum

### 10.3.2 SASH 24P 151

The AEON SASH 24P 151 was used together with the adapter by Thorlabs. However, the SOAs made by AEON requires the special adapter also mad by AEON. The AEON amplifier is thinner than amplifiers made by Thorlabs. There occurred a gap between the SOA and adapter surface(Figure 55). The SOA could not be tested, because no temperature stabilization was secured. To fill the gap were used copper plates and heatsink compound (Figure 56).

The S-band SOA was tested to achieve the gain in dependence on the input power. The SOA was deployed to the EPON network. To achieve the optical spectrums of the downstream optical signal was used the spectrum analyzer (YENISTA OSA20) which was once connected to splitter before the SOA and then to splitter after the SOA. The optical attenuator near the ONU serves to protect the ONU unit before the high optical power. The optical attenuator near the OLT was changed from the 5 dB to 35 dB. The Figure 57 shows the topology to obtain S band SOA's gain.

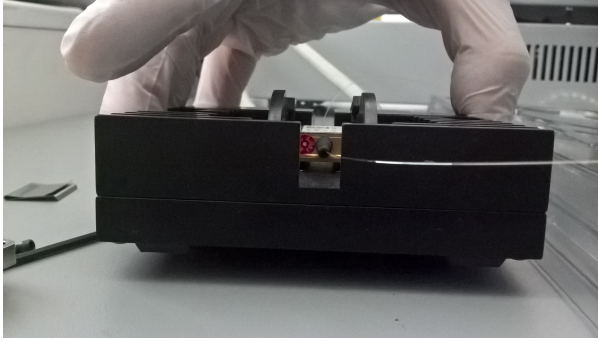


Figure 55: Gap between the SOA and adapter

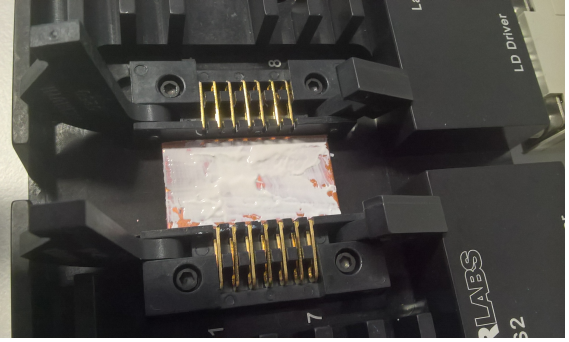


Figure 56: Gap filling

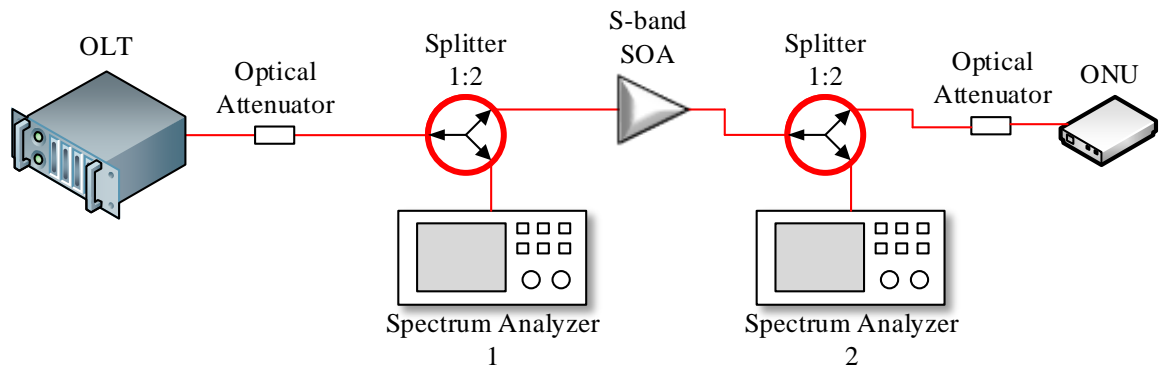


Figure 57: Topology to obtain S band SOA's gain in dependence on input power

Table 17 shows the values of attenuation, input power to SOA, and output power from the SOA and the gain. These values were calculated on the basis of known splitter insertion loss values.

Table 17: Measured values of gain depending on input power

Attenuation [dB]	$P_{IN}$ [dBm]	$P_{OUT}$ [dBm]	G [dB]
0	0,639	-2,853	-3,492
4,101	-3,462	-3,194	0,268
11,523	-10,884	-5,592	5,292
19,787	-19,148	-10,495	8,653
23,007	-22,368	-12,919	9,449
25,873	-25,234	-15,484	9,75
35,323	-34,684	-24,088	10,596



The Figure 58 shows the output from the spectrum analyzer 1, when optical attenuator is not used.

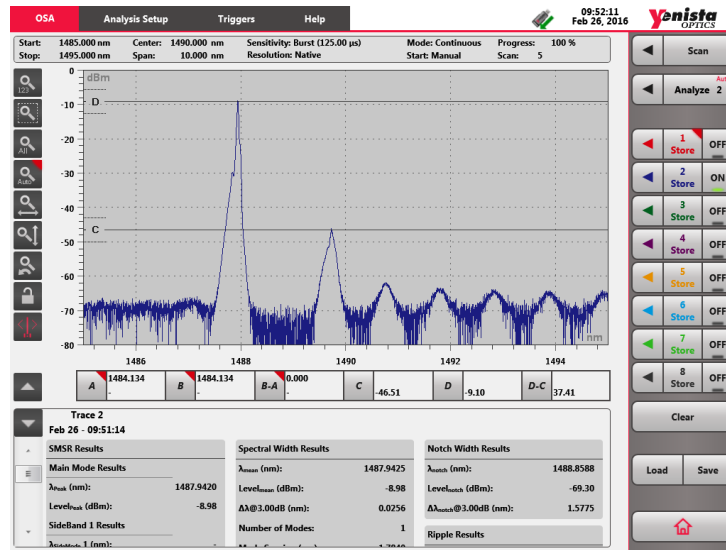


Figure 58: Downstream optical spectrum before passes the SOA

The Figure 59 shows the output from the spectrum analyzer 2, when the optical attenuator is not used. From figure can be seen that optical amplifier attenuates the optical signal, when the input power is high.

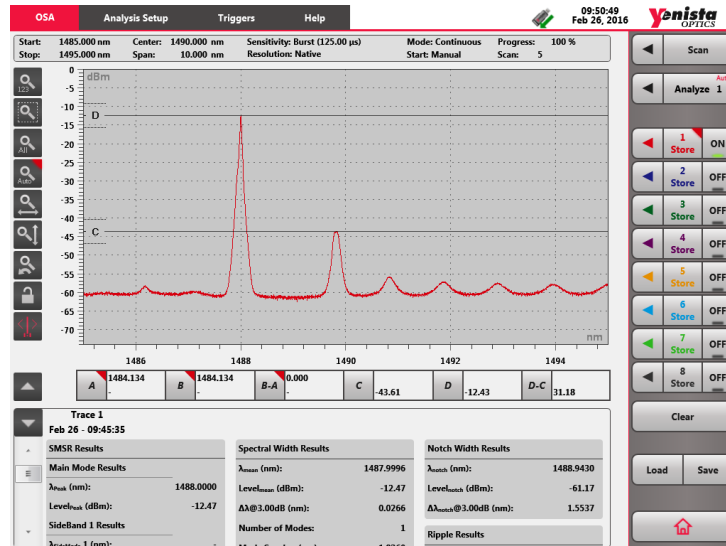


Figure 59: Downstream optical spectrum after passes the SOA

Figure 60 shows the comparison of the optical spectrums, when the optical attenuator was not used.  $P_{IN}$  is the spectrum from spectrum analyzer 1 and  $P_{OUT}$  is the optical spectrum from spectrum analyzer 2. From figure can be seen that the optical signal is attenuated after passes the SOA. The amplified is only noise and the small peak.

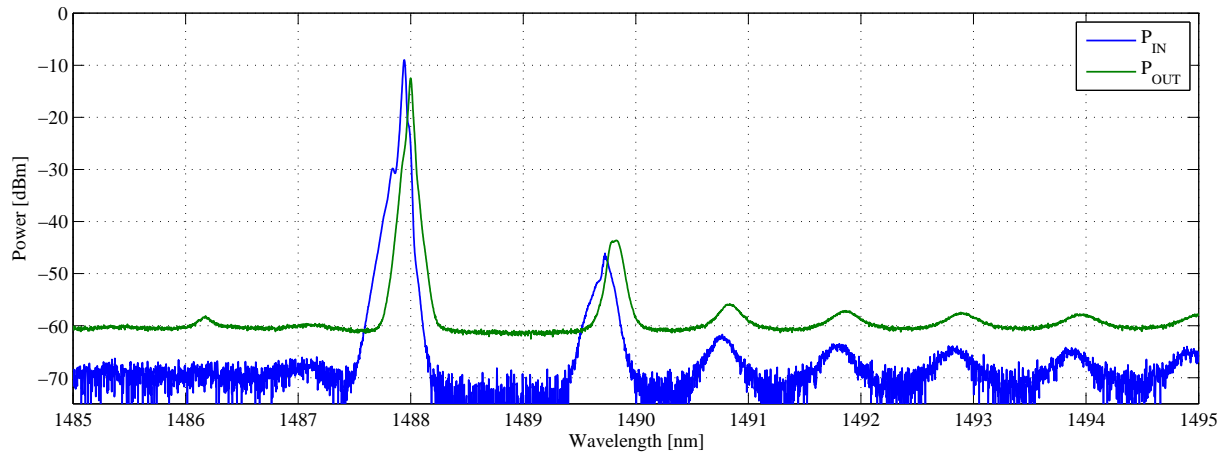


Figure 60: Optical spectrum before and after passes SOA -  $A = 0$  dB

Figure 61 shows the comparison of the optical spectrums, when the optical attenuator with loss of 11 dB is used. This time is visible amplification of the SOA.

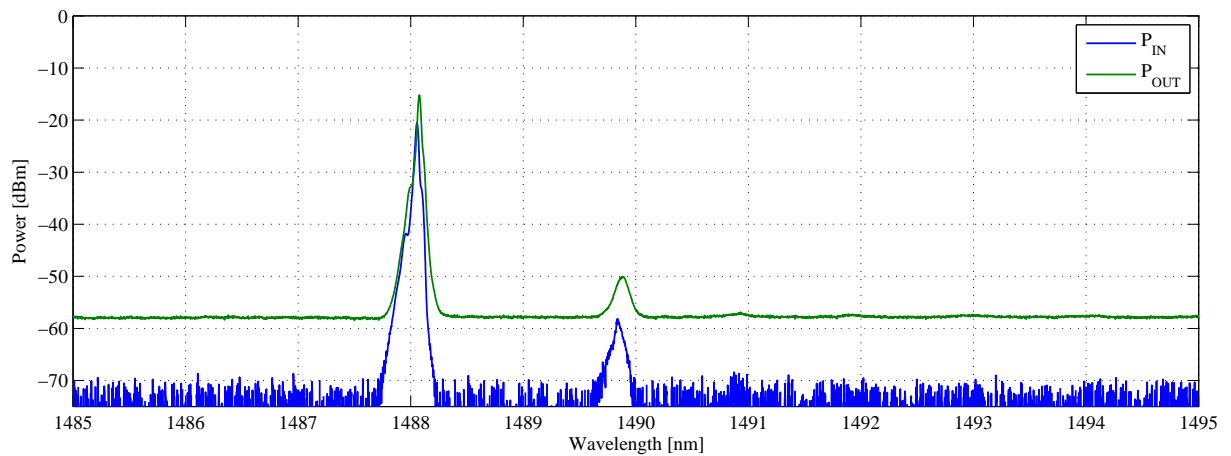


Figure 61: Optical spectrum before and after passes SOA -  $A = 11$  dB

Figure 62 shows the the comparison of the optical spectrums, when the optical attenuator with loss of 20 dB is used. This time is visible higher amplification of the SOA against the previous case.

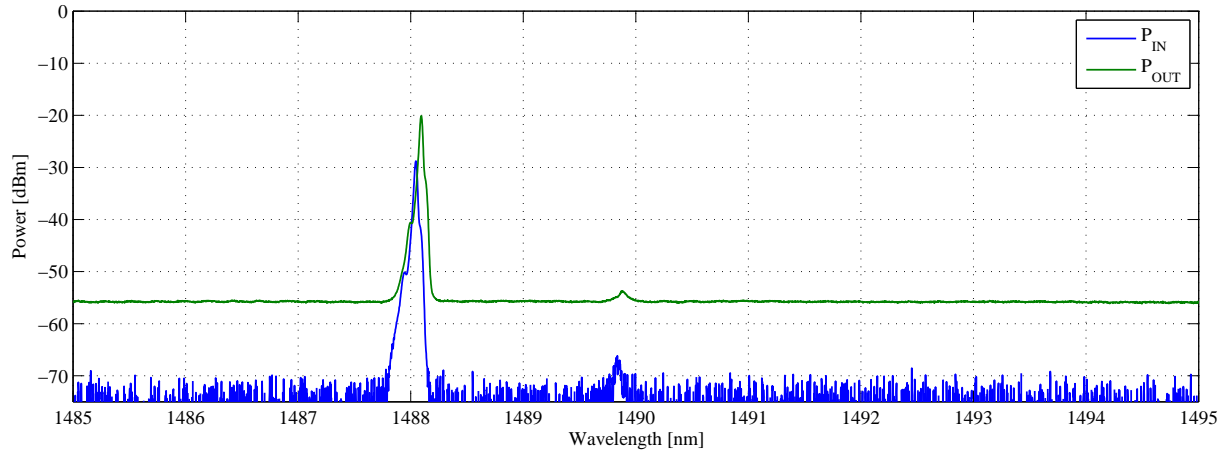


Figure 62: Optical spectrum before and after passes SOA -  $A = 20$  dB

The Figure 63 shows the gain saturation of the semiconductor optical amplifier.

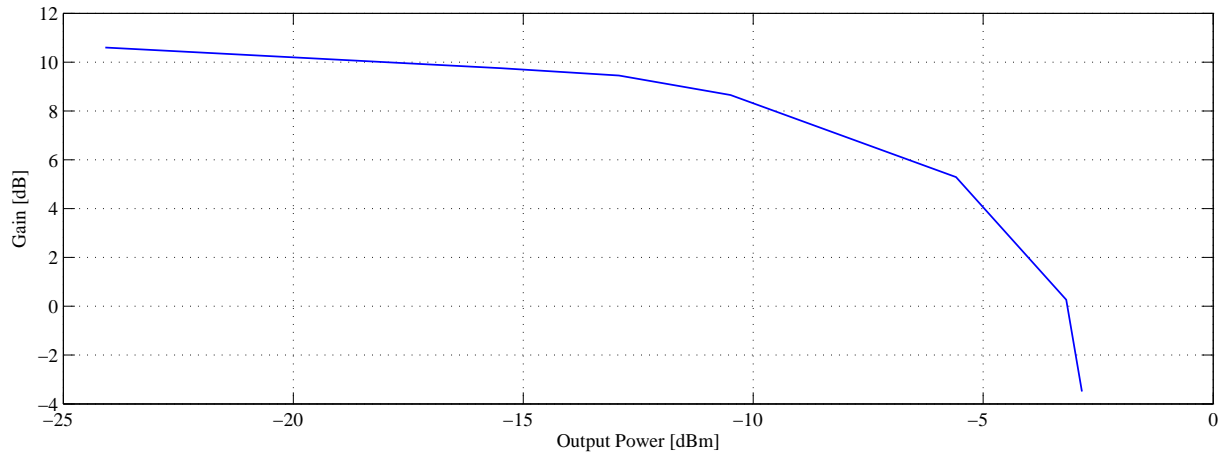


Figure 63: S band SOA's gain saturation

From the previous figures is obvious that the optical amplifier has the highest gain when the input optical power is low. This means that the AEON finds application as pre-amplifier.

## 10.4 Metallic Wires

To test the reach of the DSL technologies was used metallic cable type: SYKY 2x2x0.5. The cable was manufactured by Kabelovna Děčín-Podmokly. The mark 2x2 means that cable carries two twisted pairs. The mark 0.5 means that diameter of the cable core is 0.5 mm. The core of the cable is made from copper. The cable-lives are isolated by PVC material. The cable is suitable for low frequency distributions, transport signals and measured values. To achieve primary and secondary parameters of the cable were measured a resistance and a capacitance of the pairs. Measurements were realized by the digital multimeter Lini-T UT70A. The resistance was measured as short termination and the capacitance was measured as open termination. The

Figure 64 shows the schematic diagram of the open termination (A) and the short termination (B).

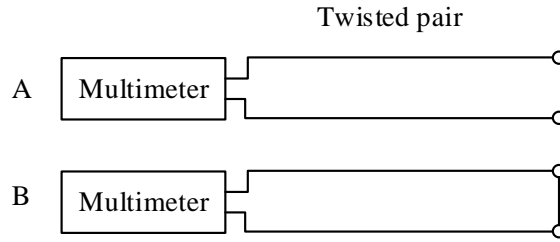


Figure 64: Open termination (A) and the short termination (B).

The wire low frequency resistance  $R_W$  in ohms  $[\Omega]$  is defined as:

$$R_W = 2 \cdot \frac{\rho}{S} \left[ \Omega \cdot km^{-1} \right] \quad (14)$$

where  $\rho$  is the resistivity (for copper  $\rho = 17.5 \Omega \cdot mm^2 \cdot km^{-1}$ , and  $S$  ( $S = \pi \cdot r^2$ ) is the wire cross section in  $mm^2$ . Calculated resistance  $R_W$  is  $178.25 \Omega \cdot mm^2 \cdot km^{-1}$ . The measured values of the resistance and the capacitance are shown in Table 18.

Table 18: Measured resistance and capacitance

	Wire pair		Average
	A - B	C - D	
<b>Resistance</b> $[\Omega]$	178.3	178	178.15
<b>Capacitance</b> $[nF]$	72.2	72.4	72.3

The loop length is defined by equation:

$$l = \frac{R_{AVG}}{R_W} [km] \quad (15)$$

where  $R_{AVG}$  is an average resistance of the two wires. The calculated loop length is 0.99 km. The calculated loop length is equal to length of loop marked on the top of pin. The capacitance of the the cable is defined as:

$$C = \frac{C_{AVG}}{l} \left[ nF \cdot km^{-1} \right] \quad (16)$$

where  $C_{AVG}$  is an average capacitance of the two wires. The calculated capacitance is  $73.03 nF \cdot km^{-1}$ . The series impedance (the inductance  $L$  is neglected) of the conduction is defined as:

$$\bar{Z} = R + j\omega L = R \left[ \Omega \cdot km^{-1} \right] \quad (17)$$

where  $\omega = 2\pi f$  and  $j = \sqrt{-1}$ . The shunt admittance (the conductance  $G$  is neglected) is given by equation:

$$\bar{Y} = G + j\omega C = j\omega C \left[ S \cdot km^{-1} \right] \quad (18)$$

The characteristic impedance, when the conductance and inductance are neglected, is defined as:

$$\bar{Z}_0 = \sqrt{\frac{\bar{Z}}{\bar{Y}}} = \sqrt{\frac{R + j\omega L}{G + j\omega C}} = \sqrt{\frac{R}{j\omega C}} \left[ \Omega \right]. \quad (19)$$

The attenuation of the wire is calculated from the propagation constant defined as:

$$\bar{\gamma} = (\alpha + j\beta) = \sqrt{\bar{Z} \cdot \bar{Y}} = \sqrt{(R) \cdot (j\omega C)} \quad (20)$$

where  $\alpha$  is an attenuation coefficient (real component of the propagation constant in  $Np \cdot km^{-1}$ ) and  $\beta$  is a phase shift coefficient (imaginary component of the propagation constant in  $rad \cdot km^{-1}$ ). The attenuation coefficient expressed in dB is calculated by equation:

$$\alpha_{dB} = 8.686 \cdot \alpha_{Np} \quad (21)$$

The attenuation of the cable with length  $l$  is calculated as:

$$A = \alpha_{dB} \cdot l. \quad (22)$$

The dependence of the characteristic impedance and attenuation coefficient on frequency is shown in Figure 65. The upper limit for frequency is set to 30 MHz, what is the maximum frequency used by the VDSL2. The attenuation is 300 dB/km at frequency 30 MHz.

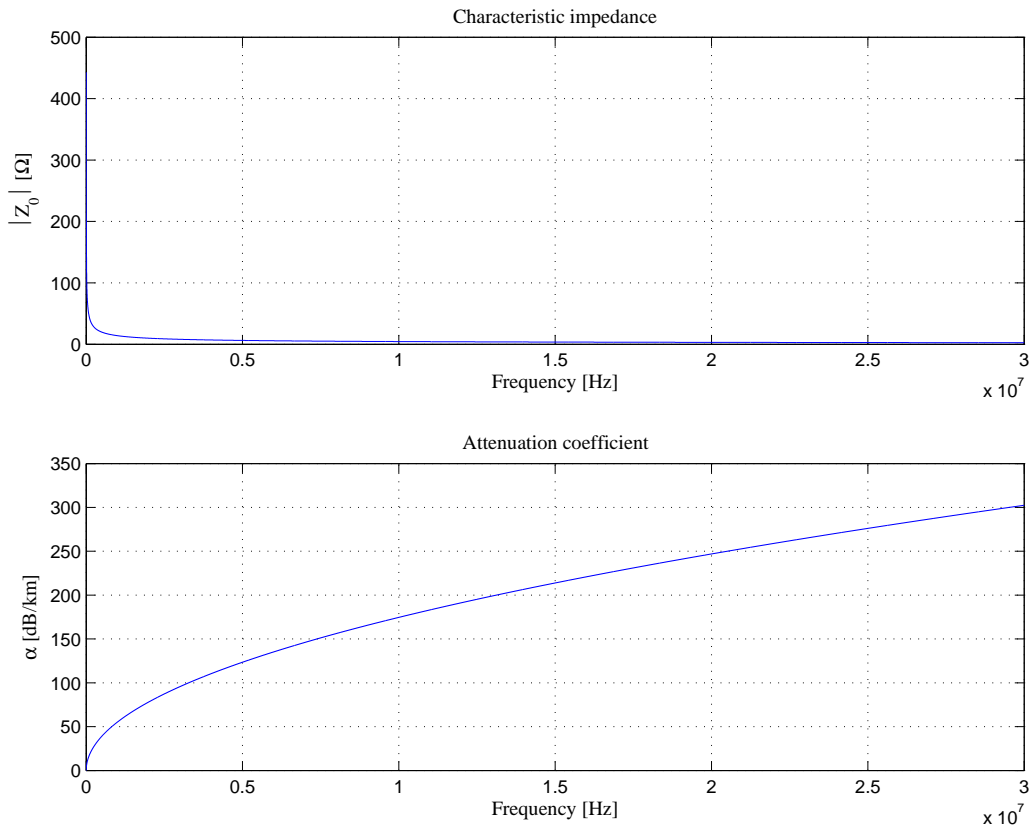


Figure 65: Charasteristic impedance and attenuation coefficient for SYKY metallic wire

### 10.5 ADSL2+ and VDSL2 Link Rates

To achieve the maximum throughput of xDSL links through the cables mentioned above was used modem emulator VeEX VePAL BX100V for ADSL2+ and the VDSL modem by himself.

The modem emulator was set to Customer-Premises Equipment (CPE) modem type and ADSL2+ mode. Besides the displaying link rates in upstream and downstream direction supports graphical visualization of transmitted bits per tones. The Figure 66 shows the number of transmitted bits per tone (yellow colour for upstream and blue colour for downstream). On the left side is the modem emulator directly connected to the DSLAM and on the right side is used 2 km long wire. From this figure is obvious that the wire length has a significant impact on the number of transmitted bits.

Several pirns of the SYKFY cables was available to test link rates dependence on the conduction length. To test ADSL2+ was used pirns with a nominal length of 1 km, the pirns with a length of 50 m were applied to test VDSL. Table 19 shows the measured ADSL2+ link rates of two set profiles depending on the wire length. Graphic representation of the measured ADSL2+ link rates depending on the wire length for higher profile is shown in Figure 67. Downstream link

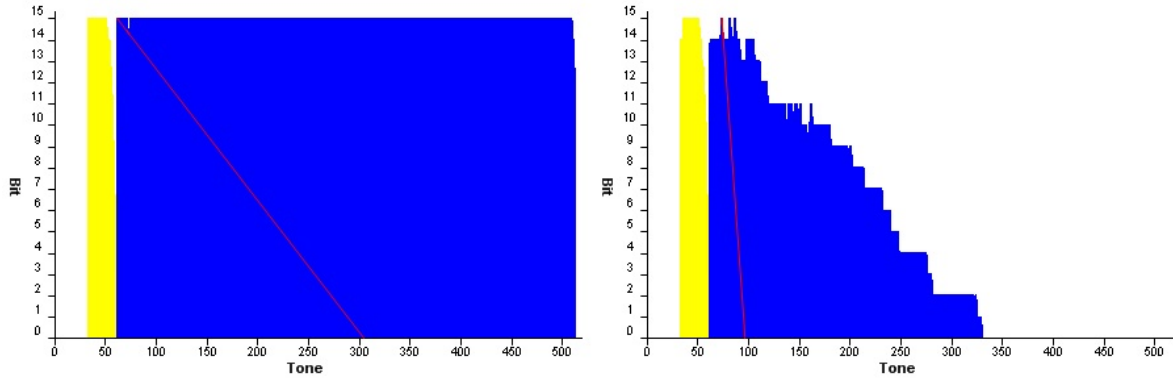


Figure 66: Transmitted bits - wire length 0 km (left) and 2 km (right)

Table 19: Measured ADSL2+ Link rates

Link Rates [Mbps]							
Set		Wire Length [km]					
		0		1		2	
Up	Down	Up	Down	Up	Down	Up	Down
4.096	16.384	1.367	16.383	1.349	11.229	1.269	8.033
4.096	32.000	1.346	26.035	1.326	11.143	1.322	7.738
Set		3		4		5	
Up	Down	Up	Down	Up	Down	Up	Down
4.096	16.384	0.913	1.757	0.694	0.701	Not Connected	
4.096	32.000	0.879	1.753	0.648	0.681	Not Connected	

rate at higher profile was decreased more than half already at the wire length of 1 km. In case of the wire length of 5 km, the modem emulator was not able to establish a connection.

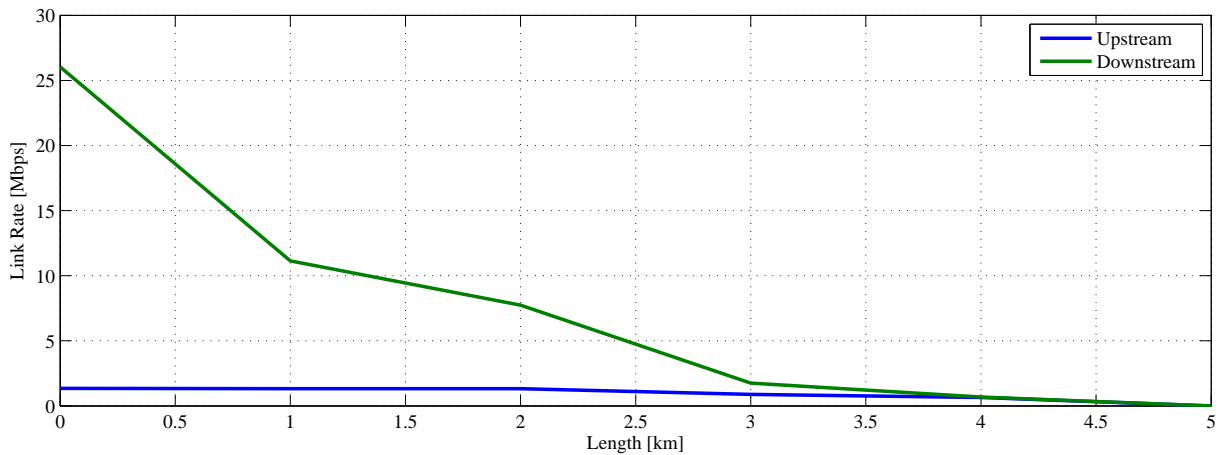


Figure 67: Link rate depending on wire length - ADSL2+

Link rates for VDSL were obtained from the VDSL modem because no special device to test VDSL was available. To access the VDSL2 modem was used terminal emulator PuTTY and

established telnet session. Figure 68 shows the main menu of the modem. There was selected option System Maintenance.

```
Copyright (c) 1994 - 2006 ZyXEL Communications Corp.

P-870MH-C1 Main Menu

Getting Started                                Advanced Management
 1. General Setup                               23. System Password
 3. LAN Setup                                   24. System Maintenance

Advanced Applications

99. Exit

Enter Menu Selection Number: 24
```

Figure 68: Main Menu - VDSL2 modem

In the system maintenance menu was selected option Command Interpreter Mode (Figure 69).

```
Menu 24 - System Maintenance

1. System Status
2. System Information and Console Port Speed
3. Log and Trace

7. Upload Firmware
8. Command Interpreter Mode

Enter Menu Selection Number: 8
```

Figure 69: System Maintenance - VDSL2 modem

To obtain the VDSL rates, command `<vdsl status>` was written to the CLI (Figure 70).

The measured VDSL link rates depending on the wire length are shown in Table 20, then the graphic representation is shown in Figure 71. Because the VDSL2 uses higher frequencies (up to 30 MHz) than ADSL2+ (up to 2.204 MHz), the connection decay occurs at the wire length of 250 meters. The both set profiles are highly degraded already at the wire length of 50 meters. The upstream link rate at the wire length of 100 meters do not reaches not even the 3% of the original link rate, but for the rest wire lengths is not changing.



```

ras> vdsl status
=====
VDSL DSP Firmware Version: 1.60.00-A1
VDSL Line State: DATA Total Transmit Power:14.5 dB
DS Payload Rate: 63968kbps Local Attenuation: 0.0 dB
US Payload Rate: 35968kbps Local SNR Margin: 53.0 dB
=====
COE Parameters:
Remote Transmit Power: 0.0 dB
Remote Init SNR: 0.0 dB
Remote SNR Margin: 0.0 dB
Remote Attenuation: 0.0 dB
=====
Counters since last reset
RX Packet Count: 41 TX Packet Count: 429
RX Error Packet Count: 0
Local FEC Error: 0 Remote FEC Error: 0
Local CRC Error: 0 Remote CRC Error: 0
Local SEF Error: 0 Remote SEF Error: 0
Local LOS Error: 0 Remote LOS Error: 0
=====
Failure Condition
Overall: 0
Watch Dog Timer: 83
Local LOS: 0 Remote LOS: 0
Local SEF: 0 Remote SEF: 0
Local NCDI: 0 Remote NCDI: 0
Local LCDI: 0 Remote LCDI: 0
=====

```

Figure 70: List of command <vdsl status> - VDSL2 modem

Table 20: Measured VDSL2 Link rates

Link Rates [Mbps]							
Set		WireLength [m]					
		0		50		100	
Up	Down	Up	Down	Up	Down	Up	Down
32.000	32.000	31.968	31.968	15.968	26.176	0.672	12.736
45.440	80.000	35.968	60.928	15.987	25.568	0.672	12.672
Set		15		200		250	
Up	Down	Up	Down	Up	Down	Up	Down
32.000	32.000	0.640	3.584	0.672	1.344	Not Connected	Not Connected
45.440	80.000	0.704	3.776	0.672	1.344	Not Connected	Not Connected

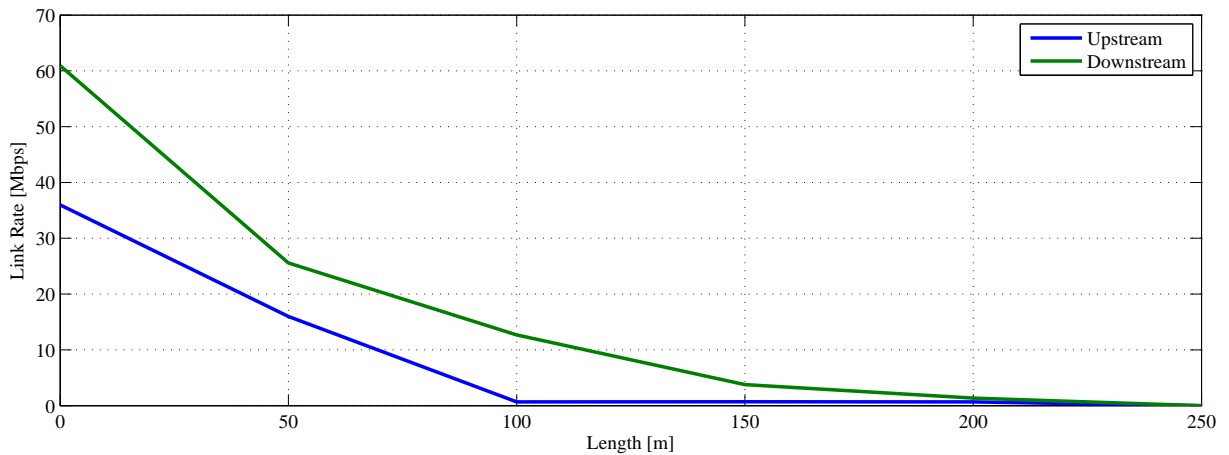


Figure 71: Link rate depending on wire length - VDSL2

## 11 EPON Testing

This chapter is focused to testing the EPON network with deployment of semiconductor optical amplifiers. For testing were used WDM splitters to split the downstream and upstream wavelengths onto the two fibers. Power levels of an optical signal were obtained from the PON Power Meter (PPM-350B EG). Also, the spectral analysis of an optical signal was done by spectrum analyzer (FTB-2540B). The splitters 1:2 had split ratio 90:10, where the 10% of an optical signal was brought to the optical spectrum analyzer and the 90% of an optical signal continued to the optical trace. Firstly, the reference power levels and the optical spectrums were recorded. The topology was built according to Figure 72.

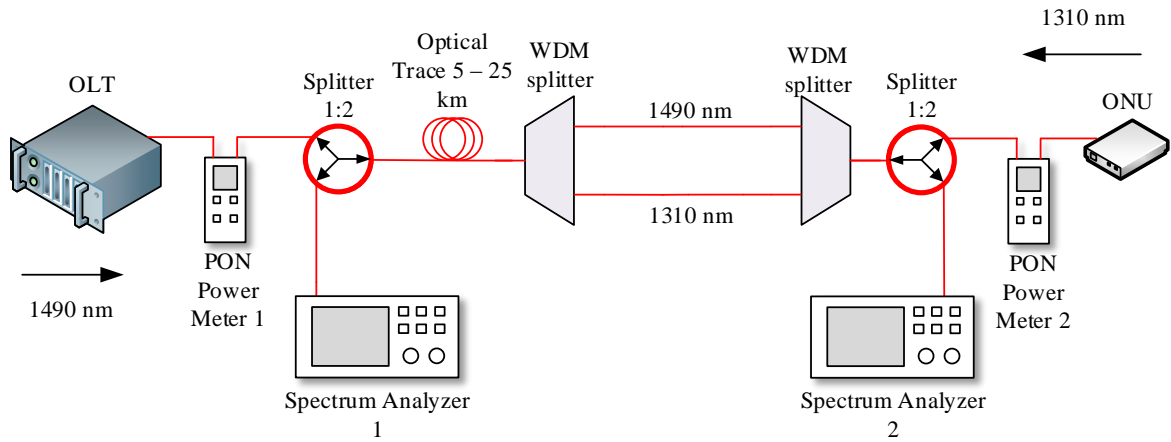


Figure 72: Reference (original) topology to SOA testing

The PON Power Meter 1 (PPM1) and Spectrum Analyzer 1 is to measure the power level of the upstream optical signal at 1310 nm. The PON Power Meter 2 (PPM2) and the Spectrum Analyzer 2 is to measure the downstream optical signal at 1490 nm. The output power from the OLT is 3.7 dBm, also measured by PON Power Meter 1. The output power from the ONU is 2.4 dBm, measured by PON Power Meter 1. Table 21 shows the measured values of the power levels, where the length of the optical traces was changed from the 5 km to the 25 km with 5 km step.

Table 21: Measured values of power - reference topology

l [km]	Optical Power [dBm]	
	PPM1	PPM2
5	-9.70	-4.80
10	-12.10	-7.10
15	-13.90	-9.70
20	-17.60	-10.30
25	-20.50	-12.80

From the table is obvious that the optical signal at the wavelength 1310 nm is more attenuated than the optical signal at the wavelength 1490 nm. The higher attenuation can be caused by the higher insertion loss at the O-band branches of the WDM splitters. The length of 25 km of the optical trace is the last length when the ONU was able to register.

The Figure 73 shows the optical spectrum of the upstream signal after the 5 km and the 25 km of the optical trace. After the 25 km, the optical signal is almost lost in noise. The difference between the peak powers at lengths of 5 and 25 km is 10.06 dB. The Figure 74 shows the same situation in the downstream direction. The difference between the powers at the peak of optical signal is 7.99 dB.

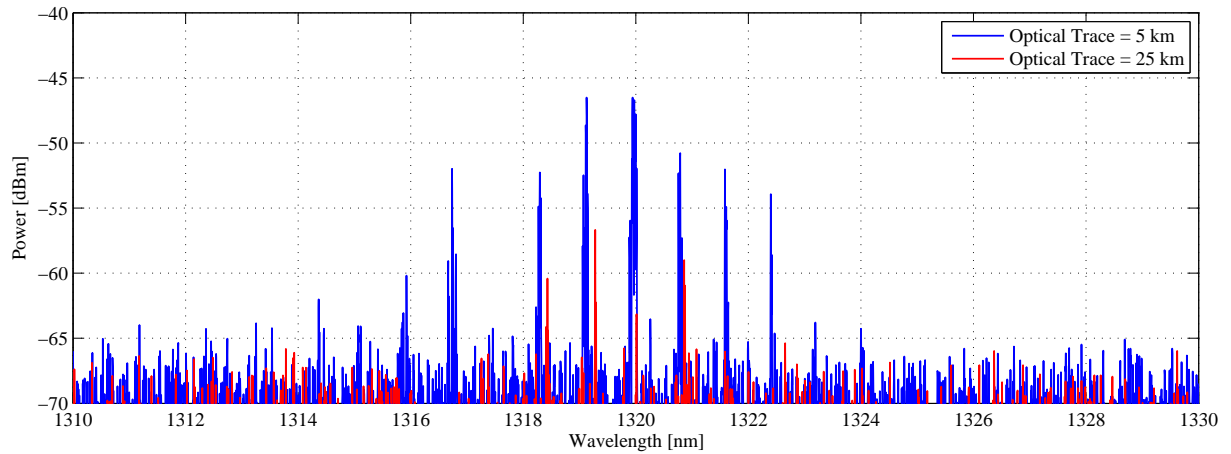


Figure 73: Upstream optical spectrum - optical trace 5 and 25 km - reference topology

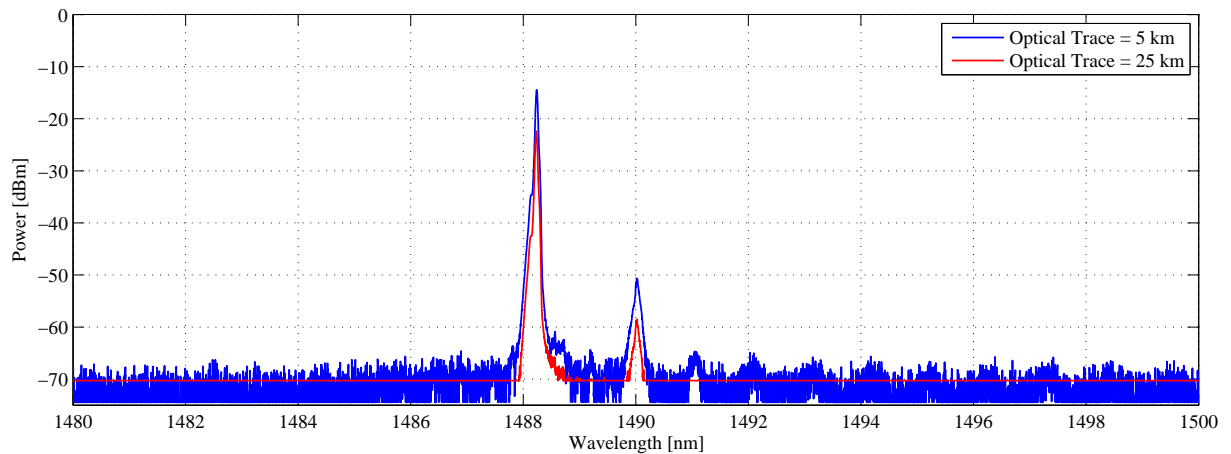


Figure 74: Downstream optical spectrum - optical trace 5 and 25 km - reference topology

## 11.1 Semiconductor Optical Amplifiers deployment

The SOAs were deployed between the WDM splitters to amplify each of the optical signals independently. In case of amplifiers deployment on the one fiber, the O-band SOA attenuates

the wavelengths outside the O-band range (1260 – 1360 nm) and the S-band SOA makes the same with the wavelengths outside the S-band range (1460 – 1530 nm).

### 11.1.1 Topology A

The Figure 75 shows the topology with the deployment of the semiconductor optical amplifiers.

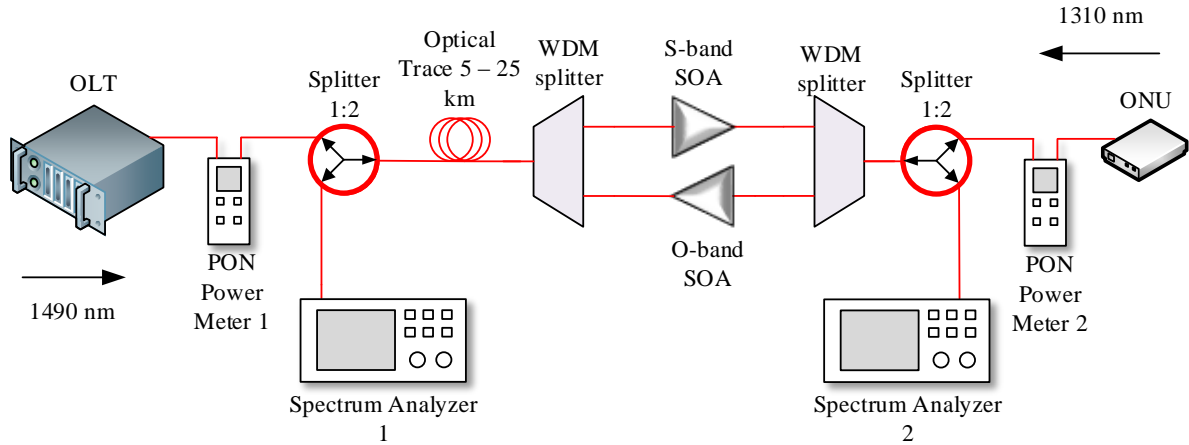


Figure 75: Topology A - SOA deployment

The topology is the same as in the previous case except the deployment of the SOAs. Table 22 shows the values of the power measured by the PON Power Meters placed in the topology and gain of the SOAs. The gain is calculated against the reference power levels.

Table 22: Measured values of power - calculated gain - topology A

l [km]	Optical Power [dBm]		O-band SOA Gain [dB]	S-band SOA Gain [dB]
	PPM1	PPM2		
5	2.10	7.70	8.10	12.50
10	0.10	7.20	8.60	14.30
15	-1.50	6.30	8.80	16.00
20	-5.30	6.00	8.10	16.30
25	-8.10	5.00	8.20	17.80

From table can be seen that the gain of the O-band amplifier is almost the same in every case. The gain of the S-band amplifier increases with the length of the trace before the optical signal passes the SOA. It confirms that the S-band semiconductor optical amplifier is a pre-amplifier and it should be placed at the end of the optical traces to amplify the low power entering the photodetector.

The Figure 76 shows the optical spectrum of the amplified upstream optical signal after reaching the 5 and the 25 km. The difference between the powers of the strongest peaks is 11.57 dBm.

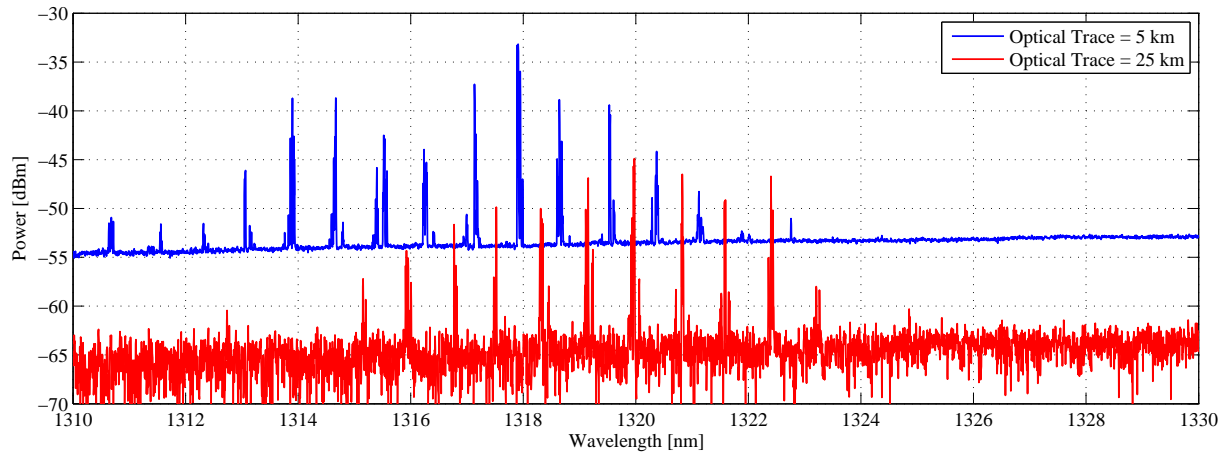


Figure 76: Upstream optical spectrum - optical trace 5 and 25 km - Topology A

In the Figure 77 is shown spectral analysis of the amplified downstream signal. The difference between the powers of the peaks is 2.75 dBm.

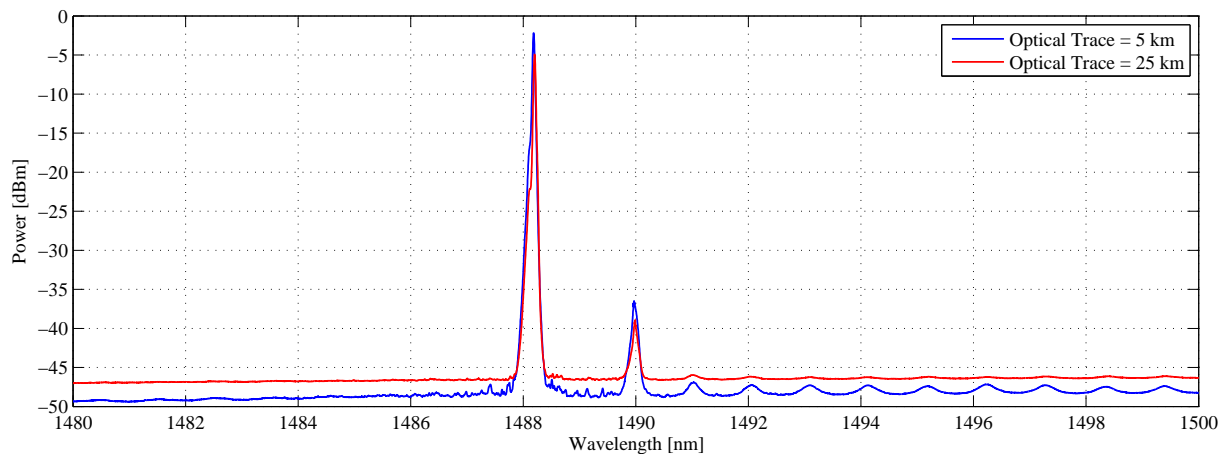


Figure 77: Downstream optical spectrum - optical trace 5 and 25 km - Topology A

### 11.1.2 Topology B

The Figure 78 shows the topology where the optical trace is situated between the ONU and the WDM splitter.

Table 23 shows the powers measured on the PON power meters and the gain calculated against the reference powers. Although, the O-band SOA is the booster amplifier and it should be placed right behind the source to increase the power to the maximum, is evident that it has a higher gain when the some attenuation is inserted before the signal passes the SOA. In case of the 25 km of inserted optical trace, the ONU already was not able to register. Therefore, no power level is recorded.

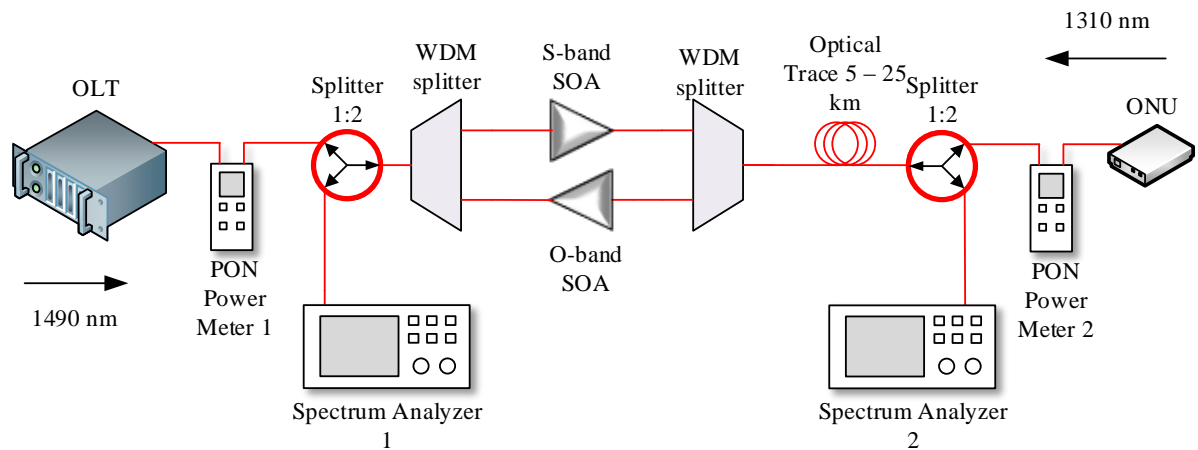


Figure 78: Topology B - SOA deployment

Table 23: Measured values of power - calculated gain - topology B

l [km]	Optical Power [dBm]		O-band Gain [dB]	S-band Gain [dB]
	PPM1	PPM2		
5	2.10	5.50	11.80	10.30
10	1.70	3.40	13.80	10.50
15	-1.80	0.60	12.10	10.30
20	-4.60	0.00	13.00	10.30
25	-	-2.30	-	10.50

Figure 79 show the optical spectrum of the upstream signal. Because of the ONU was not registered at the 25 km, no peaks are visible.

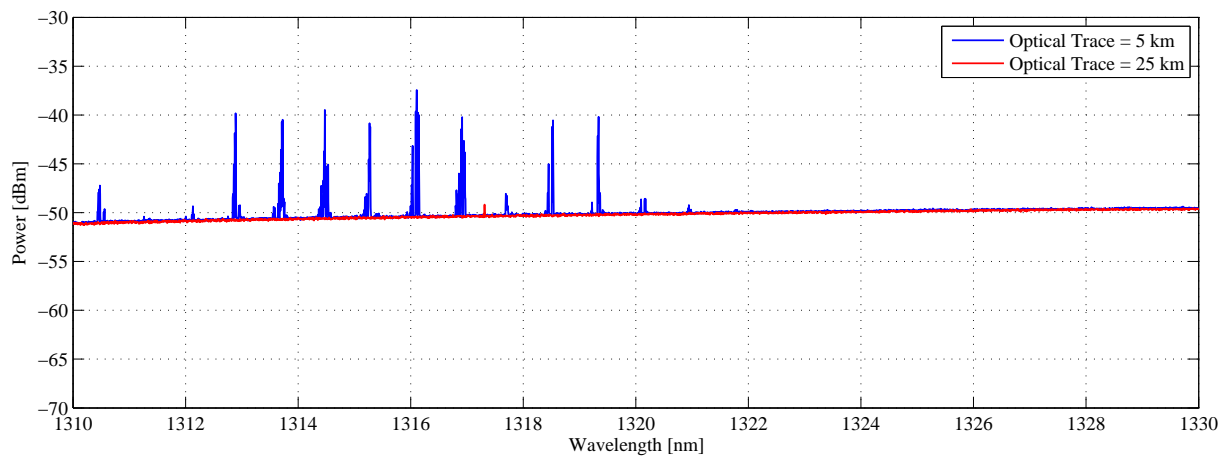


Figure 79: Upstream optical spectrum - optical trace 5 and 25 km - Topology B

The Figure 80 shows the downstream amplified optical signal. The difference between the powers of the peaks is 5.57 dBm.

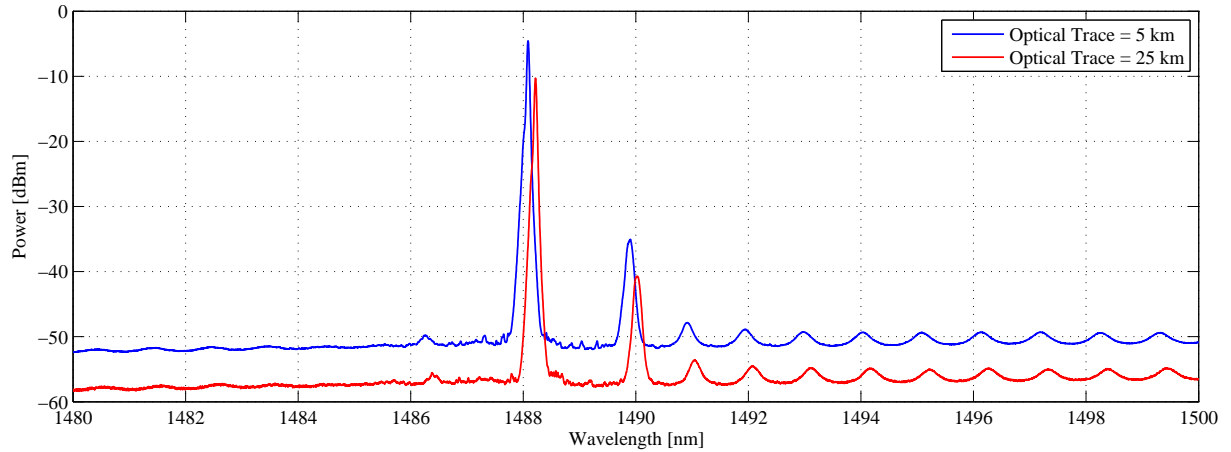


Figure 80: Downstream optical spectrum - optical trace 5 and 25 km - Topology B

## 11.2 Comparison of optical signals depending on topology

This section compares the original optical signals against the amplified optical signals.

The Figure 81 shows the full O-band, where can be seen the original upstream optical signal after the 5 km of optical trace, and the amplified optical signals according to the topologies A and B.

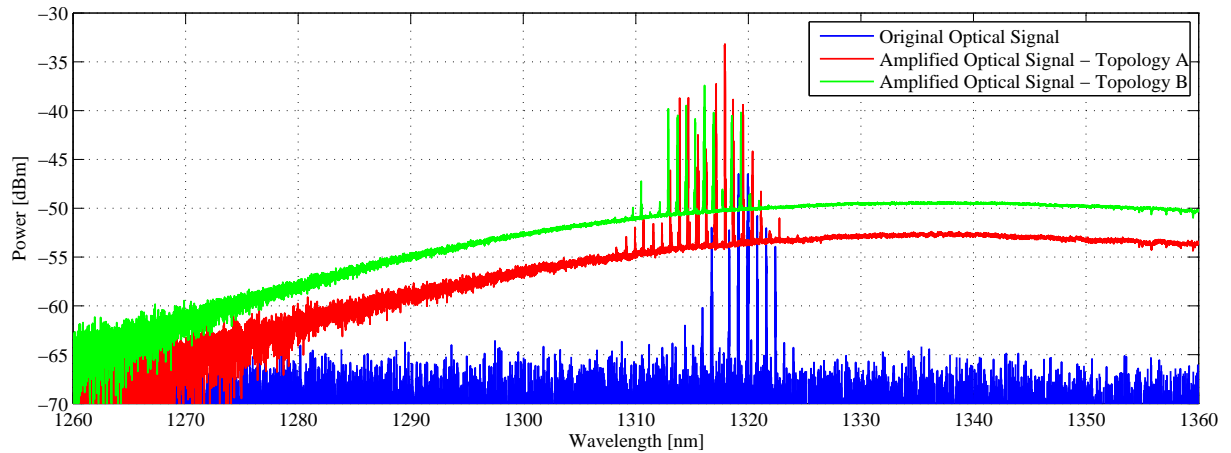


Figure 81: Comparison of upstream signals depending on topology - 5 km

From Figure 81 can be seen that is not amplified only optical signal, but the noise is amplified, too. Table 24 shows the measured values from the spectrum analyzer. While with the Topology A is amplified mainly optical signal, in case of topology B the noise amplification is dominant. Although, the topology B has the highest gain regarding to optical power as is shown in Table 24, the very optical signal has not so significant gain. Also, an optical signal-to-noise (OSNR) ratio is the lowest.

Table 24: Comparison of peak gain and noise gain - upstream - 5 km

Topology	Peak power [dBm]	Noise power [dBm]	Peak Gain [dB]	Noise Gain [dB]	OSNR [dB]
Original	-46.47	-63.92	-	-	17.45
A	-33.21	-52.68	13.26	11.24	19.47
B	-37.41	-49.83	9.06	14.09	12.42

The Figure 82 shows the situation after the 25 km of the optical trace. Then the Table 25 shows the measured parameters of the optical signal from the optical spectrum analyzer.

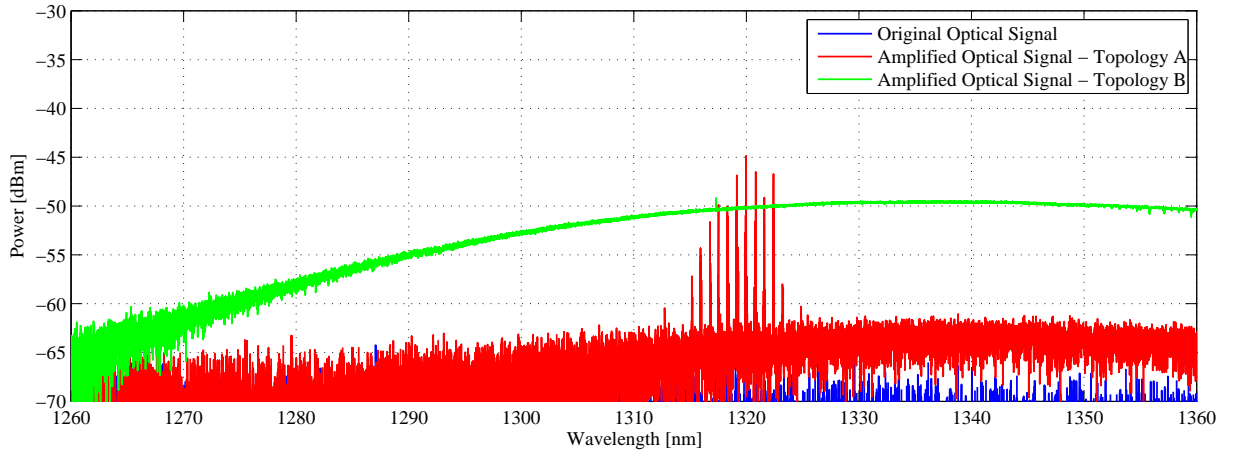


Figure 82: Comparison of upstream signals depending on topology - 25 km

Table 25: Comparison of peak gain and noise gain - upstream - 25 km

Topology	Peak power [dBm]	Noise power [dBm]	Peak Gain [dB]	Noise Gain [dB]	OSNR [dB]
Original	-56.69	-66.03	-	-	8.65
A	-45.06	-61.23	11.63	4.8	16.17
B	-	-49.44	-	16.59	-

From table can be seen that the noise has almost the same values in the original topology and with the deployed SOAs in Topology A. The OSNR and the peak power in topology A is high enough, nevertheless the ONU unit was not able to register when the length of the optical trace was more than 25 km. In case the topology B, the ONU unit was not able to register at the length of 25 km. The Figure 83 shows the optical spectrum, where the length of the optical trace is 20 km (Topology B).



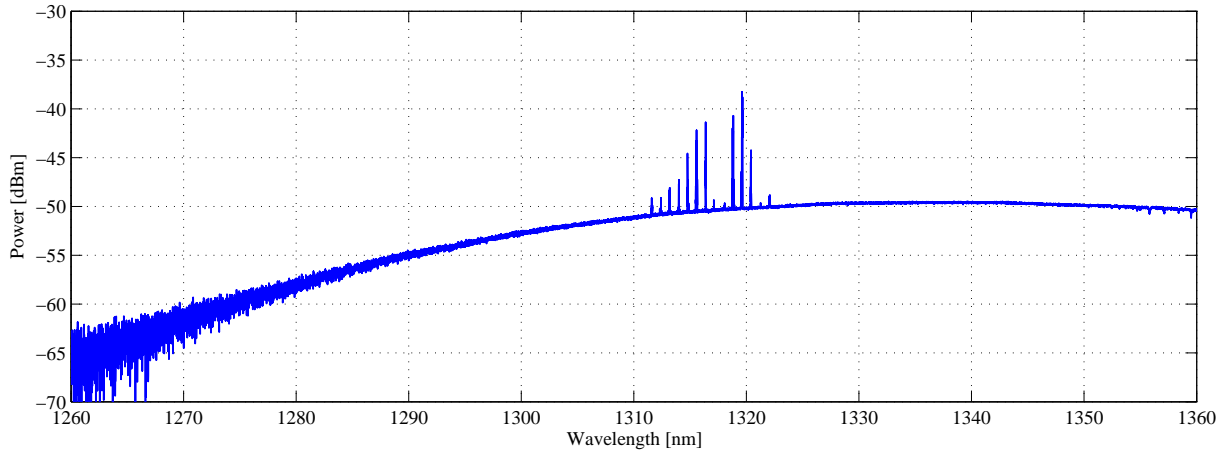


Figure 83: Upstream optical signal - 20 km - Topology B

From the Figure 83 can be seen that the optical signal is quite weak and the optical signal-to-noise ratio is only the 11.03 dB. After the 25 km of the optical trace will be signal-to-noise ratio even lower, so probably due to this, the ONU unit is not able to register.

The Figure 84 shows the downstream optical signal. In comparison are the original optical signal, amplified optical signal according to topology A and the amplified signal according to topology B. The length of the optical trace is 5 km.

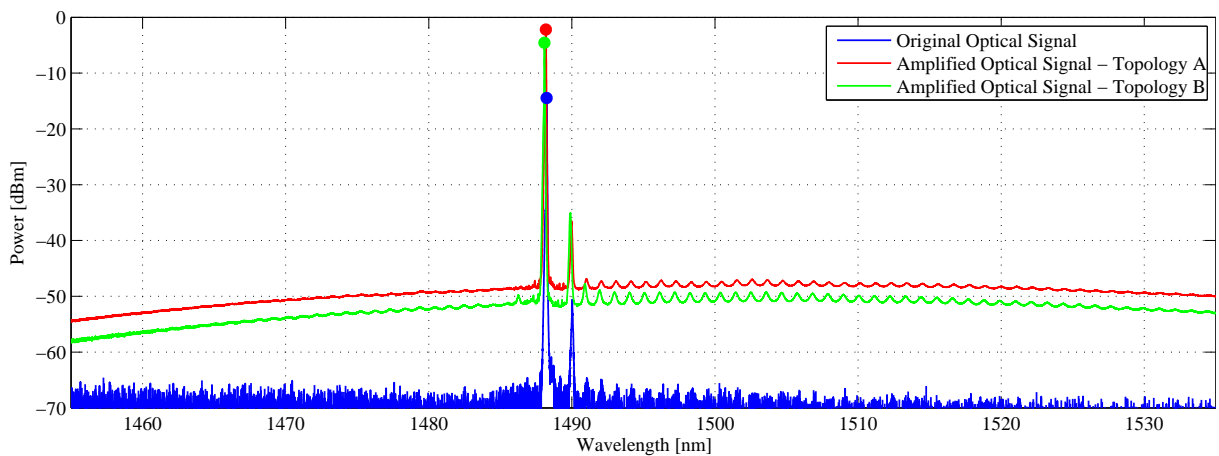


Figure 84: Comparison of downstream signals depending on topology - 5 km

From the figure can be seen that the topology A has better amplification of the downstream signal. But also, the amplification of the noise is the most significant. Because of that, the optical signal according to topology A has the lowest signal-to-noise ratio. Table 26 shows the measured values of the downstream optical signal.

Table 26: Comparison of peak gain and noise gain - downstream - 5 km

Topology	Peak power [dBm]	Noise power [dBm]	Peak Gain [dB]	Noise Gain [dB]	OSNR [dB]
Original	-14.59	-65.02	-	-	50.59
A	-2.34	-47.58	12.25	17.44	45.24
B	-4.38	-50.96	10.21	14.06	46.57

The Figure 85 shows the downstream optical signal after the 25 km of the optical trace. From the Table 27 is obvious that the peak gain is increased. But with the increasing length of the optical trace, the signal-to-noise is decreasing.

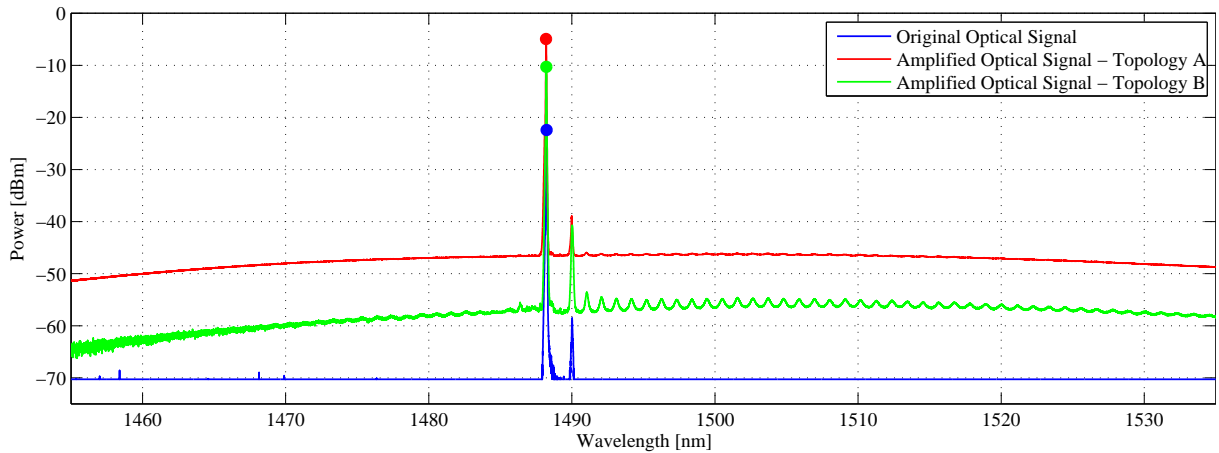


Figure 85: Comparison of downstream signals depending on topology - 25 km

Table 27: Comparison of peak gain and noise gain - downstream - 25 km

Topology	Peak power [dBm]	Noise power [dBm]	Peak Gain [dB]	Noise Gain [dB]	OSNR [dB]
Original	-22.42	-70	-	-	47.58
A	-4.39	-46.27	17.49	23.73	41.34
B	-10.3	-56.08	12.12	13.92	45.78

### 11.3 Summary

From the previous figures and tables can be seen the significant gain of the semiconductor optical amplifiers. However, the optical noise is also increased. Although, the optical amplifiers has such a gain, the EPON network coverage was not increased. In each of the tested case, the ONU unit was not able to register when the length of the optical trace was the 30 km or more. In case of the topology B, the ONU was not registered even the optical trace was the 25 km. It can be caused due to small signal-to-noise ratio, when the photodetector is not able to recognize the signal. In case of the topology A, the upstream signal still had enough power and the high

Table 28: Resulting attenuation

<b>Component</b>	<b>IL @1310 nm [dB]</b>
Optical Trace 19.811 km	10,58
Optical Trace 5.039 km	3,09
Splitter 1:2	0,88
Splitter 1:2	0,82
WDM splitter	0,69
WDM splitter	0,58
<b>Total</b>	<b>16,64</b>

OSNR, but the registration of the ONU was not able. However, the EPON network coverage is limited by the upstream, because the downstream still had enough power and the ONU still detected the optical signal at wavelength of 1490 nm. It follows that EPON network is able to overcome attenuation of about 16.64 dB. This attenuation is calculated as the sum of the used components mentioned in previous sections and summary is shown in Table 28.

## 12 Hybrid EPON/xDSL Performance Testing

Hybrid EPON/xDSL network was build according to Figure 86, where the OLT of the EPON network is placed in the laboratory EB316 and the ONU unit, both DSLAMs and modems are placed in the laboratory EB215. For hybrid network integrity testing were applied two base tests according to standards RFC2544 and ITU-T Y.1564 EtherSAM.

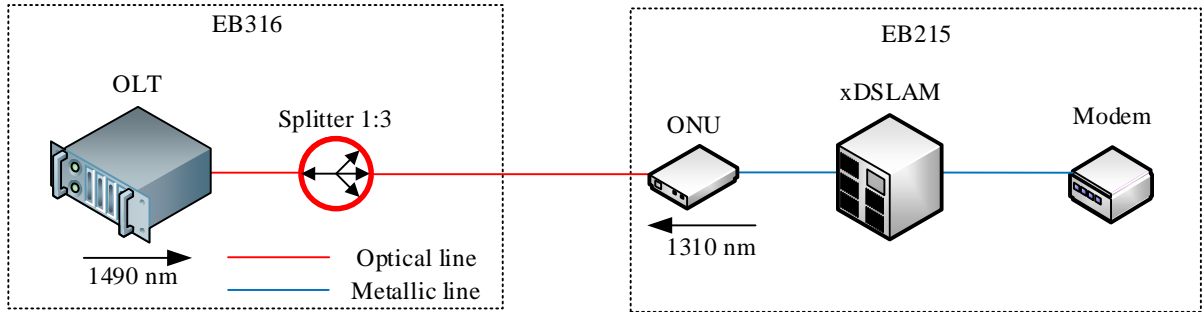


Figure 86: Base topology of hybrid xPON/xDSL network

### 12.1 RFC2544

The RFC2544 standard is the methodology that describes the tests required to measure performance criteria for carrier Ethernet networks. Throughput, back-to-back, frame loss and latency tests are for evaluate the performance of network, when each test validates a specific part of service-level-agreements (SLAs). To simulate various traffic conditions, the RFC supports seven pre-defined frame sizes (64, 128,256, 512, 1024, 1280 and 1518 bytes). Small frame sizes increase the number of transmitted frames.

#### 12.1.1 Throughput Test

The throughput test defines the maximum number of frames per second that can be transmitted without any error. The test starts at maximum frame rate and then compares the number of transmitted and received frames. If frame loss occurs, the transmission rate is divided by two and the test is restarted. If no frame occurs, then the transmission rate is increased by half of the difference from the previous trial. This trial-and-error methodology is repeated until the transmission rate, when no frame loss occurs.

#### 12.1.2 Back-to-Back Test

The back-to-back test reviews the buffering ability of a switch. It measures the maximum number of frames received at full line rate before a frame is lost. A burst of back-to-back frames is transmitted across the network with minimum interframe gap. If a frame is dropped, the burst length is decreased. If a frame is received, the burst length is increased [41].

### 12.1.3 Frame Loss Test

The frame loss test measures the network's response in overload conditions—a critical indicator of the network's ability to support real-time applications, when a large number of frame loss will rapidly degrade service quality [41].

The test sends traffic at maximum line rate and then measures if the network dropped any frames. If the frames are dropped, the test is restarted and the line rate is decreased. The test is repeated until there is no frame loss for the three consecutive iterations. The test results are presented as a percentage of frames that were dropped. The percentage indicates variable between the transmitted rate and the received frames [41].

### 12.1.4 Latency Test

The latency test measures the time, when the frame travels from the originating device through the network to the destination device. The another configuration is to test round trip time, when the frame travels from the originating device to the destination device and then back to originating device.

The test starts by measuring the throughput for each frame size to ensure the frames are transmitted without being discarded. This fills all device buffers to measure latency in the worst conditions. After that the device sends traffic for 120 seconds. At mid-point in the transmission, a frame must be tagged with a time-stamp and when it is received back at the test instrument, the latency is measured. The transmission should continue for the rest of the time period [41].

## 12.2 ITU-T Y.1564 EtherSAM

EtherSAM is a standard testing method, which supports complete validation of the Ethernet Service Level Agreements (SLA) in one test. The test is significantly faster and with higher accuracy than RFC2544. The standard ITU-T Y.1564 was released in 2010. Traffic is divided into the three traffic classes where each of the classes have assigned a specific colour: green traffic indicates the Committed Information Rate (CIR): green for committed traffic, yellow for excess traffic and red for discarded traffic (Figure 87) [42].

### 12.2.1 EtherSAM Traffic Classes

Committed Information Rate (CIR, green traffic) – is a guaranteed bandwidth for a specific service; this bandwidth has to be available at all times, minimum performance objectives are guaranteed.

Excess Information Rate (EIR, yellow traffic) – is a bandwidth above the CIR; availability depends on network loading and usage; minimum performance objectives are not guaranteed.

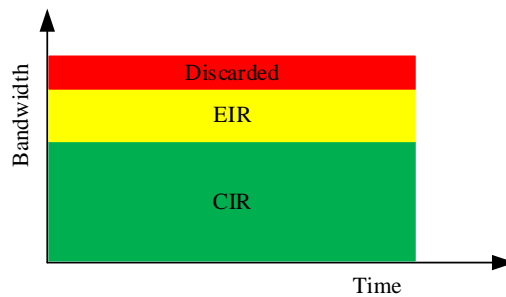


Figure 87: Traffic Classes [42]

## 12.2.2 Key Performance Indicators

Key performance indicators (KPIs) are characteristics that indicates the minimum performance of a particular traffic profile. The network has to guarantee minimum performance requirements under green traffic condition.

### 12.2.2.1 Bandwidth

Bandwidth refers to the maximum amount of data that can be forwarded. This measurement is a ratio of the total amount of traffic forwarded during a measurement window of one second.

### 12.2.2.2 Frame Delay (Latency)

Frame delay is measurement of the time delay between a packet's transmission and its reception. This measurement is a key factor for voice applications where too high frame delay can affect call quality [42].

### 12.2.2.3 Frame Loss

Frame loss can occur for many reasons, as a transmission errors or network overload. Errors caused by a physical phenomenon can occur during frame transmission, resulting in frame discard by network devices based on the frame check sequence field comparison. Network overload also causes frame discard when network device has to drop frame to prevent link overload [42].

### 12.2.2.4 Packet Jitter

Packet jitter means variability in arrival time between packet receipts. Packets are sorted to fronts and transmitted in bursts. Random priority can cause random transmission speeds. Therefore, the packets are received in an occasional intervals. Jitter seems as a confusion on the receiving buffers of the end nodes, when the buffers can be overused or underused [42].

### 12.2.3 Service Configuration Test

The service configuration test is a per-service test that verifies the bandwidth and performance requirements of a specific service, as defined by the user. The test is based on ramp test when the three phases of data traffic are generated:

- Minimum data rate to CIR,
- CIR to EIR,
- Traffic Policing (above the EIR).

These tests are resulting in a clear assessment of whether the network elements and path have been properly configured to forward the services while meeting minimum KPI performance objectives.

### 12.2.4 Service Performance Test

The service performance test generates all configured services at the same time and at the same CIR. During this period, each of the services is individually monitored [42].

### 12.2.5 Quality of Services

To ensure the quality of services, the SLAs have to meet requirements shown in Table 29. Table shows the maximum values.

Table 29: QoS requirements [43]

Service	Frame Loss [%]	Latency [ms]	Jitter [ms]
VoIP	1	150	30
Interactive Video	1	150	30
Streaming Video	5	4000-5000	-

In case of VoIP, frame loss causes voice clipping and skips. The loss of two or more consecutive packets results in a degradation of voice quality. Excessive latency also causes voice quality degradation. Interactive video has a such high demands because of use audio codec for voice and requires the same loss, latency, and jitter as VoIP. Streaming video applications have smaller requirements because they are not delay sensitive (the video can take several seconds to restoration). Because of application buffering is not sensitive to jitter [43].

## 12.3 Hybrid EPON/ADLS2+ network – RFC2544

The RFC2544 test was executed according to Figure 88. Optical fiber lines were 0 and 10 km long, where 0 km means the direct connection between the laboratory EB316 and the laboratory

EB215 (32.4 m). Metallic lines were 0 and 2 km long, where 0 km means direct connection with the length of cable about 1 m. For the testing was chosen the port with set downstream rate of 32 Mbps and the upstream rate of 4.096 Mbps. The RFC2544 Dual Test was applied, where the Ethernet Analyzer (AXS-200/350) was enabled as the Local unit and the Multiservice Tester (FTB-860) was enabled as the Remote unit. For the throughput were set the same rates as the set rates on the port of the ADSL2+ DSLAM.

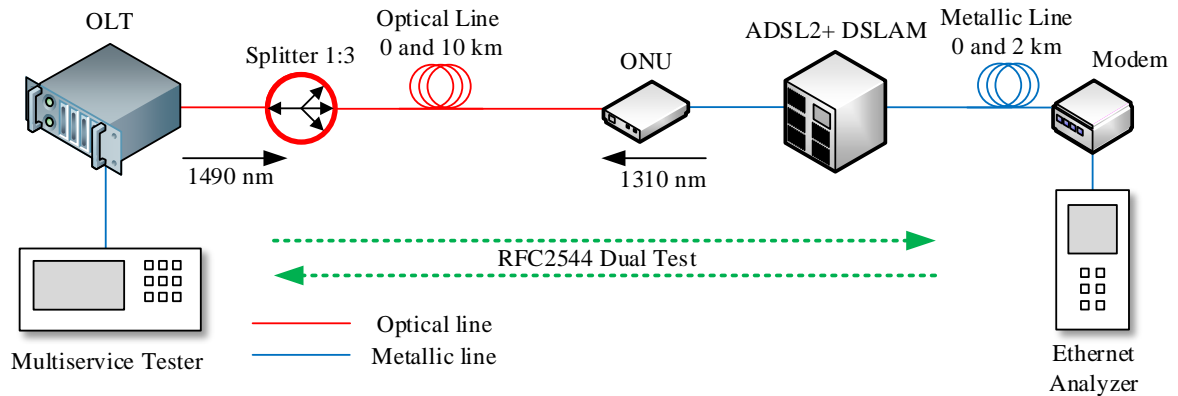


Figure 88: Topology for test hybrid EPON/ADSL2+ network (RFC2544)

The second used topology (Figure 89) for the ADSL2+ testing is with deployment of the semiconductor optical amplifiers. In this case, the length of the optical fiber line was 10 km. The lengths of the metallic line is the same as in previous topology i.e, 0 and 2 km.

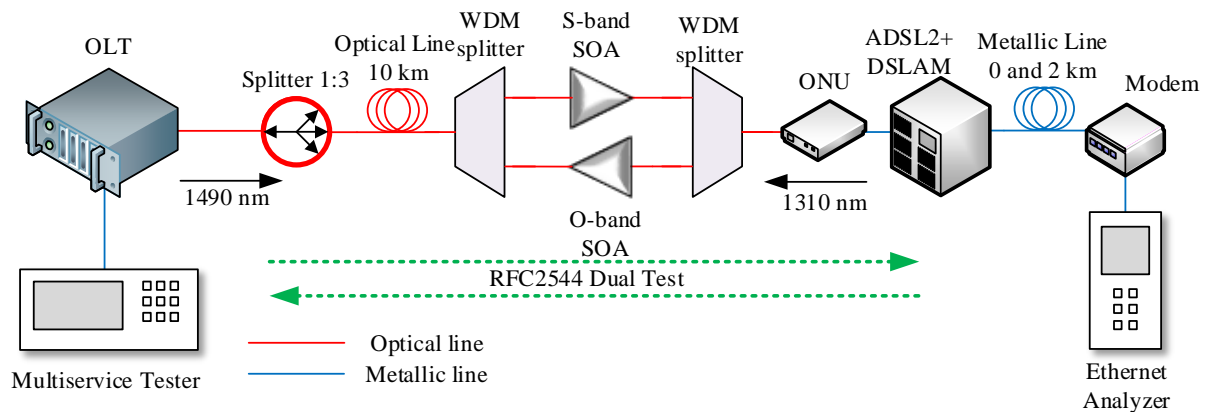


Figure 89: Topology for test hybrid EPON/ADSL2+ network (RFC2544) - SOA deployment

### 12.3.1 RFC2544 - EPON/ADSL2+ - Throughput

Frame sizes with the length of 64, 512, and 1518 bytes were chosen. The Figure 90 shows the throughput results in the upstream direction. The SOA mark in legend of the figure means the topology with the deployment of the semiconductor optical amplifiers.



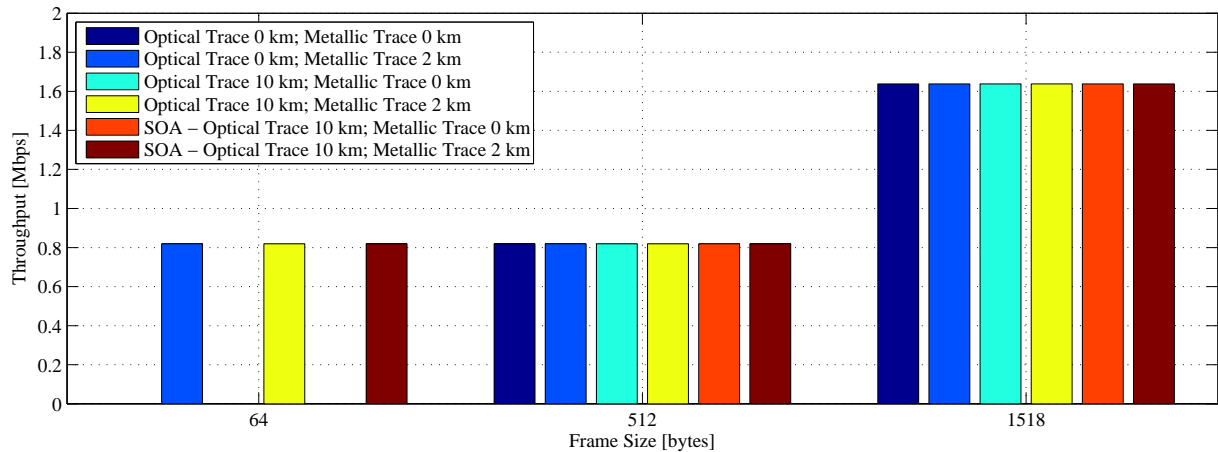


Figure 90: RFC2544 - EPON/ADSL2+ - Throughput - Upstream

From the bar chart is obvious that the upstream throughput is not dependent on the optical fiber length or the metallic line length. Only in case of metallic line = 0 is the upstream throughput 0 Mbps. Difference occurs between the frame sizes 64 respectively 512 bytes and 1518 bytes. Throughput when the frame sizes are the 64 bytes and 512 bytes is equal i.e., 0.819 Mbps. Throughput, when frame size is the 1518 bytes is at maximum ,i.e., 1.638 Mbps. This can be caused by modem, when the modem is not capable to process the high amount of the small frames. This link rate is slight higher than the link rate measured by ADSL2+ modem emulator.

The Figure 91 shows the downstream throughput of the ADSL2+. There is no visible dependence on the length of the optical fiber line, even the SOAs deployment does not have any influence on the downstream throughput. However, the downstream throughput is decreased with the increased length of the metallic line. The maximum downstream throughput is 22.4 Mbps when the frame size is 1518 bytes. When the length of the metallic line is 2 km, the throughput is 10.4 Mbps. Throughput is highly dependent on the length of the metallic line. A decrease in the length of the 2 km is more than 53

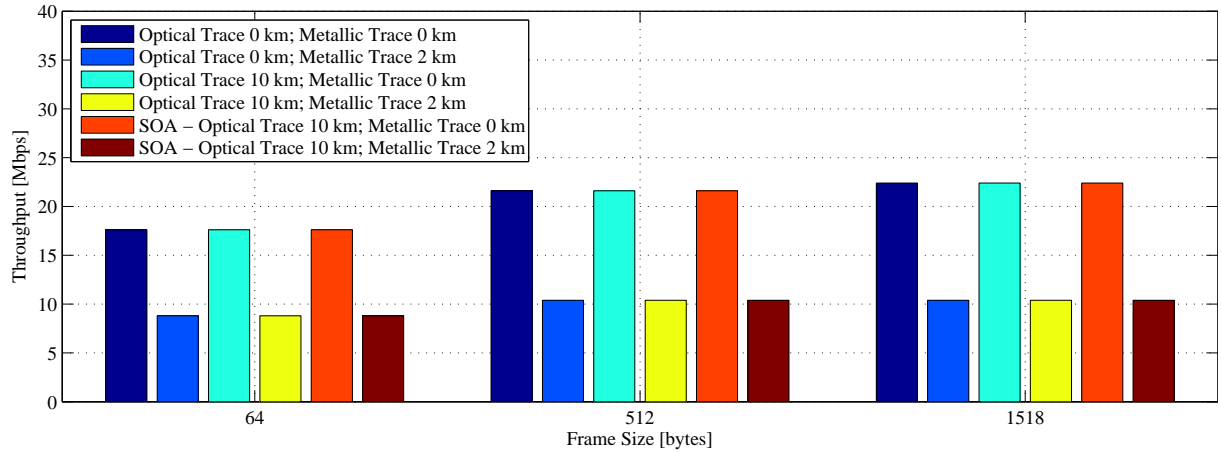


Figure 91: RFC2544 - EPON/ADSL2+ - Throughput - Downstream

### 12.3.2 RFC2544 - EPON/ADSL2+ - Back-to-Back

The Figure 92 shows the upstream Back-to-Back test results of the ADSL2+. There is no dependence on the length of the optical line or the metallic line. The differences occurs only with the changing the frame size. However, the back-to-back shows the extremely low values. The RFC2544 standard is adapted to test only the one active device in network. In this hybrid network are four active devices: OLT, ONU, DSLAM, and modem. That is the reason of the low values obtained by back-to-back tests.

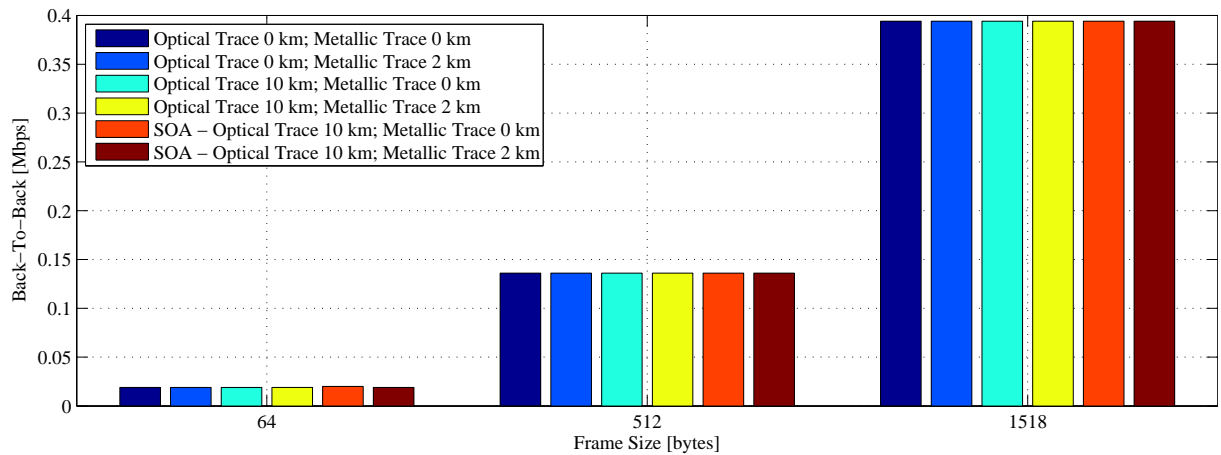


Figure 92: RFC2544 - EPON/ADSL2+ - Back-to-Back - Upstream

The Figure 93 shows the results of the back-to-back test for the downstream direction. Again there is not any dependence on the fiber length. The back-to-back is slight lower when the metallic line has the length of the 2 km. Also, the back-to-back is increasing with the frame size. However, the same applies as in the previous case.

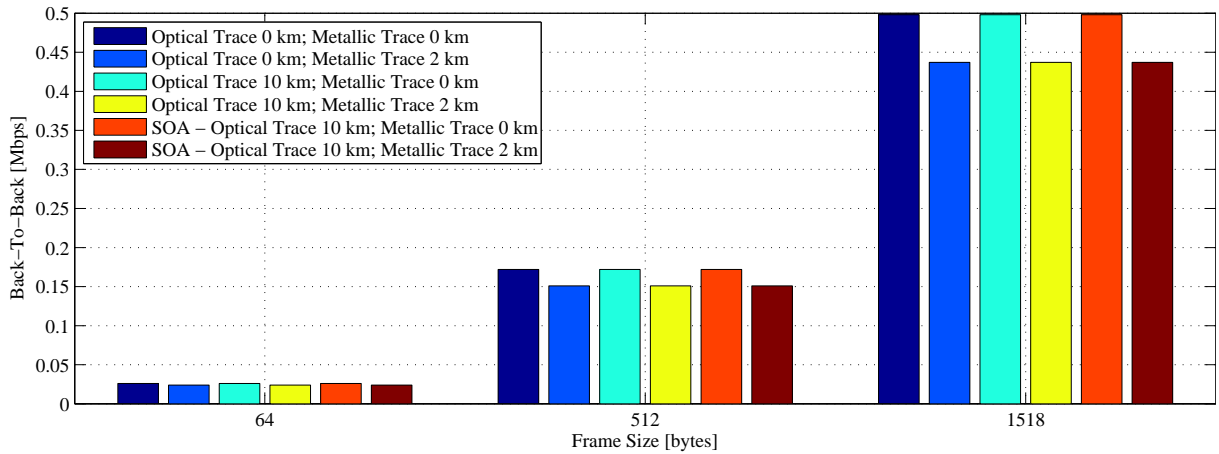


Figure 93: RFC2544 - EPON/ADSL2+ - Back-to-Back - Downstream

### 12.3.3 RFC2544 - EPON/ADSL2+ - Frame Loss

The Figure 94 shows the results of frame loss test in the upstream direction. The highest frame losses are at frame size of 64 bytes. The high frame losses are due to low throughput of the ADSL2+ link.

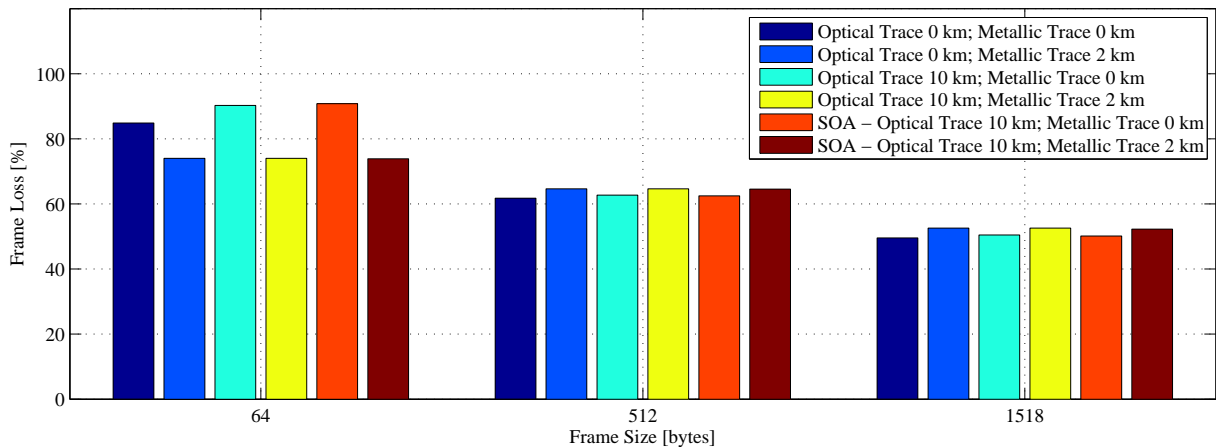


Figure 94: RFC2544 - EPON/ADSL2+ - Frame Loss - Upstream

The Figure 95 shows the results of the frame loss test in the downstream direction. From this figure can be seen that the highest frame losses occurs with the metallic line length of 2 km. Also, the small frame size has an influence on the frame losses.

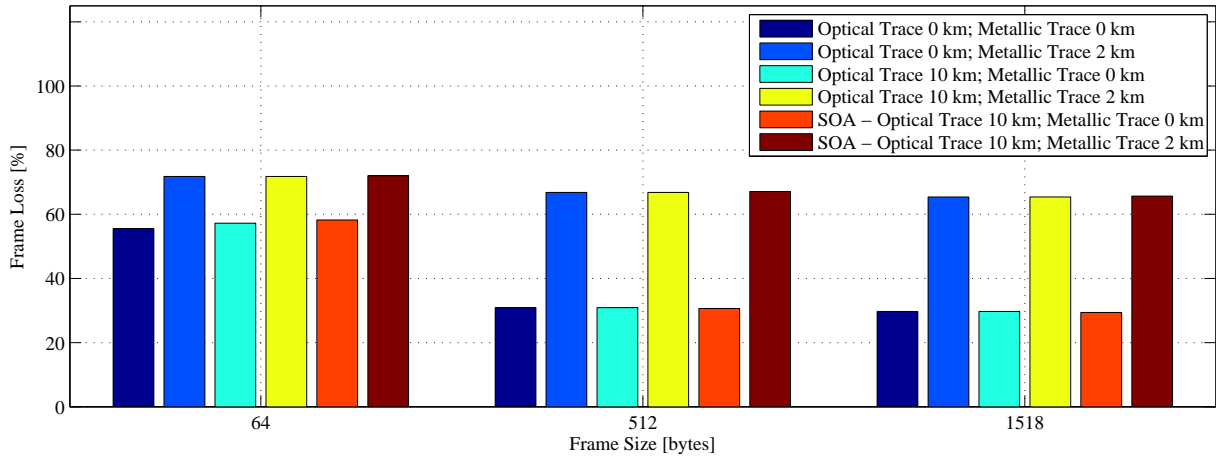


Figure 95: RFC2544 - EPON/ADSL2+ - Frame Loss - Downstream

### 12.3.4 RFC2544 - EPON/ADSL2+ - Latency

The Figure 96 shows the results of the latency test. The higher latency is at frame size of 1518 bytes (almost 250 ms). Again can be seen that the latency is increased with the length of the metallic line. However, this time is latency also increased with the length of the fiber.

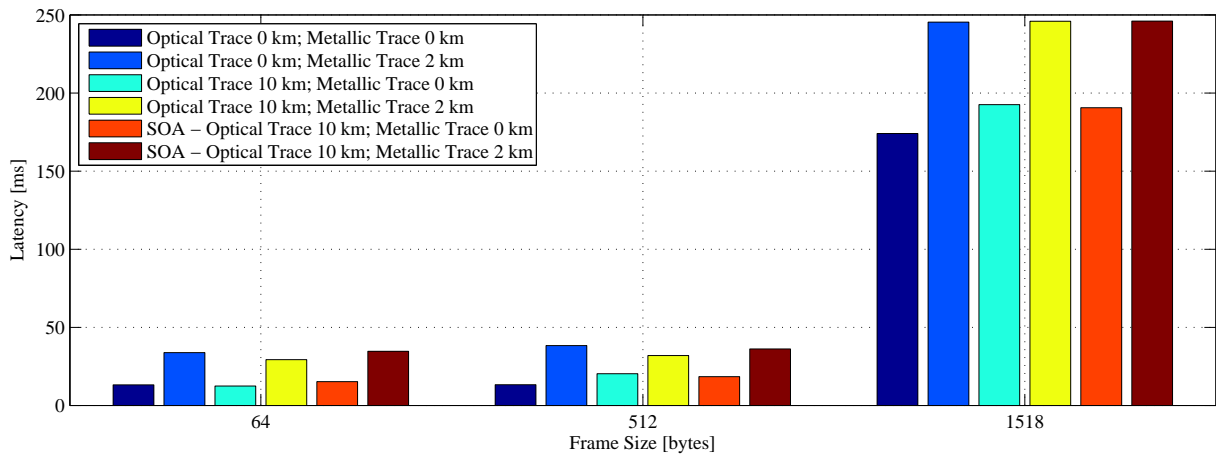


Figure 96: RFC2544 - EPON/ADSL2+ - Latency

## 12.4 Hybrid EPON/VDSL2 network – RFC2544

To test hybrid EPON/VDSL2 network were used the same topologies as in case of the EPON/ADSL2+ network except the used lengths of the metallic lines were 0 and 100 m. This time were tested two VDSL2 profiles. The first one (profile A) had set the downstream bit rate to 32 Mbps and the upstream bit rate to 32 Mbps. The second one (profile B) had set the downstream bit rate to 80 Mbps and the upstream bit rate to 45.44 Mbps. The same bit rates were set in RFC2544 Dual Test. The Figure 97 and the Figure 98 show the constructed topologies.

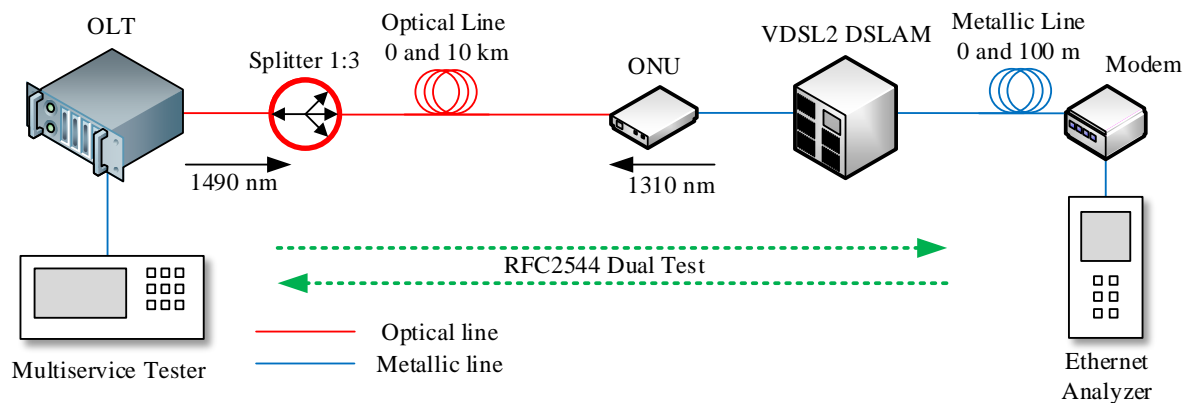


Figure 97: Topology for test hybrid EPON/VDSL2 network (RFC2544)

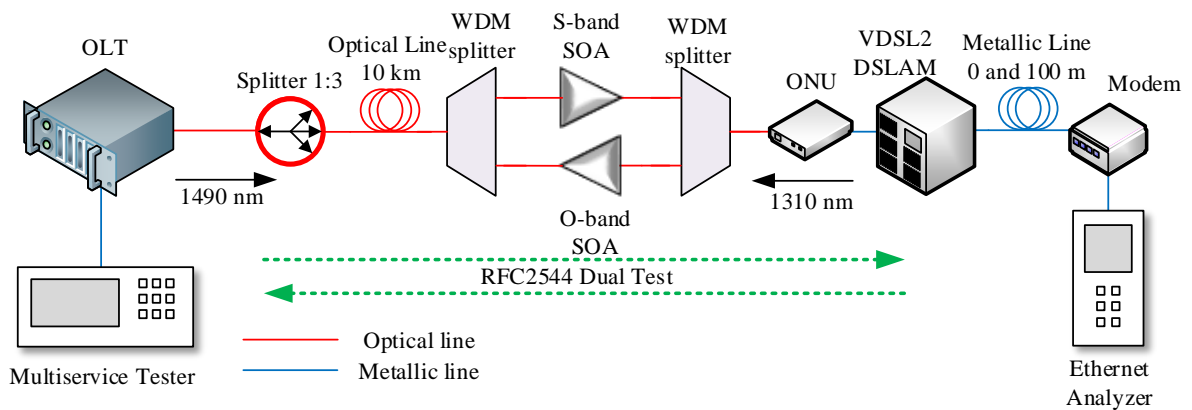


Figure 98: Topology for test hybrid EPON/VDSL2 network (RFC2544) - SOA deployment

### 12.4.1 RFC2544 - EPON/VDSL2 - Throughput

The Figure 99 (profile A) and Figure 100 (profile B) show the results of the throughput for the upstream. From the both figures can be seen that the throughput is highly dependent on the length of the metallic line. The maximum upstream throughput for the profile A is 32.028 Mbps at frame size of 512 bytes. For the profile B is maximum upstream throughput 35.218 Mbps at frame size of 1518 bytes.

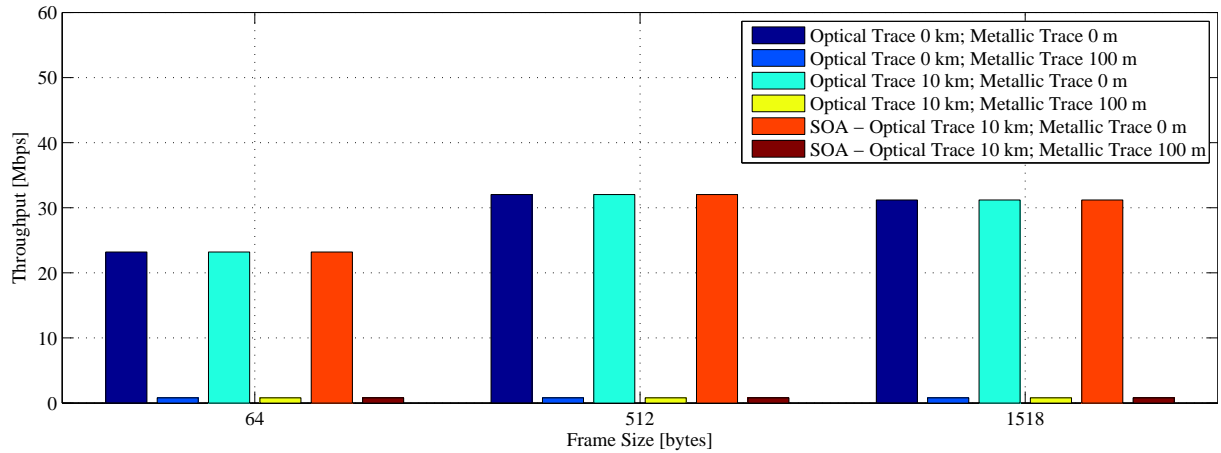


Figure 99: RFC2544 - EPON/VDSL2 - Throughput - Upstream - profile A

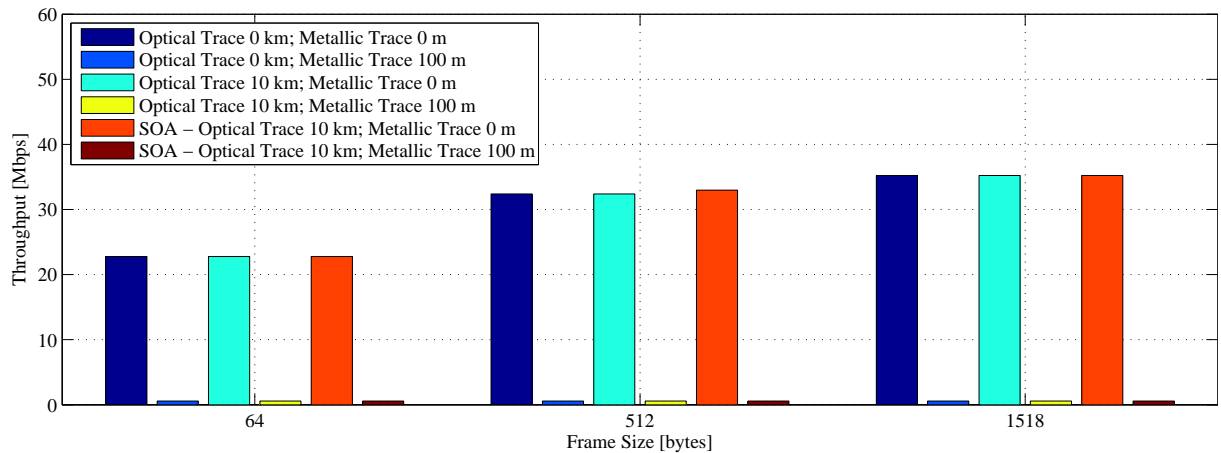


Figure 100: RFC2544 - EPON/VDSL2 - Throughput - Upstream - profile B

The Figure 101 (profile A) and Figure 102 (profile B) show the results of the throughput for the downstream. In this case, frames with the size of 64 bytes are the most suitable for the transmission. Also is visible that the downstream throughput is dependent especially on the length of the metallic wire. The maximum downstream throughput for the profile A is 32.028 Mbps, for the profile B is maximum downstream throughput 76.362 Mbps. The both profiles have the same throughput at wire length of 100 m, what is given by the wire attenuation.

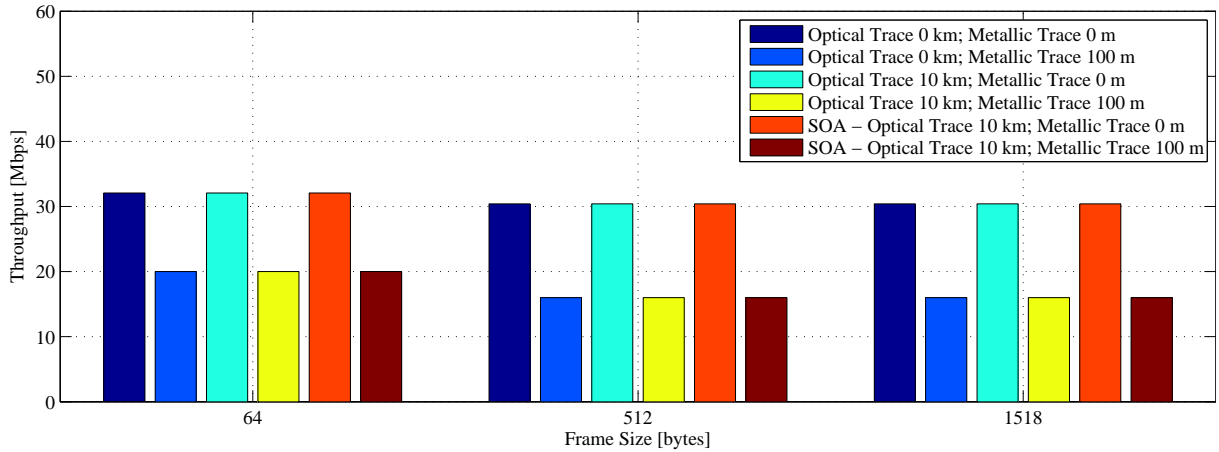


Figure 101: RFC2544 - EPON/VDSL2 - Throughput - Downstream - profile A

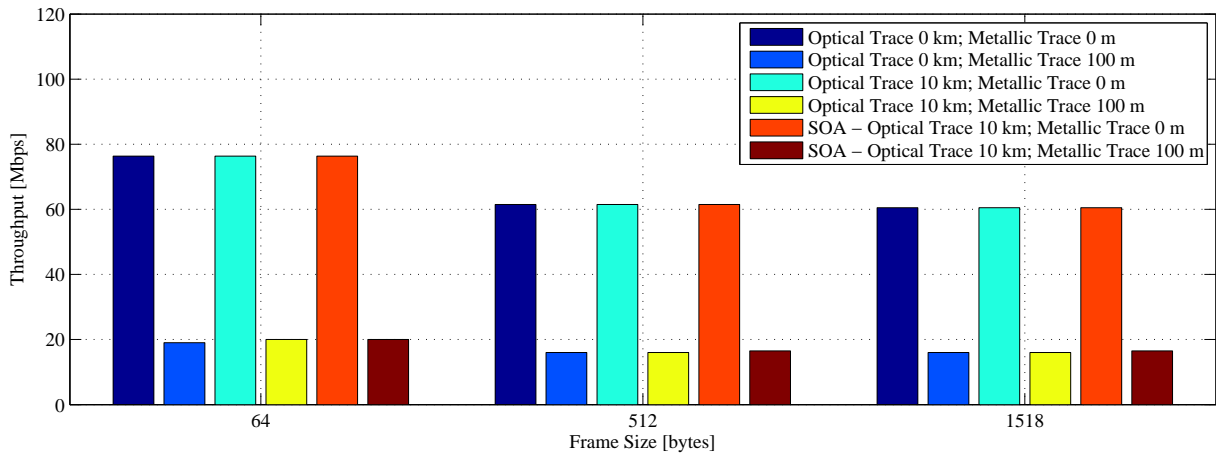


Figure 102: RFC2544 - EPON/VDSL2 - Throughput - Downstream - profile A

#### 12.4.2 RFC2544 - EPON/VDSL2 - Back-to-Back

The Figure 103 (profile A) and the Figure 104 (profile B) show the result of the back-to-back test for the upstream direction. In this case, the same applies as in the previous case with the ADSL2+. The RFC2544 standard is suitable for the one active device in the network. That is the reason of a such low values. Nevertheless, from figures can be seen that the length of the metallic line affects the results of the back-to-back testing.

The Figure 105 (profile A) and the Figure 106 (profile B) show the results of the back-to-back test in the downstream direction. The results show that the highest back-to-back is able at frame size of 1518 bytes.

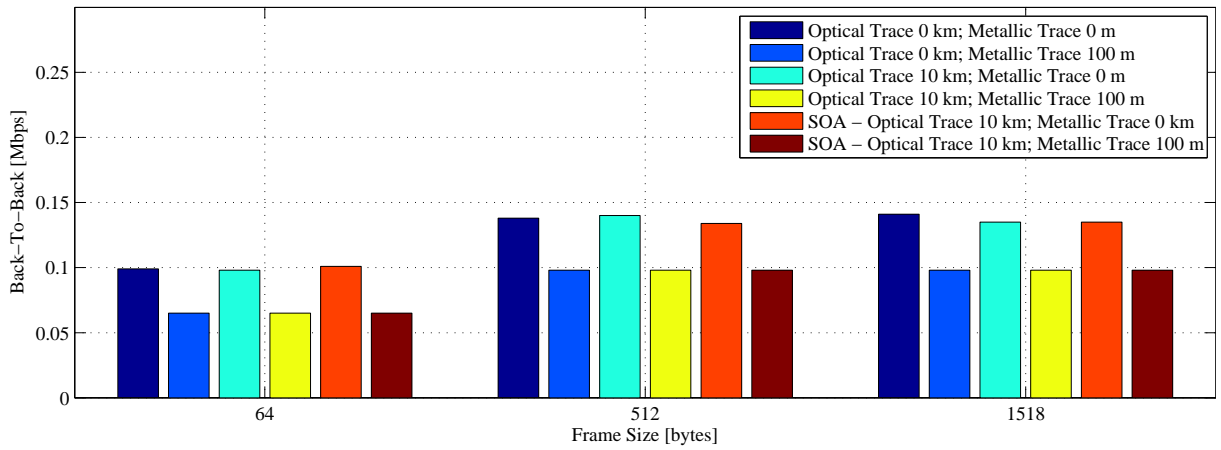


Figure 103: RFC2544 - EPON/VDSL2 - Back-to-Back - Upstream - profile A

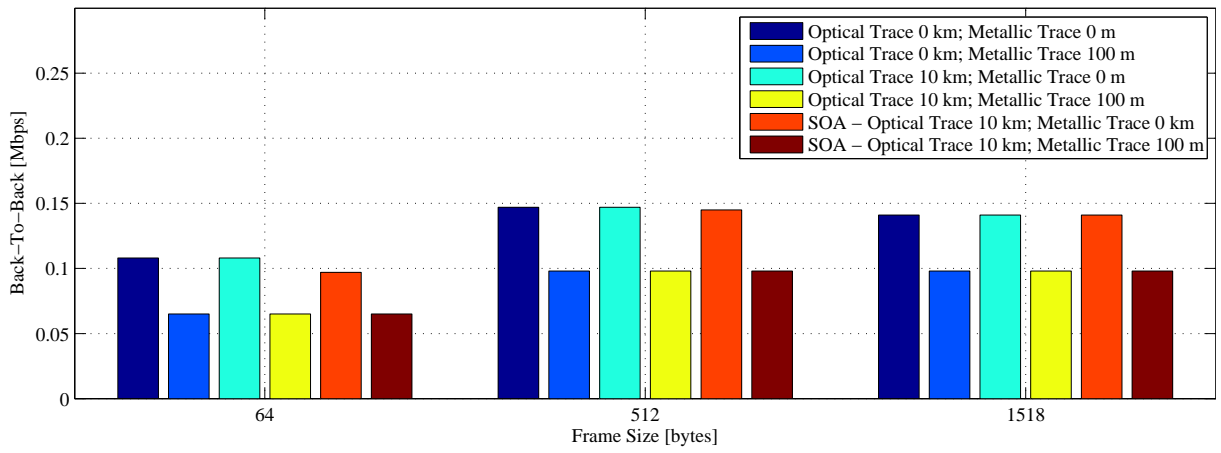


Figure 104: RFC2544 - EPON/VDSL2 - Back-to-Back - Upstream - profile B

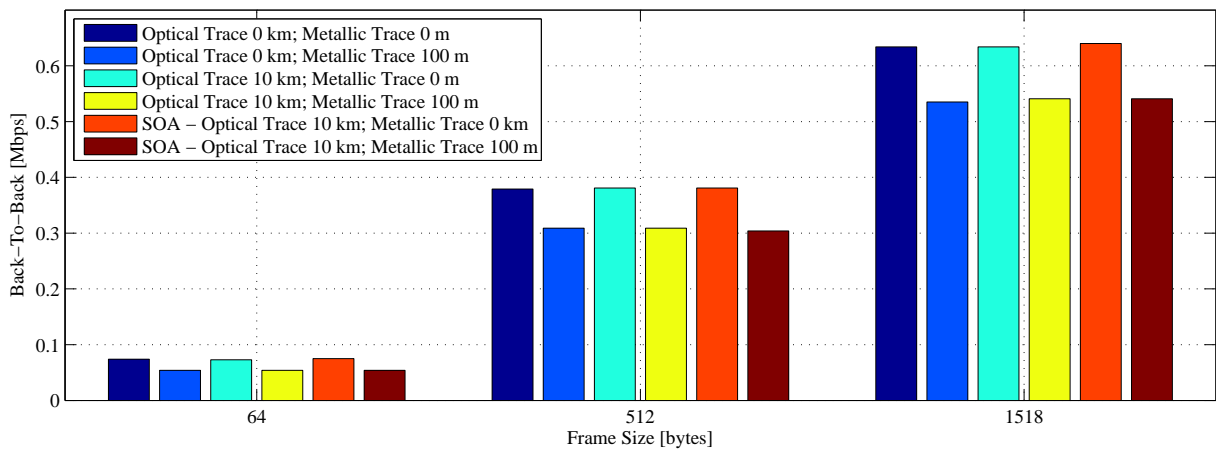


Figure 105: RFC2544 - EPON/VDSL2 - Back-to-Back - Downstream - profile A



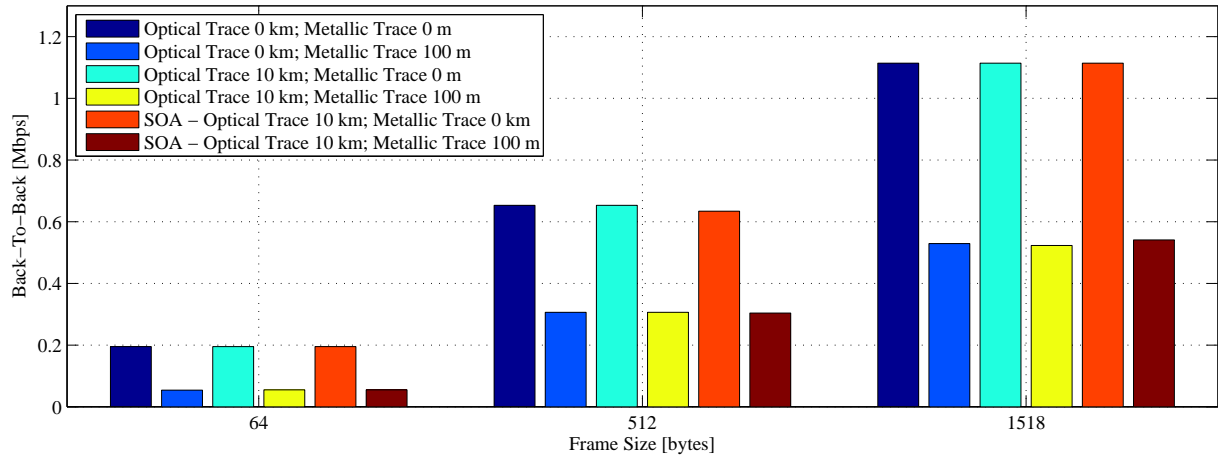


Figure 106: RFC2544 - EPON/VDSL2 - Back-to-Back - Downstream - profile B

### 12.4.3 RFC2544 - EPON/VDSL2 - Frame Loss

The Figure 107 (profile A) and the Figure 108 (profile B) show the results of the frame loss for the upstream direction. According the results of throughput for the upstream, frame loss is almost 100% in case of the length of the metallic line 100 m. In other cases is frame loss close to zero.

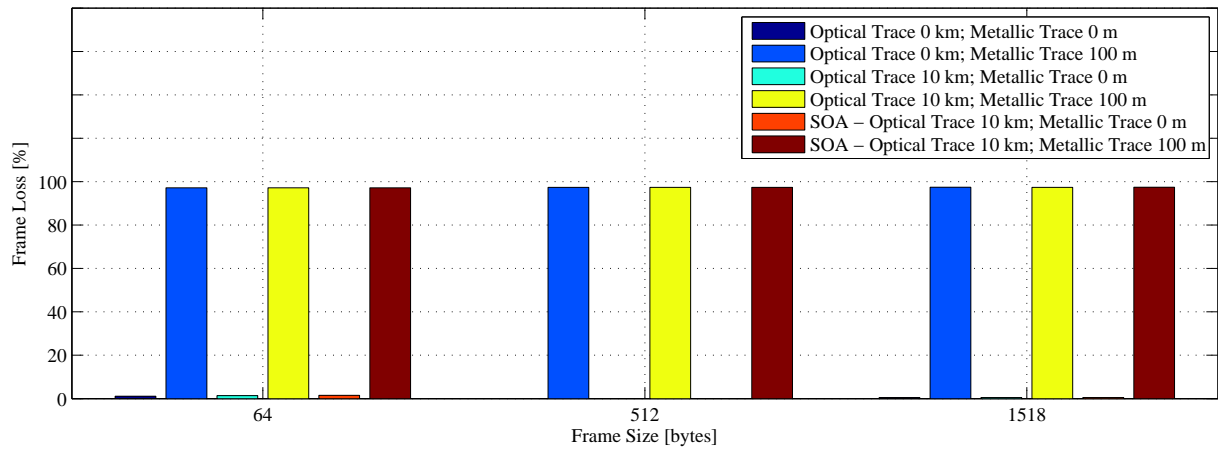


Figure 107: RFC2544 - EPON/VDSL2 - Frame Loss - Upstream - profile A

The Figure 109 (profile A) and the Figure 110 (profile B) show the results of the frame loss for the downstream direction. Because of the frame loss dependence on the throughput are the results so high in case of the metallic line length of the 100 m. Frame loss also increases with the increasing frame size.

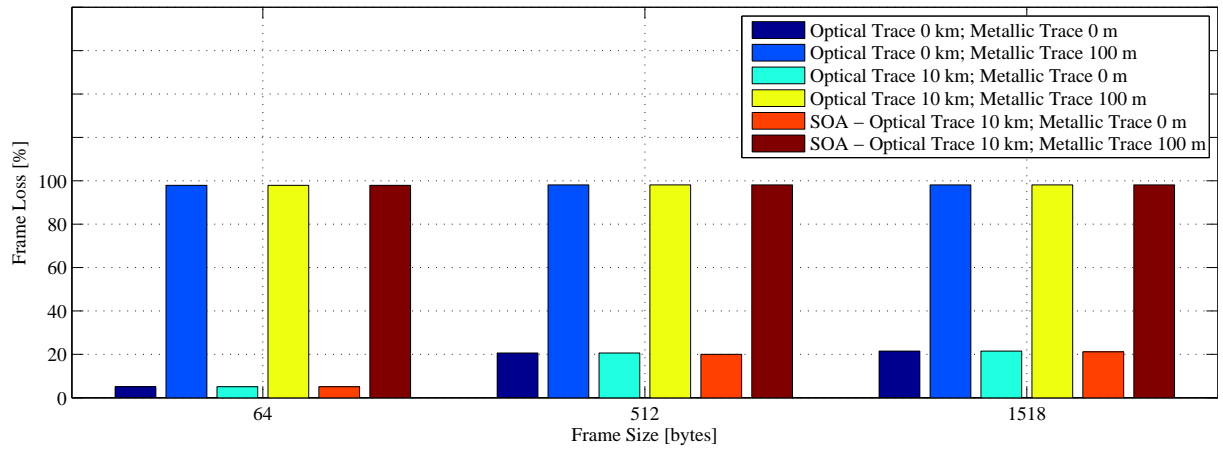


Figure 108: RFC2544 - EPON/VDSL2 - Frame Loss - Upstream - profile B

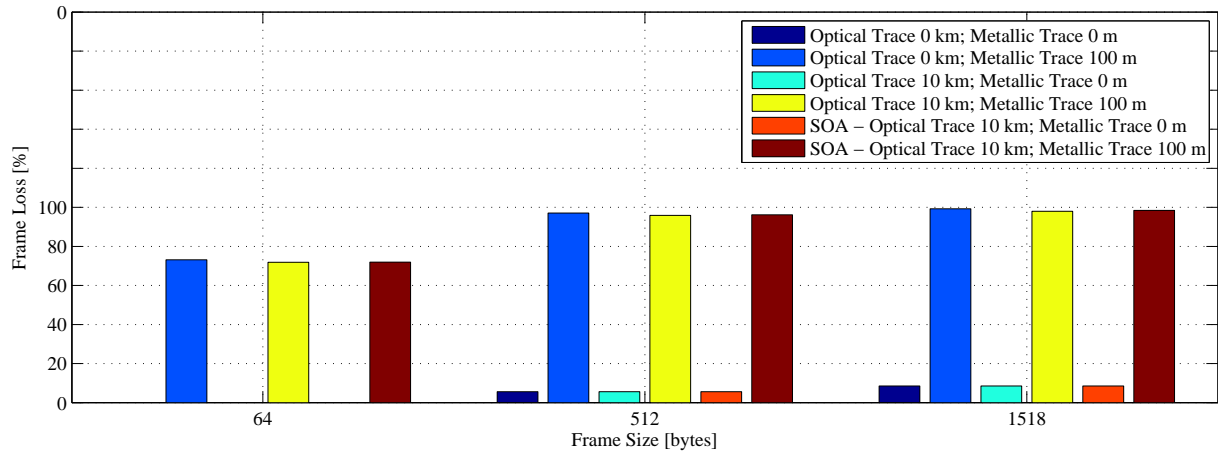


Figure 109: RFC2544 - EPON/VDSL2 - Frame Loss - Downstream - profile A

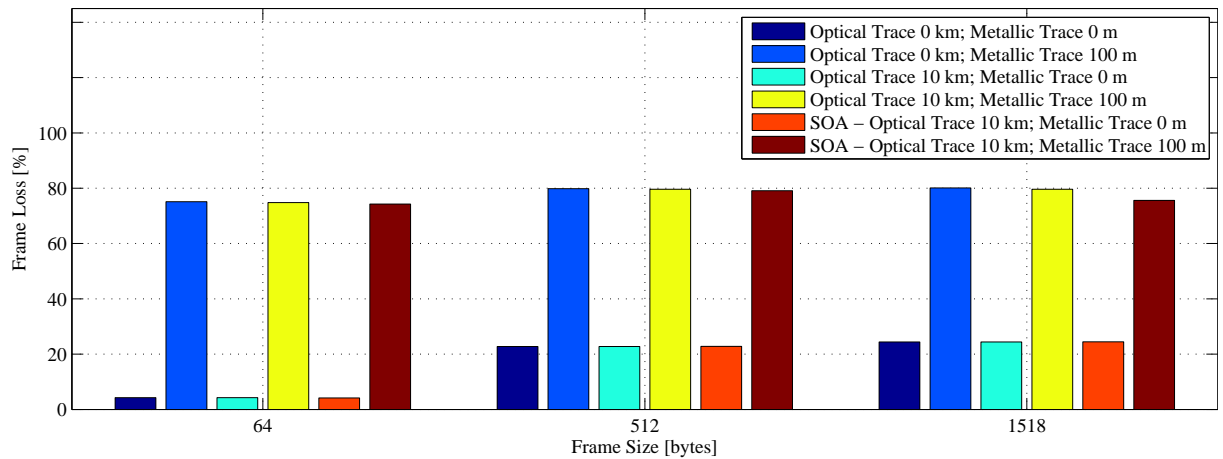


Figure 110: RFC2544 - EPON/VDSL2 - Frame Loss - Downstream - profile B

#### 12.4.4 RFC2544 - EPON/VDSL2 - Latency

The Figure 111 (profile A) and the Figure 112 (profile B) shows the latency results. Again can be seen that the latency is highly dependent on the metallic line. Dependence on the length of the fiber is not visible.

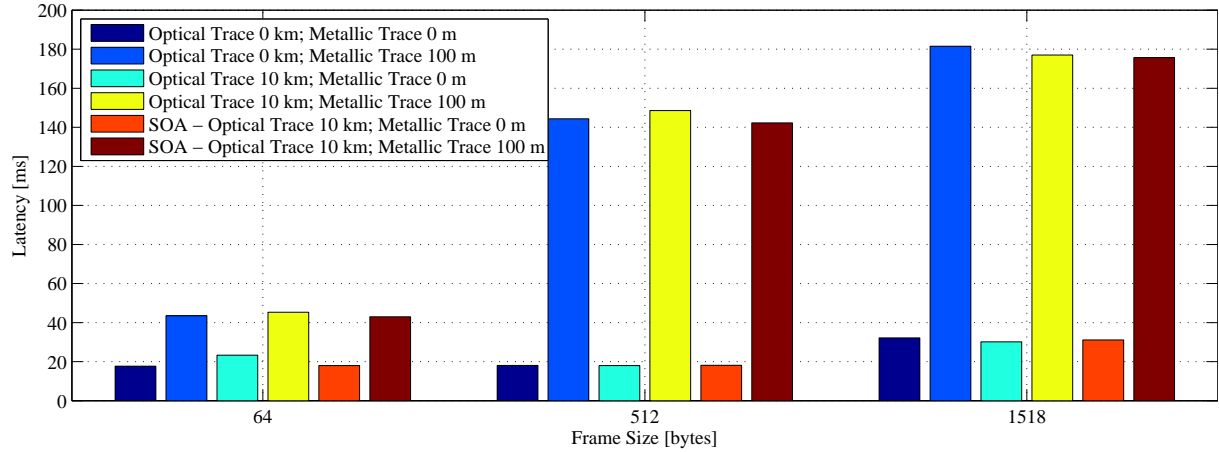


Figure 111: RFC2544 - EPON/VDSL2 - Latency - profile A

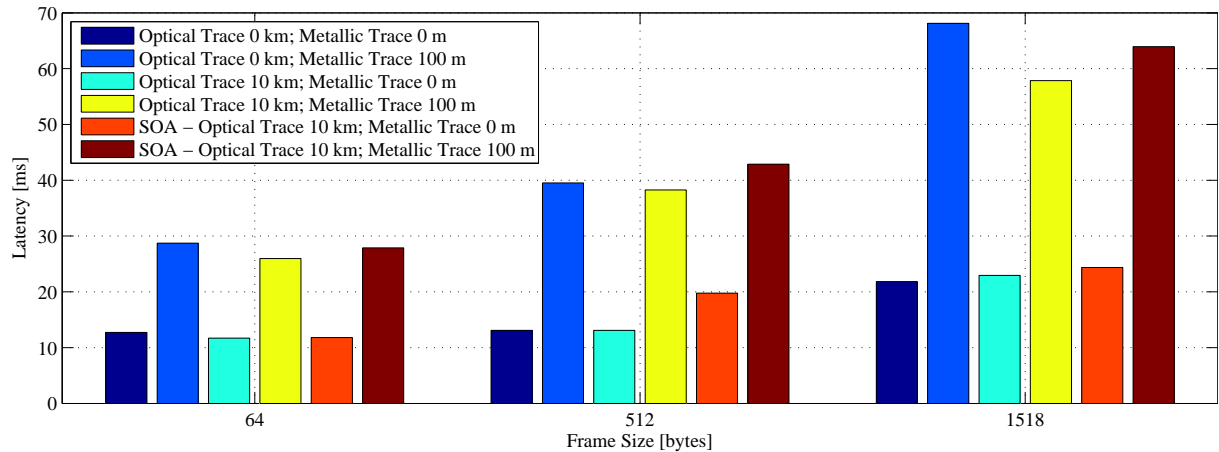


Figure 112: RFC2544 - EPON/VDSL2 - Latency - profile B

## 12.5 RFC2544 – Summary

Results from the RFC2544 show that there is not visible dependence on the length of the optical fiber line. Not even when the semiconductor optical amplifiers are implemented to the topology. However, the tests were not executed at higher length of the fiber, because every attempt to test RFC 2544 at the length of the optical fiber higher than 10 km was aborted. For that reason is highly likely that results would be significantly different. High influence of the metallic line is visible. ADSL2+ can support only the fraction of its original bit rates at the length of the metallic line 2 km in the downstream direction. In case of the upstream direction, the parameters are not affected by the metallic line because ADSL2+ upstream uses the low frequencies. The performance metrics of the hybrid EPON/VDSL2 network are mostly affected by the metallic line. The metallic line 100 m long causes the extremely high degradation of network parameters and it is evident that use of this line length is not very useful.

## 12.6 Hybrid EPON/ADSL2+ network – ITU-T Y.1564 EtherSAM

To test hybrid EPON/ADSL2+ network was also applied EtherSAM test. Unfortunately, there was not any device to apply the EtherSAM Dual Test. For that reason was applied the basic EtherSAM test according to the Figure 113 and the Figure 114. The modem was connected with the multiservice tester (FTB-860), where the EtherSAM test was launched. The OLT was connected with the Ethernet analyzer which served as the loopback unit. The test was limited by the upstream link rate, so the EtherSAM profile had to be set in accordance with the following Table 30. On the basis of the RFC2544 test results, the bit rates higher than 1.5 Mbps cause the distortion of the results. From the RFC2544 test is obvious that the length of the metallic line has a great impact to the hybrid network characteristics. For that reason, I decided to underline the impact of the length of the optical fiber and the semiconductor optical amplifiers deployment. Thereby, the following analysis are aimed to analyze the impact of the fiber length on the quality of services. The same is applied in testing hybrid EPON/VDSL2 network by EtherSAM. Full graphs are shown in attachments.

Table 30: Set profile to test EtherSAM ITU-T Y.1564 - EPON/ADSL2+

<b>Service</b>	<b>Type</b>	<b>Service Profile</b>	<b>Number of services</b>	<b>CIR [Mbps]</b>	<b>Frame Size [bytes]</b>
1	DATA	DATA	1	1.0	1374 (Fixed)
2	VoIP	G.723	5	0.136	82 (Fixed)

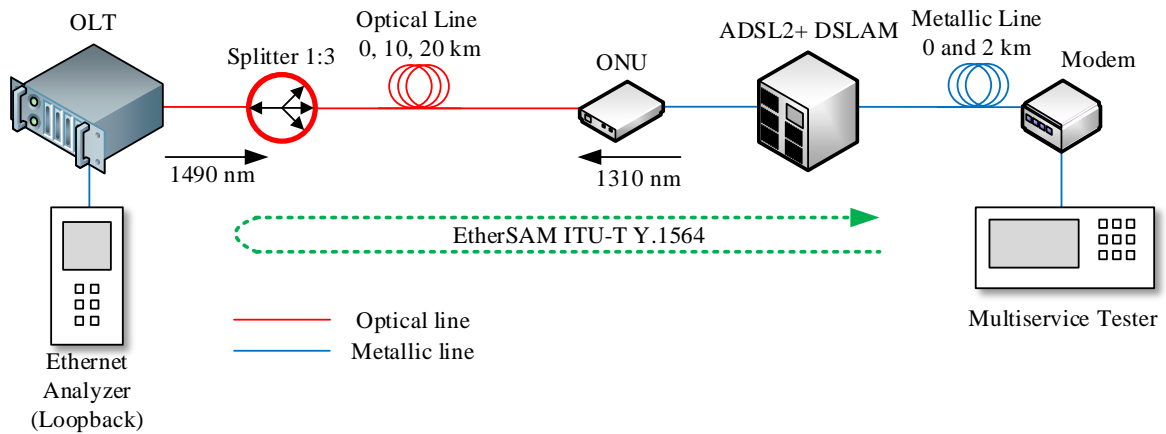


Figure 113: Topology to test hybrid EPON/ADSL2+ network (EtherSAM)

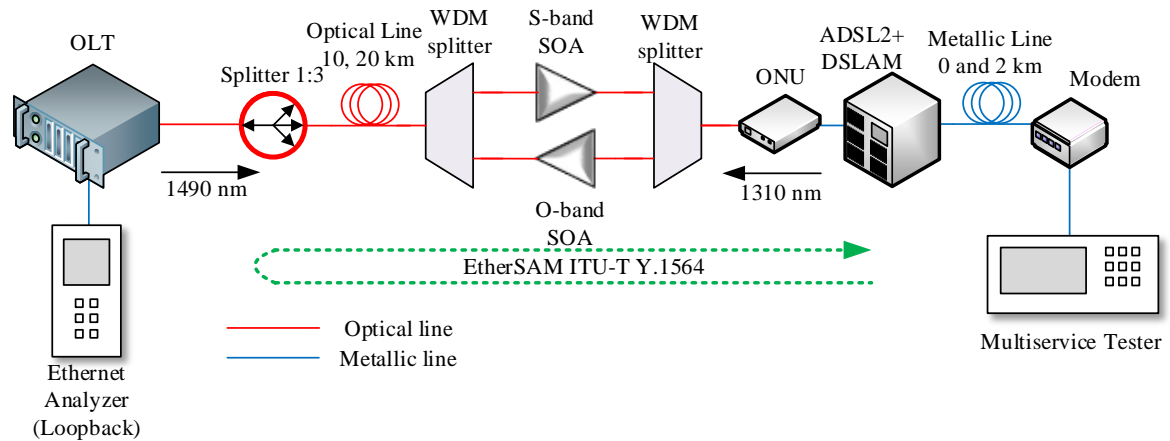


Figure 114: Topology to test hybrid EPON/ADSL2+ network (EtherSAM) - SOA deployment

### 12.6.1 EtherSAM -EPON/ADSL2+ - Average Throughput

Figure 115 shows the average throughput of the both services (data and VoIP). In every case is only direct connection between the DSLAM and the modem.

Direct connection and the optical fiber 10 km long between the OLT and and the ONU does not affect the throughput of the services. The decrease of the trthroughput occurs when the length of the fiber is 20 km. The deployment of the SOAs has also influence on the throughput. The data throughput is the same when the length of the optical trace is 20 km and in case when the length of the optical fiber is 10 km with deployment of the SOAs. Here we can see that the deployment of the SOAs has a negative impact on throughput of services. The CIR band for data can not be guaranteed in case of 20 km fiber lenght and also with deployment of SOAs. In case of VoIP, the throughput is not decreased.

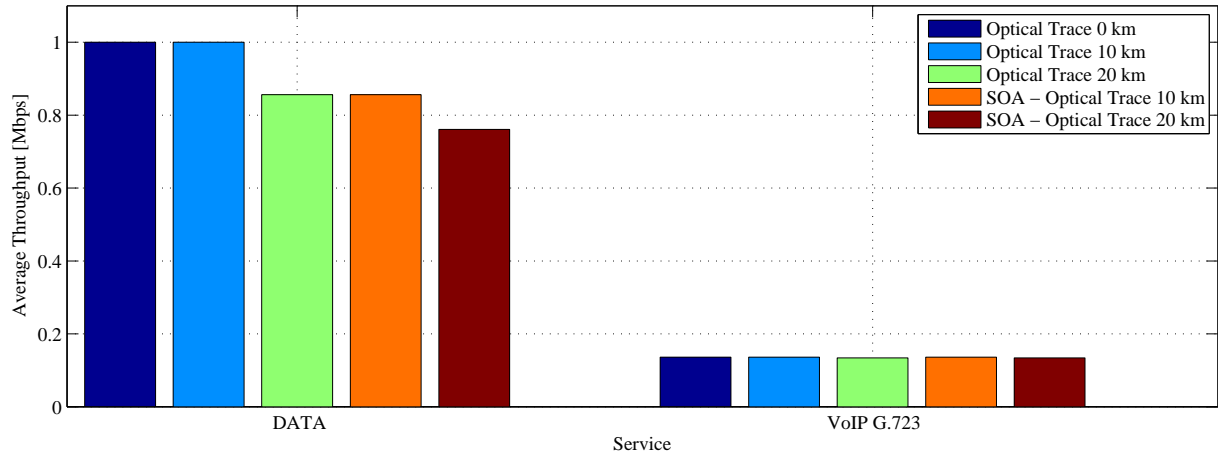


Figure 115: EtherSAM - EPON/ADSL2+ - Average Throughput

### 12.6.2 EtherSAM -EPON/ADSL2+ - Maximum Jitter

Figure 116 shows the maximum jitter depending on the length of the optical trace and deployment of the semiconductor optical amplifiers. The maximum value of the jitter occurs in case of the SOAs deployment together with the length of the fiber 20 km. The very deployment of the SOAs does not affect the jitter of the services. The used codec G.723 has almost two times higher jitter than jitter of the data. However, the jitter levels are sufficient for the service traffic.

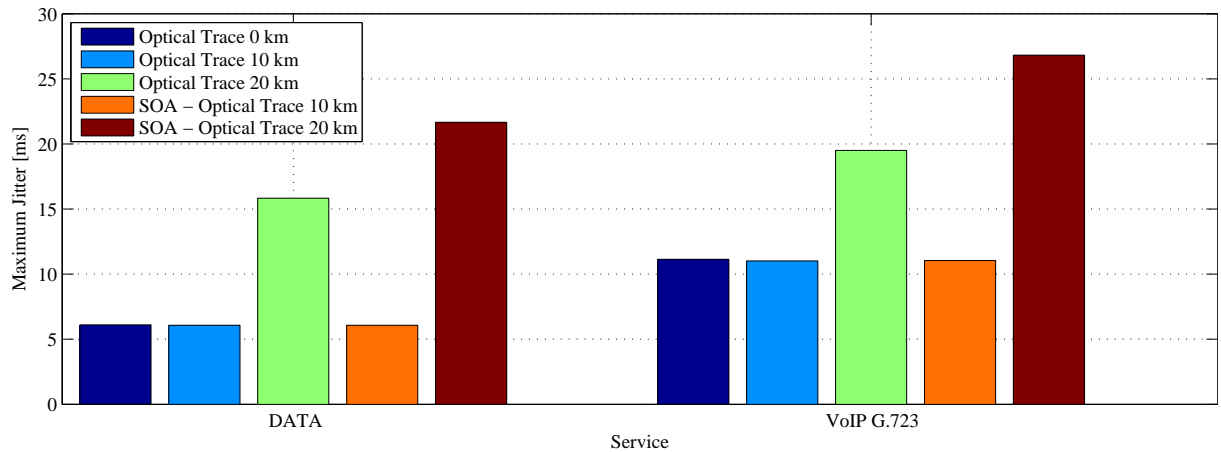


Figure 116: EtherSAM - EPON/ADSL2+ - Maximum Jitter

### 12.6.3 EtherSAM -EPON/ADSL2+ - Frame Loss

From the Figure 117 can be seen that frame loss occurs especially when the length of the optical fiber is 20 km. In case of the deployment the SOAs is the frame loss even higher. Frame loss for data is 14.2% in case 20 km fiber length and 23.5% with the SOAs deployment. Frame

loss for VoIP is 1.1% in case 20 km fiber length and 1.7% with the SOAs deployment. With the fiber length lower than 20 km is frame loss 0% for both services. The frame loss for VoIP slightly exceeds the maximum values and quality of voice service can be affected.

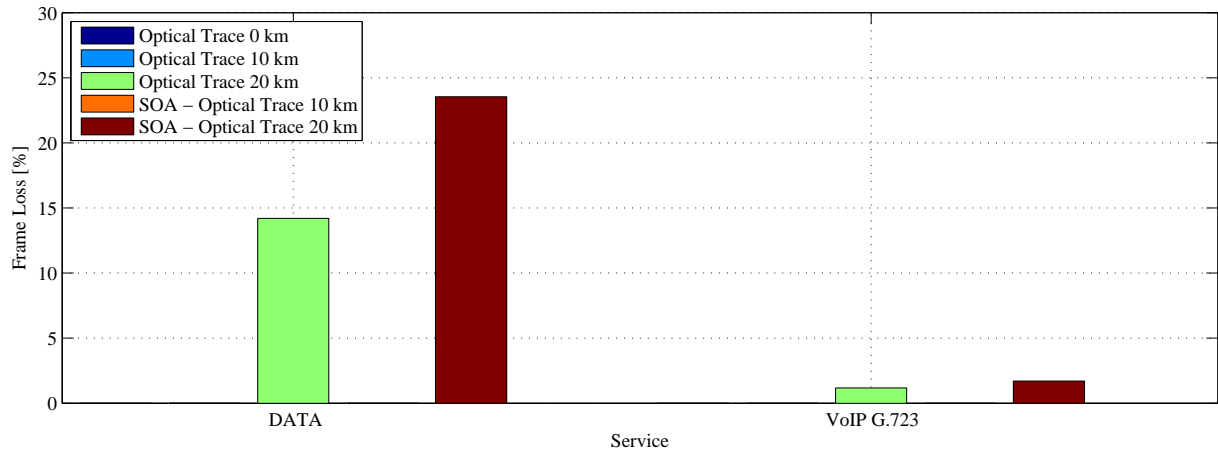


Figure 117: EtherSAM - EPON/ADSL2+ - Frame Loss

#### 12.6.4 EtherSAM -EPON/ADSL2+ - Round-trip Latency

From the Figure 118 can be seen that the latency is quite high in each of the cases. Latency increases with the length of the optical fiber line and also with the SOAs deployment. The latency to seamless traffic of VoIP is more than sufficient.

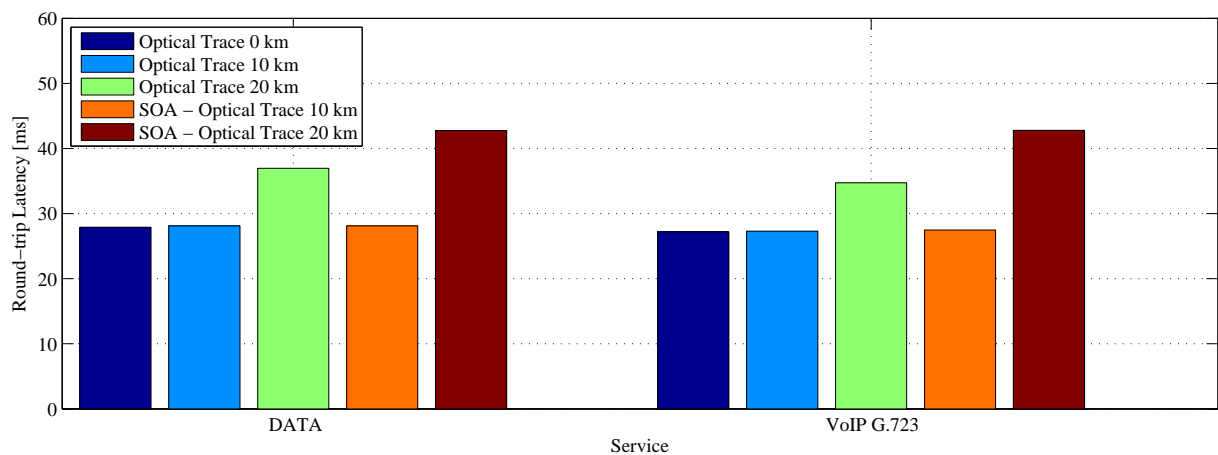


Figure 118: EtherSAM - EPON/ADSL2+ - Round-trip Latency

### 12.7 Hybrid EPON/VDSL2 network – ITU-T Y.1564 EtherSAM

The hybrid EPON/VDSL2 network was tested according the topologies in the Figure 119 and the Figure 120. The used VDSL2 profiles are the same as in case of the RFC2544 test.

To EtherSAM test over hybrid EPON/VDSL2 was created profile according to Table 31. This EtherSAM profile is set to both VDSL2 profiles, but due to similar results will be presented only the profile A. The complete results are attached on the DVD.

Table 31: Set profile to test EtherSAM ITU-T Y.1564 - EPON/VDSL2

Service	Type	Service Profile	Number of services	CIR [Mbps]	Frame Size [bytes]
1	IPTV	HDTV MPEG-4	1	10.592	1374 (Fixed)
2	VoIP	G.723	5	0.136	82 (Fixed)
3	DATA	DATA	1	20.000	Random

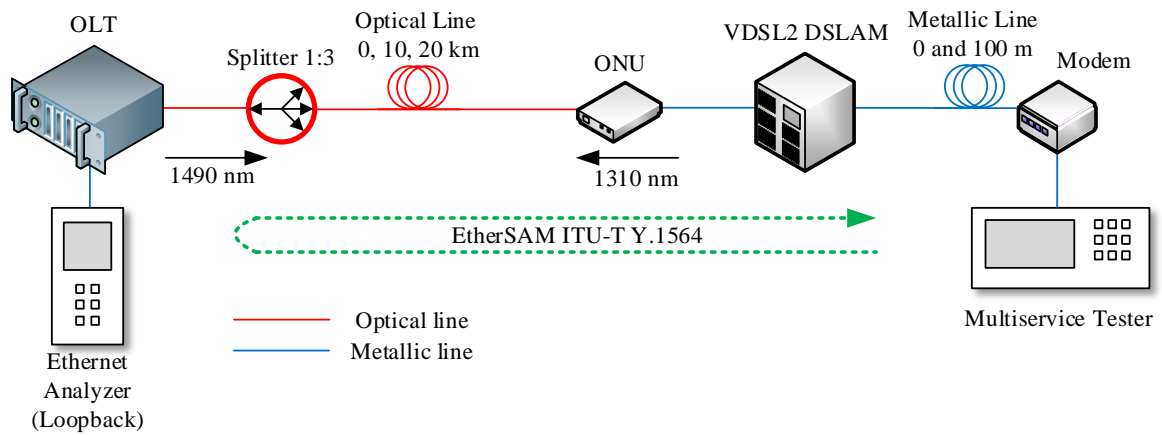


Figure 119: Topology to test hybrid EPON/VDSL2 network (EtherSAM)

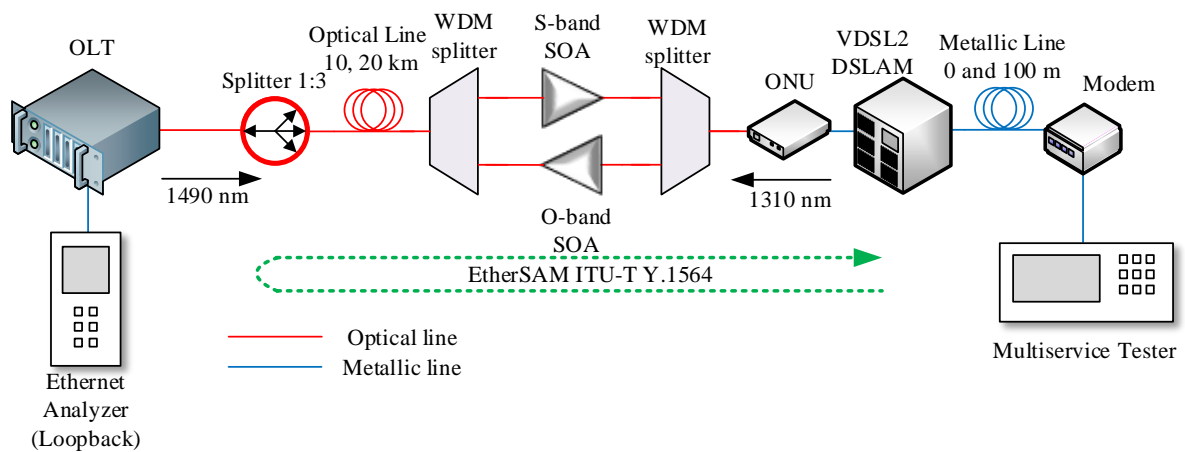


Figure 120: Topology to test hybrid EPON/VDSL2 network (EtherSAM) - SOA deployment



### 12.7.1 Average Throughput

Throughput of the services is considerably affected by the length of the metallic line. This was shown in previous sections where the results of the RFC2544 revealed a great influence of the metallic line. Again, I decided to refer the affect of the fiber length and also the SOAs deployment.

Figure 121 shows that if the fiber length is less than 20 km, the throughput of the all services is almost as the set CIR for each service. With the increasing the fiber length, the throughput of the each service is decreased. Also, the SOAs have a negative effect on the throughput. In most cases is throughput for services sufficient.

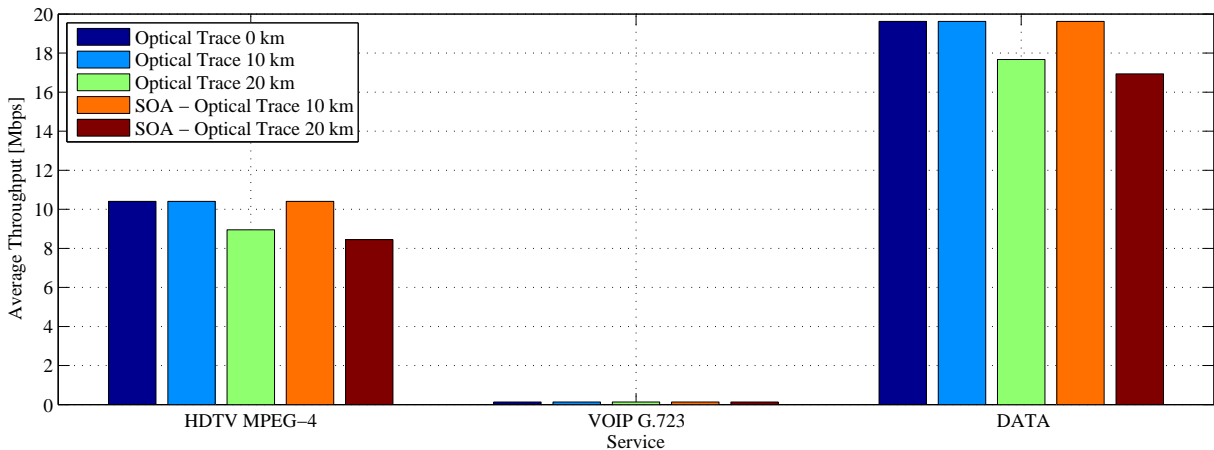


Figure 121: EtherSAM - EPON/VDSL2 - Average Throughput - profile A

### 12.7.2 Maximum Jitter

The Figure 122 shows the maximum jitter of each service. The increasing optical fiber results in the decreasing the maximum jitter of each service. In contrast, the deployment of the SOAs increases the jitter. It can be caused, that with the higher length the buffers have more time process data. However, the values of jitter are satisfactory for all services.

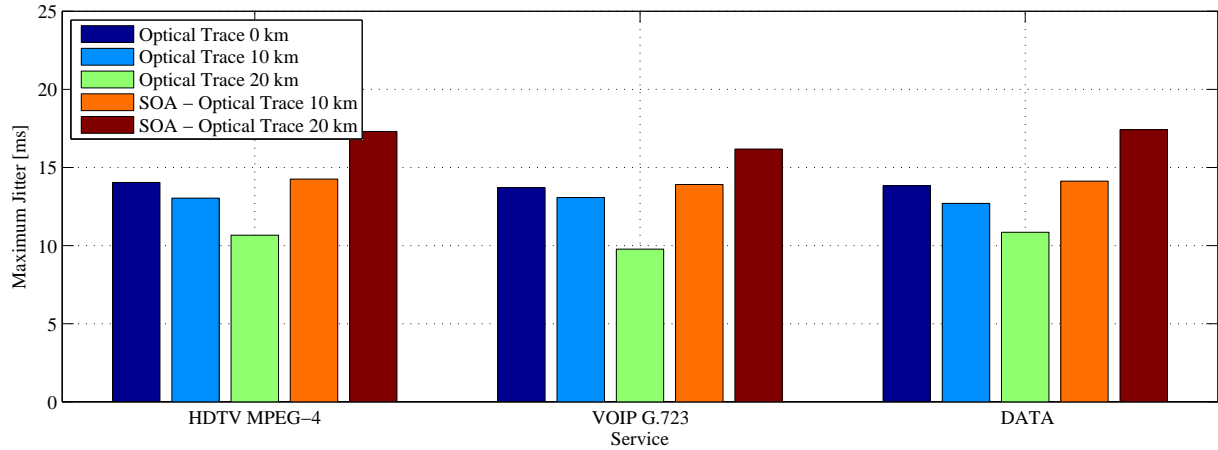


Figure 122: EtherSAM - EPON/VDSL2 - Maximum Jitter - profile A

### 12.7.3 Frame Loss

The Figure 123 shows the frame loss of the each service. From this figure is obvious, that the length of the fiber has the most impact on video and data transmission. In the other cases is the frame loss less than 3%. Although, the frame loss is more than 20% in case of deployment SOAs and fiber length of 20 km, all the time are demands for quality of services fulfilled.

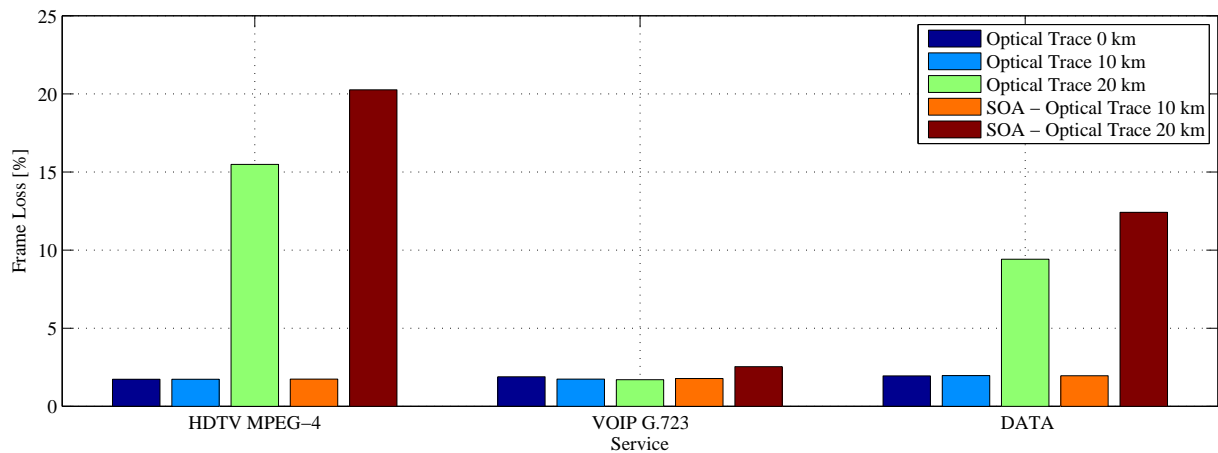


Figure 123: EtherSAM - EPON/VDSL2 - Frame Loss - profile A

### 12.7.4 Round-trip Latency

From Figure 124 can be seen that the latency is the lowest when the optical fiber is 20 km long. With the SOAs deployment is the latency increased, but still lower than in every other case. In no case is the value of latency over 150 ms, therefore the requirements for quality of services are met.

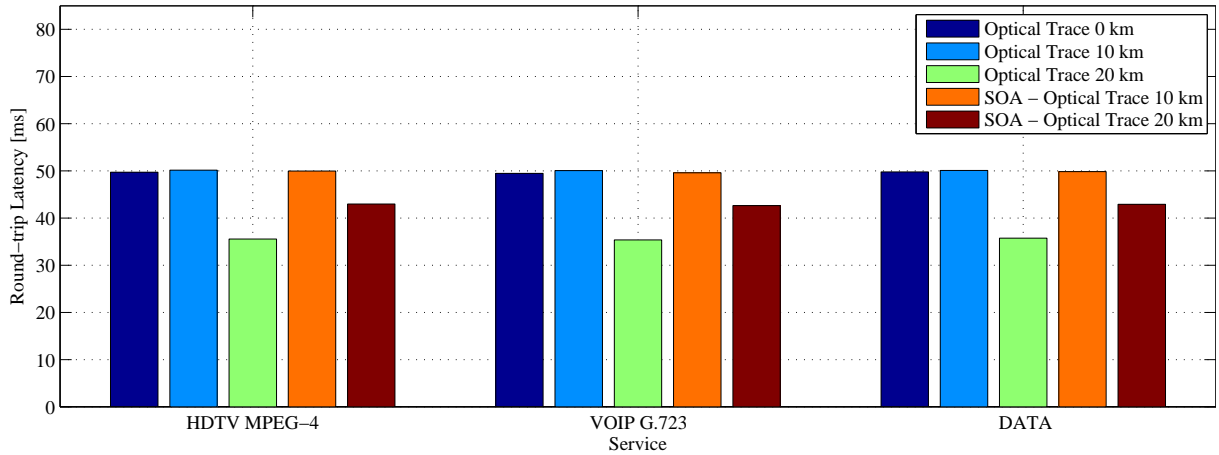


Figure 124: EtherSAM - EPON/VDSL2 - Round-trip Latency - profile A

## 12.8 ITU-T Y.1564 EtherSAM - Summary

From previous figures is obvious that the fiber length does not causes the great differences in SLA parameters except the frame loss. Frame loss is highly affected by the length of the fiber. Nevertheless, the all requirements for quality of service were fulfilled. Actually, the EIR band could be added under these conditions or the CIR could be increased. However, these demands are fulfilled in case that the modem is near the DSLAM. In case of increased length of the metallic lines, the results are far from sufficient.

## 13 Simulation of EPON network in Optiwave Software

The Optiwave OptiSystem is the simulation software to design, test, and optimization optical networks. The library offers large amount of active and passive components. With OptiSystem is able to test wide spectrum of optical networks, from an analog systems to backbone networks.

### 13.1 Optical Network Design

#### 13.1.1 Optical Line Termination

The transmitting part of the OLT unit is formed by the CW laser, which transmits at wavelength of 1490 nm and the output power is set to 7 dBm. To generate data is used Pseudo-Random Bit Sequence Generator, where the set bit rate is 1250 Mbps according to EPON. Such generated data are coded by the 8B10B Sequence Generator. 8B10B generator is connected to Non-Return-to-Zero (NRZ) pulse generator. The optical signal is modulated in external Mach-Zehnder Modulator by the NRZ pulse generator.

The receiving part of the OLT is formed by the PIN photodiode. PIN photodiode is an InGaAs (made from Indium, Gallium, and Arsenide) type. Electrical signal is processed by the linear Low Pass Bessel Filter, which remove the high frequency noise created by passing the optical trace. The 3R Regenerator recovers the shape and the time base of the signal. The BER analyzer shows the properties of the signal after passes the topology. Figure 125 shows the schematic of the OLT.

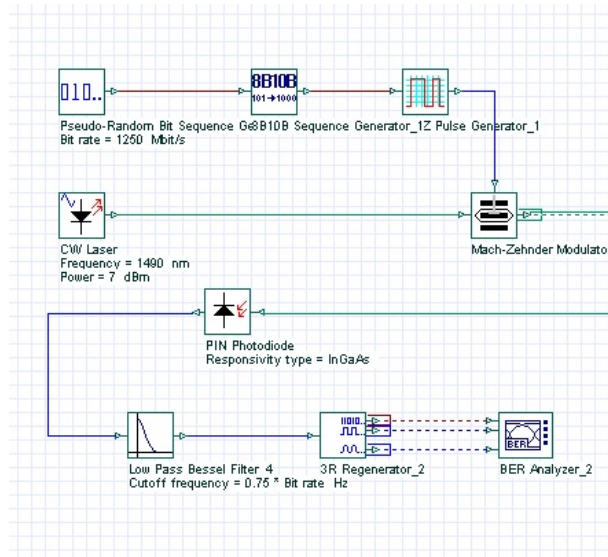


Figure 125: OLT in OptiSystem

### 13.1.2 Optical Network Unit

The ONU consists of the same components as the OLT unit. The only difference is in the CW laser settings, where the CW laser of the ONU transmits at wavelength of 1310 and the output power is 5 dBm. The Figure 126 shows the schematic of the ONU unit.

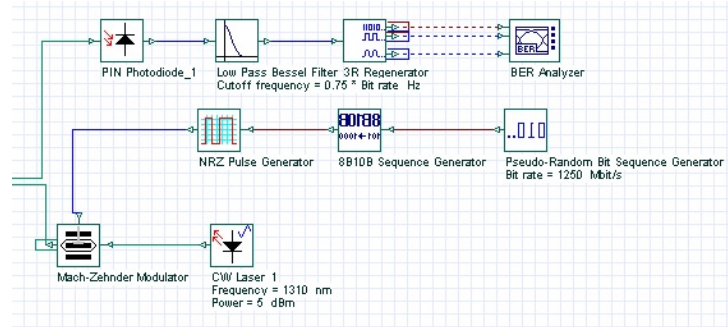


Figure 126: ONU in OptiSystem

### 13.1.3 Optical Distribution Network

The ODN consists of two bidirectional splitters with the insertion loss of 1.8 dB. In the ODN are not used the WDM splitters, because they have not any sense in the simulation. The components split the upstream and downstream direction by itself. As an optical fiber is used component Bidirectional Optical Fiber. The attenuation coefficient is set to 0.6 dB/km. Also, the PMD coefficient is set to 0.6 ps/km<sup>1/2</sup>. The fiber length is variable. Between the optical fiber and the splitter were placed optical amplifiers, where the gain of 14 dB is set to S-band SOA and the 8 dB is set to O-band SOA according to measurements. The Optical Delay component serves only for the simulation needs and its placement is necessary to bidirectional transmission. Then have to be increased number of iterations. The Figure 126 shows the schematic of the ODN.

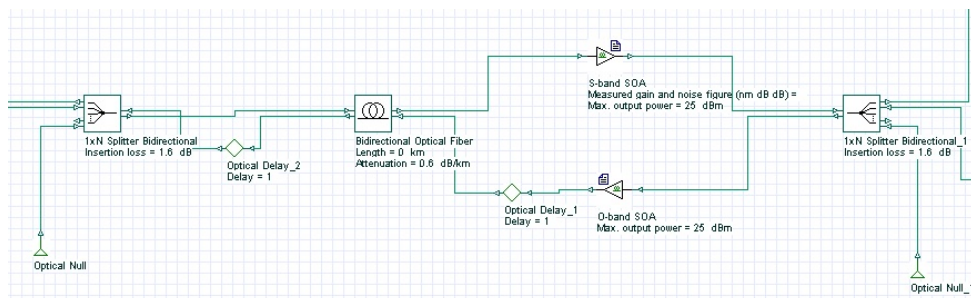


Figure 127: ODN in OptiSystem

## 13.2 Downstream Results

Figure 128 shows the BER values with the increasing fiber length. The graph is recorded from the BER analyzer in the ONU unit. It is obvious that until the fiber length of 40 km the BER value is 0. After that, the BER value has a sharp increase. The BER value after the 41 km of the optical fiber is  $8.5 \cdot 10^{-258}$ . Then follows the slow increase of the BER value. The value  $10^{-12}$  is reached after the fiber length of 55 km.

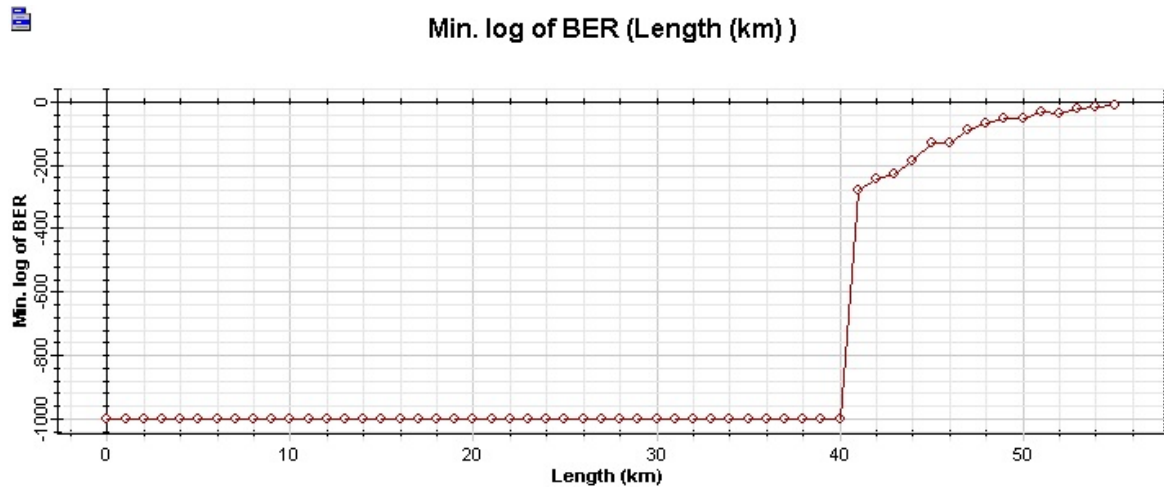


Figure 128: Downstream - BER depending on fiber length

### 13.2.1 Spectral Analysis

In the Figure 129 is shown the spectral analysis of the downstream optical signal at the output of the Mach-Zehnder modulator. The measured optical power is 3.91 dBm. Figure 130 shows the optical spectrum after overcoming the fiber length of the 55 km. The measured optical power is -33.7 dBm.

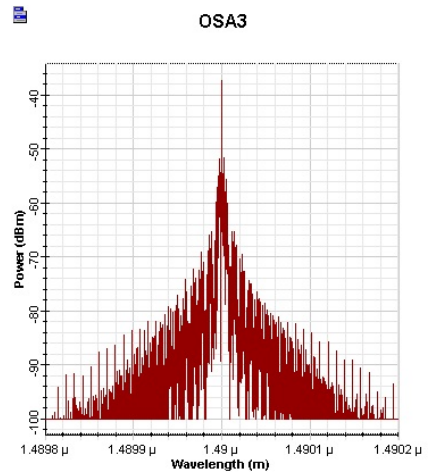
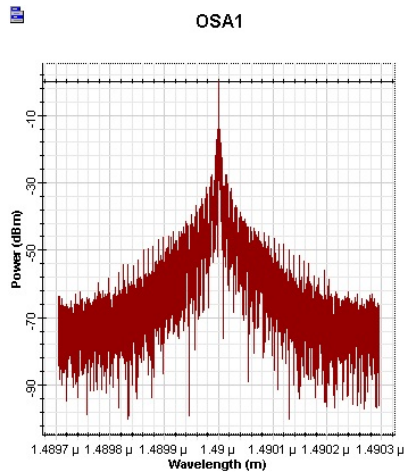


Figure 129: Opt.Spectrum (DS) - MZM output    Figure 130: Opt.Spectrum (DS) - SOA input

Then is the signal amplified by the S-band SOA. Figure 131 shows the amplified optical signal. From figure can be seen that the noise level is increased together with the optical signal. The measured optical power is -6.43 dBm. The signal gain is not so significant, however the high noise power level increases the total power. Figure 132 shows the optical spectrum of the signal on the input of the PIN photodetector. The total power is -11.04 dBm.

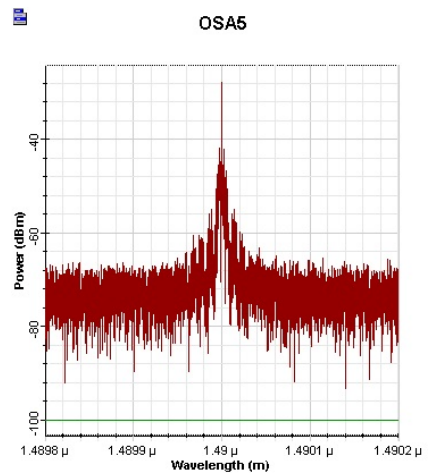
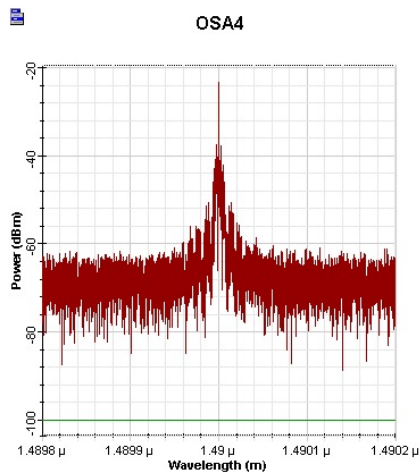


Figure 131: Opt.Spectrum (DS) - SOA output    Figure 132: Opt.Spectrum (DS) - PIN input

### 13.2.2 Eye Diagrams

The Figure 133 shows the eye diagram, when the fiber is 0 km long. The eye is almost ideal and the eye height is about 15 m a.u. (amplitude unit). The BER is 0. The Figure 134 shows the eye diagram after the 40 km of the fiber. The eye height is now only the 60  $\mu$  a.u. Is obvious that the distortion is rising. Nevertheless, the BER value is still 0.

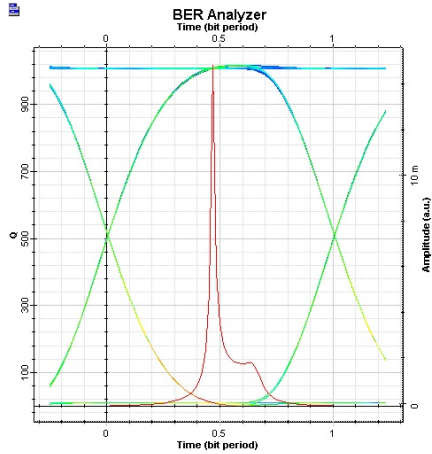


Figure 133: Eye diagram (DS) - 0 km

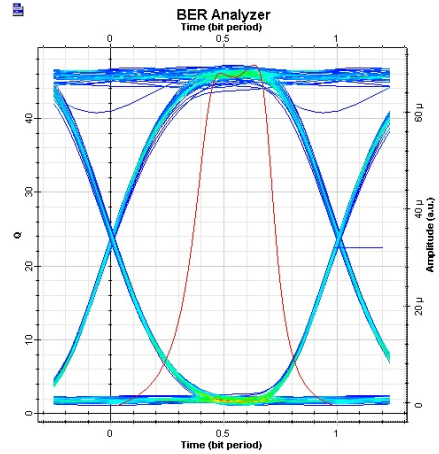


Figure 134: Eye diagram (DS) - 40 km

The Figure 135 shows the eye diagram after the 41 km of the fiber, when the BER value is increased to  $8.5 \cdot 10^{-258}$ . The Figure 136 shows the eye diagram after the fiber length of 55 km, where the BER value is  $3.10^{-12}$ . In the figure is visible distortion of the signal given by decreased signal-to-noise ratio at the sampling point.

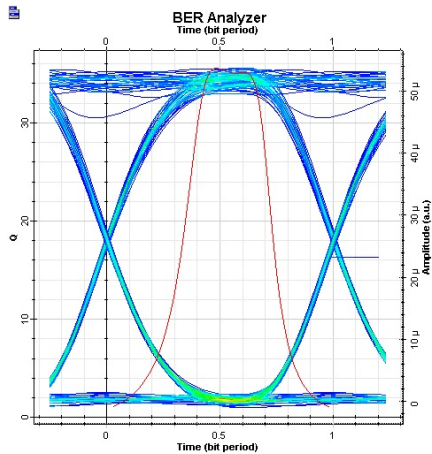


Figure 135: Eye diagram (DS) - 41 km

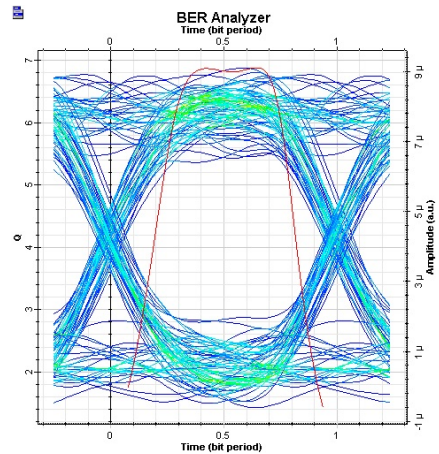


Figure 136: Eye diagram (DS) - 56 km

### 13.3 Upstream Results

Figure 128 shows the BER values depending on the fiber length. These results are obtained from the BER analyzer situated in the OLT. The BER value is 0 until the fiber length of 30 km. After reaching this distance can be again seen the sharp increase of the BER value. The BER value after overcoming the fiber length of the 31 km is  $1.5 \cdot 10^{-255}$ . Then again occurs the slow increase of the BER. The last fiber length, when the BER value is higher than  $10^{-12}$  is 44 km.



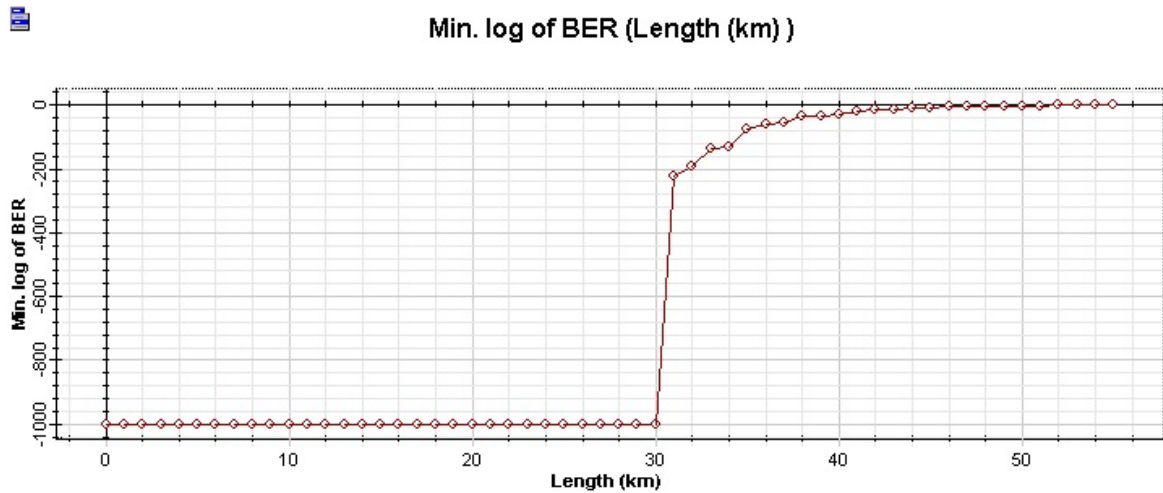


Figure 137: Upstream - BER depending on fiber length

### 13.3.1 Spectral Analysis

Figure 138 shows the optical spectrum on the output of Mach-Zehnder modulator. The optical power is 2.1 dBm. The Figure 139 shows the optical spectrum on the input of the optical amplifier. The input optical power is -2.48 dBm.

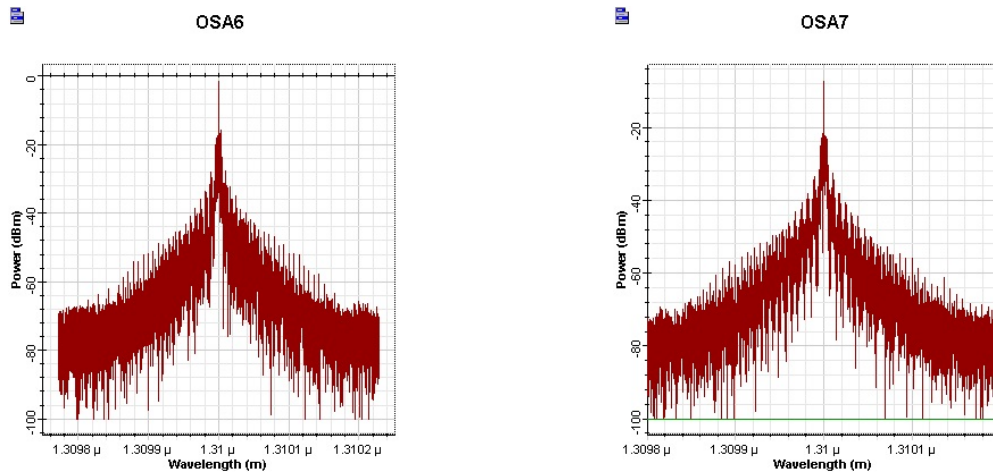


Figure 138: Opt.Spectrum (US) - MZM output Figure 139: Opt.Spectrum (US) - SOA input

The optical spectrum of the amplified signal is shown in Figure 140. The signal is not so affected by the noise as in case of the S-band SOA. The output optical power is 5.569 dBm. The Figure 141 shows the optical spectrum of upstream signal after overcoming the optical trace of 44 km. The noise is attenuated by passing the optical trace. The power at the input of PIN photodetector is -25.9 dBm.

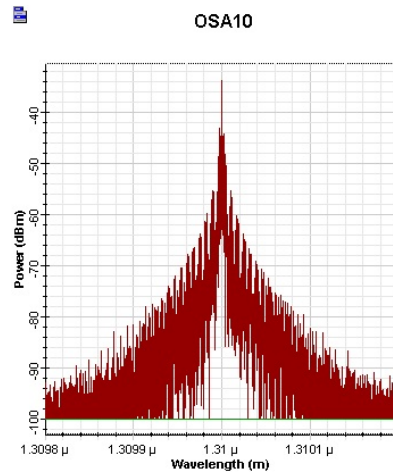
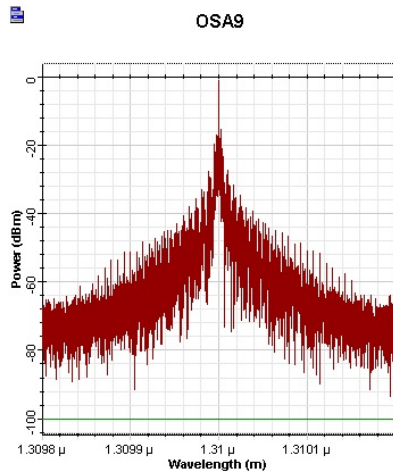


Figure 140: Opt.Spectrum (US) - SOA output    Figure 141: Opt.Spectrum (US) - PIN input

### 13.3.2 Eye Diagrams

The Figure 142 shows the eye diagram, where the length of the fiber is 0 km. The eye height is 2 m a.u. At the eye diagram are not visible any signs of the distortion. However, the eye height is considerably lower than the eye height in downstream after the 0 km of fiber. The figure 143 shows the eye diagram after overcoming the fiber length of 30 km. The BER value is still 0.

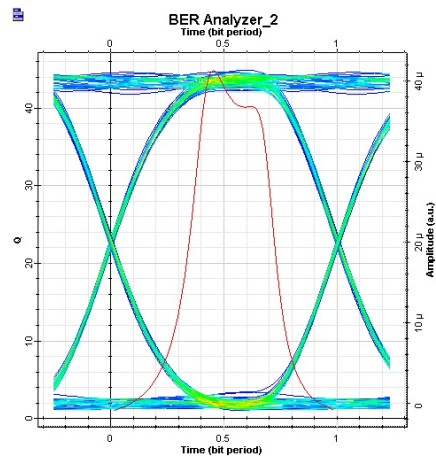
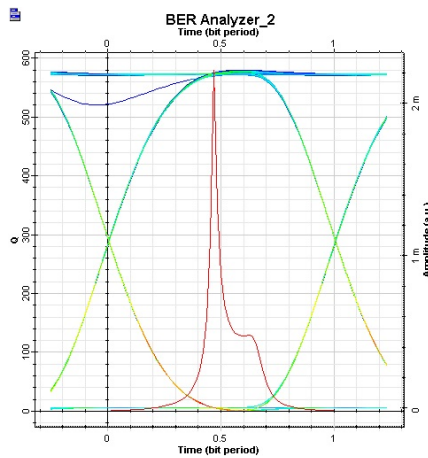


Figure 142: Eye diagram (US) - 0 km

Figure 143: Eye diagram (US) - 30 km

In the Figure 144 is eye diagram after reaching the 31 km of optical fiber, when the BER value is increased from the null to  $1.5 \cdot 10^{-255}$ . Also, from the figure can be seen the increasing distortion of the eye, but this distortion is not so significant. The Figure 145 shows the eye diagram after the fiber length of 43 km, when the BER value is  $1.1 \cdot 10^{-12}$ . The decreased signal-to-noise ratio at the sampling point causes the small eye height, what causes the higher BER.

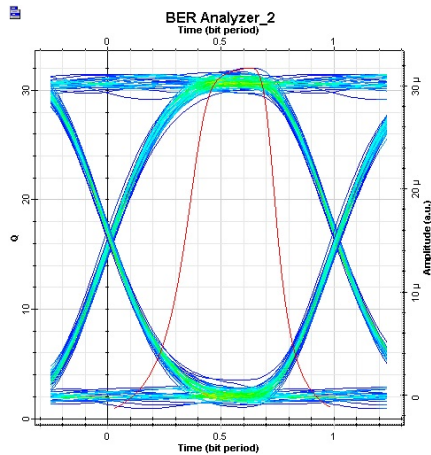


Figure 144: Eye diagram (US) - 31 km

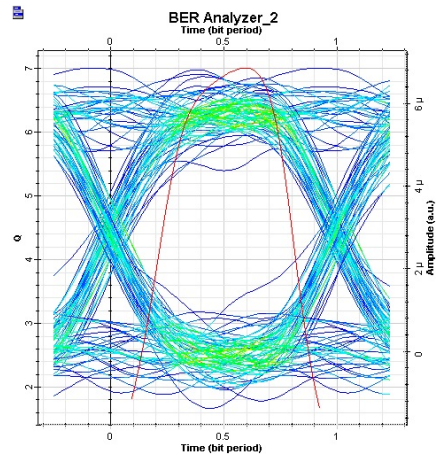


Figure 145: Eye diagram (US) - 43 km

The Figure 146 shows the eye diagram after overcoming the 52 km of the fiber. The BER value is 0 and is visible that the eye is not recognizable.

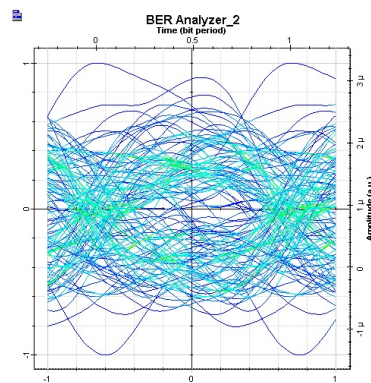


Figure 146: Eye diagram (US) - 52 km

### 13.4 Summary

From the results of simulations can be seen that the optical transmission among the OLT and the ONU is limited by the ONU and O-band amplifier. The last fiber length, when the ONU is able to communicate is 43 km while the reach of the OLT is 55 km. So the results are similar with real results expect the reach, when in the real network is ONU able to communicate with the fiber length of 25 km. However, the fact that the system is limited by the ONU reach is the same. Nevertheless, the EPON network coverage in simulation is about 18 km higher than in a real experimental workplace. This is because the simulations does not fully corresponds with the real conditions. For more precisely set of simulation, we would need to know every parameters of the used components such a sensitivity of used photodetectors.

## 14 Conclusion

The aim of the diploma thesis was to build up hybrid xPON/xDSL access network and find out, if this solution is suitable to future deployment by providers. Also, the semiconductor optical amplifiers deployment to the EPON network is included in this thesis to determine whether the maximum reach of network will be increased or not.

In the theoretical part of this thesis are described access networks considering to used physical medium for transmission. Following chapters are aimed to discuss the xDSL technologies, physical parameters of twisted pairs, impairments, and transmission techniques. Single chapter is dedicated to xDSL standards, where are discussed the most commonly used standards of xDSL. Next chapter is devoted to Ethernet passive optical network and its base properties. The fundamental protocols and operations are explained. Little of hybrid passive optical networks is also part of this thesis. The last chapter from the theoretical part discusses the semiconductor optical amplifiers, the principles of amplification, their nonlinearities, and applications.

The practical part is focused to performance tests of hybrid access network based on standards RFC2544 and ITU-T Y.1564 EtherSAM. The measurements of optical network together with deployment of semiconductor optical amplifiers were executed to find out the maximum coverage of EPON network. Also, the basic optical measurements such as power level, attenuation, dispersion, and spectral analysis of the optical network were performed on builded topologies.

The spectral analysis and power level measurements of the EPON network with deployed semiconductor amplifiers showed, that the reach of EPON network was not extended. Although the semiconductor optical amplifiers exhibits enough high gain, the ONU unit was not able to communicate with the OLT, when the fiber length was higher than 25 km. With this fiber length, the ONU was able to register also without using the amplifiers. The reasons may be more. The semiconductor amplifiers do not amplify only the optical signal, but also the noise. The amplified noise and small value of an OSNR could be the most limited factor. Also, the Fabry-Perot laser used in the ONUs, which spreads the power to the wider spectrum of wavelengths could be an issue. More suitable laser source to amplification could be with narrow spectral width.

The results of the performance tests RFC2544 and ITU-T Y.1564 showed that hybrid network seem to be good choice under certain conditions. In case of hybrid EPON/ADSL2+ network can be seen that the network parameters are not so affected by the length of the metallic wire as in case of hybrid EPON/VDSL2. At the length of the metallic wire 2 km, the EPON/ADSL2+ network is able to provide data-rates about 10 Mbps in downstream. It can be sufficient for small households. The EPON/VDSL2 hybrid network is highly affected by length of the metallic wire. With length of the metallic wire 100 m, data-rate is only a small fraction of the original data-rates. However, in case of short metallic wire are data-rates only slightly affected by the length of the optical fiber. Even, the deployment of the semiconductor optical amplifiers does not have a high affect to network parameters.

Based on results from simulations, the deployment of the semiconductor optical amplifiers seems to be good step to increase reach of the EPON network. However, the more detailed parameters of active components are necessary to simulate more precisely results. For example, the use of Fabry-Perot laser (using by ONU unit) should provide better view of real conditions. However, to set Fabry-Perot laser in OptiSystem are required real properties of this laser source.

Regarding to future research, the hybrid networks should be tested under different conditions. There would be tested different metallic wire lengths to find the optimal distance between the DSLAM and subscriber's modem. For these purposes should be used cable types suitable for high frequencies to minimize influence of the attenuation at high frequencies. Also, the hybrid networks should be tested under high load, what can cause very different results in consideration of QoS parameters. Another possibility is to build up hybrid WDM-PON/xDSL network and apply a similar tests.

## References

- [1] ŠIMÁK, Boris, Jiří VODRÁŽKA a Jaroslav SVOBODA. Digitální účastnické přípojky xDSL. 1. vyd. Praha: Sdělovací technika, 2005, 141 s. Telekomunikace (Sdělovací technika). ISBN 80-86645-07-x.
- [2] WAY, Winston I. Broadband hybrid fiber/coax access system technologies. San Diego: Academic Press, 1999, xv, 458 p. Telecommunications (Boston, Mass.). ISBN 0127387552-.
- [3] LEONID G. KAZOVSKY .. [ET AL.]. Broadband optical access networks. Hoboken, N.J.: Wiley-Interscience, 2011. ISBN 978-047-0910-924.
- [4] ABDELRAHMAN, Ramia Babiker Mohammed, Amin Babiker A. MUSTAFA and Ashraf A. OSMAN. A Comparison between IEEE 802.11a, b, g, n and ac Standards. IOSR Journal of Computer Engineering (IOSR-JCE) [online]. 2015, Oct.2015, 2015(17): 26-29 Available from: [files.figshare.com/2299003/D017532629.pdf](http://files.figshare.com/2299003/D017532629.pdf)
- [5] GORSHE, Steve. Broadband access: wireline and wireless, alternatives for internet services. Chichester, England: Wiley, 2014. ISBN 978-1-118-87880-4.
- [6] HALONEN, Timo, Javier ROMERO a Juan MELERO. GSM, GPRS, and EDGE performance: evolution towards 3G/UMTS. 2nd ed. Hoboken, NJ, USA: J. Wiley, 2003, xxxvii, 615 p. ISBN 0470866942.
- [7] ROUSE, Margaret. Free-space optics (FSO) [online]. In: . [cit. 2016-04-28]. Available from: <http://whatis.techtarget.com/definition/free-space-optics-FSO>
- [8] Free-space Optical Communications [online]. In: . [cit. 2016-04-28]. Available from: [https://www.rp-photonics.com/free\\_space\\_optical\\_communications.html](https://www.rp-photonics.com/free_space_optical_communications.html)
- [9] DORDOVÁ, Lucie. METODA STANOVENÍ CHARAKTERISTIK ATMOSFÉRICKÉHO PRENOSOVÉHO PROSTŘEDÍ V OPTICKÉ OBLASTI SPEKTRA [online]. Brno, 2009 [cit. 2016-04-28]. Dizertační práce. Vedoucí práce Prof. Ing. OTAKAR WILFERT, CSc.
- [10] PLANK, Thomas, Erich LEITGEB, Pirmin PEZZEI a Zabih GHASSEMLOOY. Wavelength-selection for high data rate Free Space Optics (FSO) in next generation wireless communications. 2012 17th European Conference on Networks and Optical Communications [online]. IEEE, 2012, , 1-5 [cit. 2016-04-28]. DOI: 10.1109/NOC.2012.6249909. ISBN 978-1-4673-0951-6. Available from: <http://ieeexplore.ieee.org/lpdocs/epic03/wrapper.htm?arnumber=6249909>
- [11] STARR, Thomas, John M. CIOFFI a Peter SILVERMAN. Understanding digital subscriber line technology. Upper Saddle River, NJ: Prentice Hall PTR, c1999. ISBN 01-378-0545-4.

- [12] BRAIN, Marshall. How the Radio Spectrum Works [online]. [cit. 2016-04-28]. Available from: <http://electronics.howstuffworks.com/radio-spectrum1.htm>
- [13] JACOBSEN, Krista. TEXAS INSTRUMENTS. XDSL Technology and Applications:: Removing the Telephone Line Bottleneck. 1999.
- [14] GOLDEN, Philip., Herve. DEDIEU a Krista. JACOBSEN. Implementation and applications of DSL technology. Boca Raton: Auerbach Publications, c2008. ISBN 08-493-3423-3.
- [15] DSL White Paper [online]. [cit. 2016-04-28]. Available from: [http://www.alliedtelesis.com/media/pdf/dsl\\_wp.pdf](http://www.alliedtelesis.com/media/pdf/dsl_wp.pdf)
- [16] ABBAS, Huda Saleh a Mark A. GREGORY. The next generation of passive optical networks: A review. Journal of Network and Computer Applications [online]. 2016, 67, 53-74 [cit. 2016-04-28]. DOI: 10.1016/j.jnca.2016.02.015. ISSN 10848045. Available from: <http://linkinghub.elsevier.com/retrieve/pii/S1084804516000989>
- [17] DIXIT, Sudhir. IP over WDM: Building the next-generation optical Internet. Hoboken, N.J.: Wiley-Interscience, 2003, xx, 557 p. ISBN 04-712-1248-2.
- [18] SAMI LALLUKKA. Passive optical networks: transport concepts. Espoo: VTT, 2006. ISBN 95-138-6706-4.
- [19] IEEE 802.3 and Ethernet [online]. [cit. 2016-04-28]. Available from: <http://www.cse.iitk.ac.in/users/dheeraj/cs425/lec06.html>
- [20] LAM, Cedric F. Passive optical networks: principles and practice. Boston: Elsevier/Academic Press, c2007, xlv, 324 p. ISBN 01-237-3853-9.
- [21] Z. Luying, C. Xiaofei, Y. Yong-Kee, and N. Lek heng, "Hybrid WDM-TDM PON architectures and DWBA algorithms," in Communications and Networking in China (CHINACOM), 2010 5th International ICST Conference on, 2010, pp. 1-6.
- [22] P. Ossieur, et al., "A 135-km 8192-Split Carrier Distributed DWDM-TDMA PON With 2 x 32 x 10 Gb/s Capacity," J.Lightw. Technol., vol. 29, pp. 463-474, 2011.
- [23] RÓKA, Rastislav. The HPON Network Configurator and its Parameters for Designing of Passive Optical Networks [online]. [cit. 2016-04-28].
- [24] G. Wellbrock, "Preparing for the future," in 36th European Conference and Exhibition on Optical Communication (ECOC), 2010, pp. 1-10.
- [25] N. Cvijetic, M.-F. Huang, E. Ip, Y.-K. Huang, D. Qian, and T.Wang, "1.2 Tb/s Symmetric WDM-OFDMA-PON over 90km Straight SSMF and 1:32 Passive Split with Digitally-Selective ONUs and Coherent Receiver OLT," in Optical Fiber Communication Conference

and Exposition (OFC/NFOEC), and the National Fiber Optic Engineers Conference 2011, pp. 1-3.

- [26] N. Kataoka, N. Wada, G. Cincotti, and K. Kitayama, "2.56 Tbps (40-Gbps x 8-wavelength x 4-OC x 2-POL) asynchronous WDM-OCDMA-PON using a multi-port encoder/decoder," in 37th European Conference and Exhibition on Optical Communication (ECOC), 2011, pp. 1-3.
- [27] ALVIZU, R., A. ARCIA a M. HERNANDÉZ. Hybrid WDM-XDM PON architectures for future proof access networks [online]. , pp. 139 - 153 [cit. 2016-04-28].
- [28] MCGARRY, Michael P., Elliott I. GURROLA a YUANQIU LUO. On the reduction of ONU upstream buffering for PON/xDSL hybrid access networks. 2013 IEEE Global Communications Conference (GLOBECOM) [online]. IEEE, 2013, , 2667-2673 [cit. 2016-04-28]. DOI: 10.1109/GLOCOM.2013.6831477. ISBN 978-1-4799-1353-4. Available from: <http://ieeexplore.ieee.org/lpdocs/epic03/wrapper.htm?arnumber=6831477>
- [29] MARQUES, Alessandro. Nonlinear Applications of Semiconductor Optical Amplifiers for All-Optical Networks. 2007. Dissertation thesis. Elektrotechnik und Informatik der Technischen Universität Berlin.
- [30] THAMBIRATNAM, KAVINTHERAN. A MULTI-WAVELENGTH SOURCE BASED ON SAGNAC LOOP AND SEMICONDUCTOR OPTICAL AMPLIFIER. Kuala Lumpur, 2008. Dissertation thesis. UNIVERSITY OF MALAYA.
- [31] DUTTA, N. K. a Qiang WANG. Semiconductor optical amplifiers. Hackensack, NJ: World Scientific Pub., c2006. ISBN 981-256-397-0.
- [32] SALEH, Bahaa E. A. a Malvin Carl. TEICH. Fundamentals of photonics. New York: Wiley, c1991. ISBN 04-718-3965-5.
- [33] CARNEY, Kevin, Robert LENNOX, Ramon MALDONADO-BASILIO, Severine PHILIPPE, Frederic SURRE, Louise BRADLEY a Pascal LANDAIS. Method to improve the noise figure and saturation power in multi-contact semiconductor optical amplifiers: simulation and experiment. Optics Express [online]. 2013, 21(6), 7180-. DOI: 10.1364/OE.21.007180. ISSN 1094-4087. Available from: <https://www.osapublishing.org/oe/abstract.cfm?uri=oe-21-6-7180>
- [34] KEISER, Gerd. Optical fiber communications. 3rd ed. Boston, MA: McGraw-Hill, 2000. ISBN 00-723-6076-3.
- [35] MICHAEL J. CONNELLY. Semiconductor Optical Amplifiers. Boston, MA: Kluwer Academic Publishers, 2004. ISBN 03-064-8156-1.



- [36] MICHIE, C., A. E. KELLY a I. ANDONOVIC. Reflective Semiconductor Optical Amplifiers for passive optical networks. 2009 11th International Conference on Transparent Optical Networks [online]. IEEE, 2009, , 1-4 . DOI: 10.1109/ICTON.2009.5185149. ISBN 978-1-4244-4825-8. Available from: <http://ieeexplore.ieee.org/lpdocs/epic03/wrapper.htm?arnumber=5185149>
- [37] ODROBIŇÁK, Radoslav. Four-wave mixing application in semiconductor optical amplifier [online]. Available from: <http://advances.utc.sk/index.php/AEEE/article/view/365/409>
- [38] MEHRA, Rekha a Sheersh ACHARYA. XPM based optical switch using SOA. 2014 International Conference on Signal Propagation and Computer Technology (ICSPCT 2014) [online]. IEEE, 2014, , 351-354. DOI: 10.1109/ICSPCT.2014.6884918. ISBN 978-1-4799-3140-8. Available from: <http://ieeexplore.ieee.org/lpdocs/epic03/wrapper.htm?arnumber=6884918>
- [39] Fiber Characterization and Testing Long Haul, High Speed Fiber Optic Networks:: Chromatic Dispersion, Polarization Mode Dispersion and Spectral Attenuation [online]. Available from: [http://www.thefoa.org/tech/ref/testing/test/CD\\_PMD.html](http://www.thefoa.org/tech/ref/testing/test/CD_PMD.html)
- [40] HANSON, Tom (ed.). Optical fibres, cables and systems: OPTICAL FIBRES CHARACTERISTICS. Geneva: ITU-T, 2010.
- [41] GIGUERE, Bruno. EXFO. RFC2544: HOW IT HELPS QUALIFY A CARRIER ETHERNET NETWORK. Exfo [online]. Canada, 2008 [cit. 2016-04-28]. Available from: [http://www.3-edge.de/export/sites/default/.content/3Edge\\_Datasheets-pdf/RFC2544-Howithelps-qualify-a-carrierEthernet-Network.pdf](http://www.3-edge.de/export/sites/default/.content/3Edge_Datasheets-pdf/RFC2544-Howithelps-qualify-a-carrierEthernet-Network.pdf)
- [42] THIerno, Diallo a Marquis DORAIS. EtherSAM: THE NEW STANDARD IN ETHERNET SERVICE TESTING. Rateart [online]. 2013 [cit. 2016-04-28]. Available from: [http://www.rateart.pl/public\\_files/spec/appnote230.3-ang.pdf](http://www.rateart.pl/public_files/spec/appnote230.3-ang.pdf)
- [43] Enterprise QoS Solution Reference Network Design Guide: Quality of Service Design Overview [online]. [cit. 2016-04-28]. Available from: [http://www.cisco.com/c/en/us/td/docs/solutions/Enterprise/WAN\\_and\\_MAN/QoS\\_SRND/QoS-SRND-Book.pdf](http://www.cisco.com/c/en/us/td/docs/solutions/Enterprise/WAN_and_MAN/QoS_SRND/QoS-SRND-Book.pdf)

## List of Appendices

Appendix A - Building drawings with marked traces - The second floor

Appendix B - Building drawings with marked traces - The third floor

Appendix C - Results of ITU-T Y.1564 EtherSAM test - EPON/ADSL2+

Appendix D - Results of ITU-T Y.1564 EtherSAM test - EPON/VDSL2

### List of Appendices on DVD:

- EtherSAM results - EPON-ADSL2+
- EtherSAM results - EPON-VDSL2
- Chromatic Dispersion Measurements
- Method C results between laboratories
- OTDR - between laboratories
- OTDR - optical traces
- Photos from measurements
- PMD measurements
- RFC results - EPON-ADSL2+
- RFC results - EPON-VDSL2
- Simulation - OptiSystem
- Spectral Analysis

## A Building drawings with marked traces - The second floor

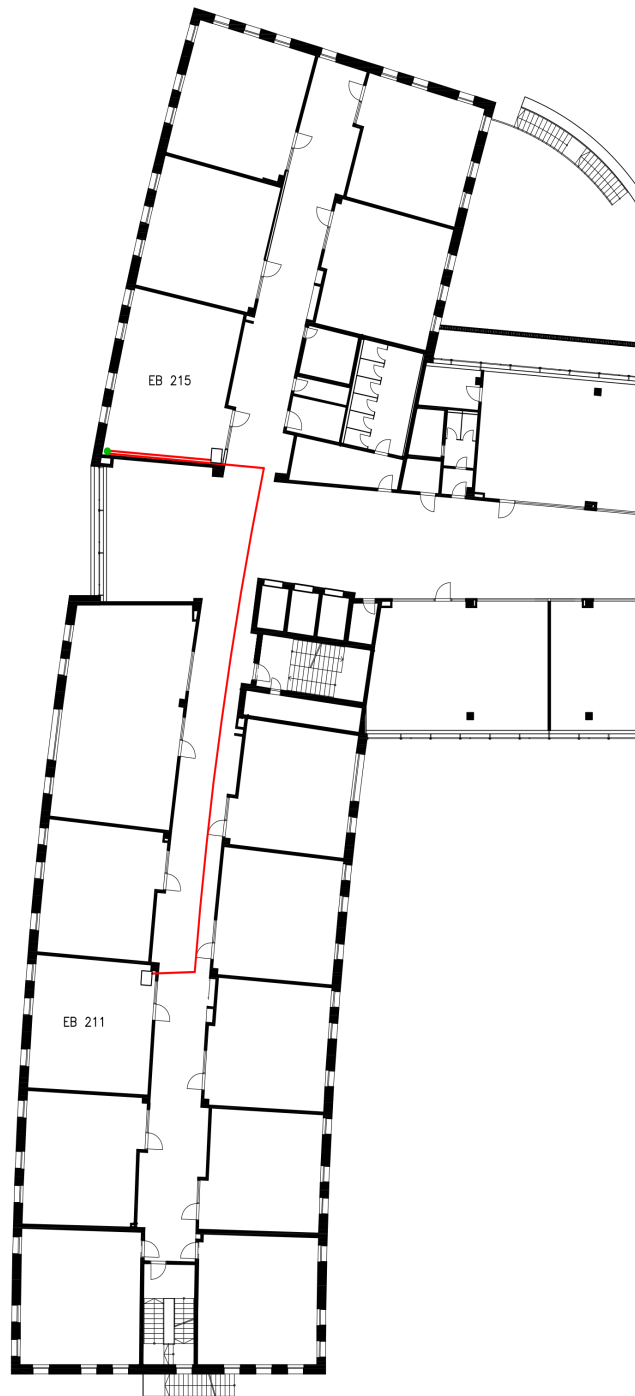


Figure 147: Second floor drawing

## B Building drawings with marked traces - The third floor



Figure 148: Third floor drawing

## C Results of ITU-T Y.1564 EtherSAM test - EPON/ADSL2+

From figures below can be seen that the metallic wire length does not have great impact on the network parameters, because of small CIR band for all services. Greater impact has a fiber length as was mentioned in section 12.6.

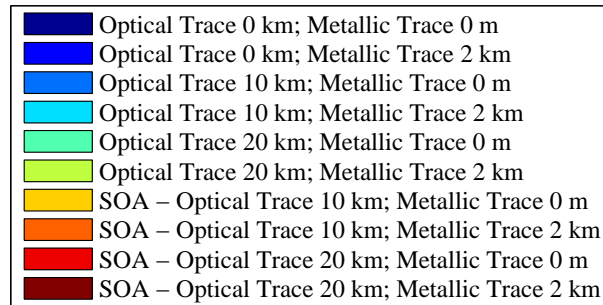


Figure 149: Legend for EPON/ADSL2+

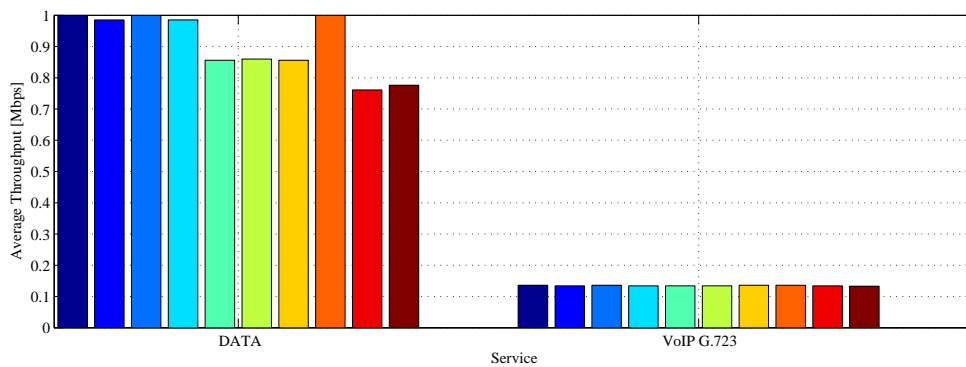


Figure 150: EtherSAM - EPON/ADSL2+ - Average Throughput - Full results

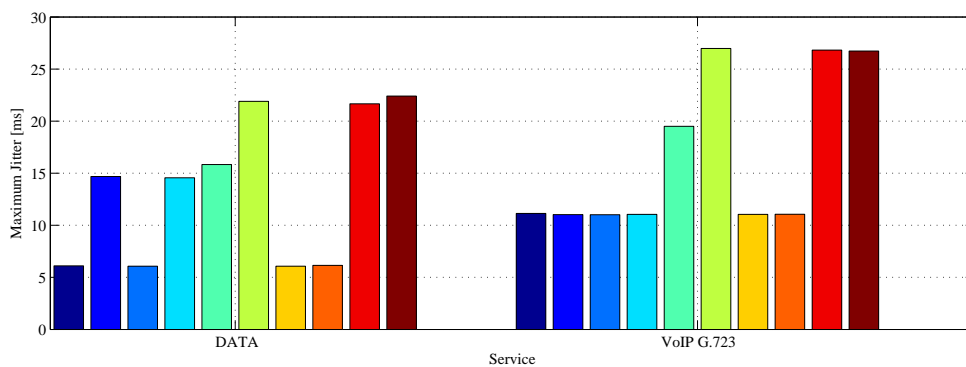


Figure 151: EtherSAM - EPON/ADSL2+ - Maximum Jitter - Full results

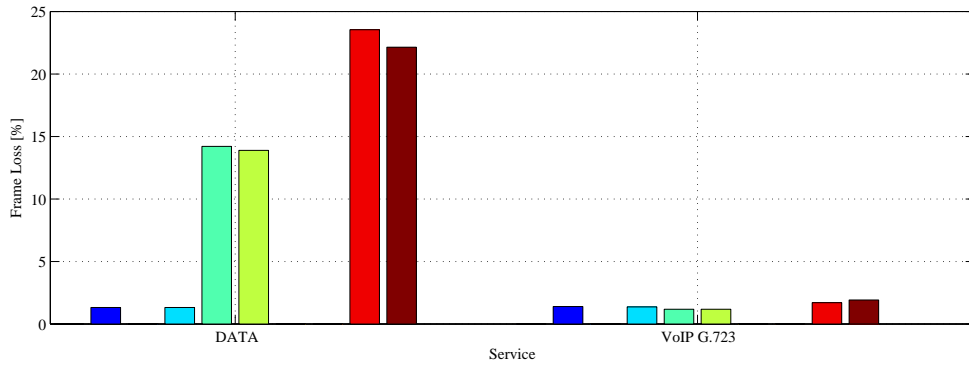


Figure 152: EtherSAM - EPON/ADSL2+ - Frame Loss - Full results

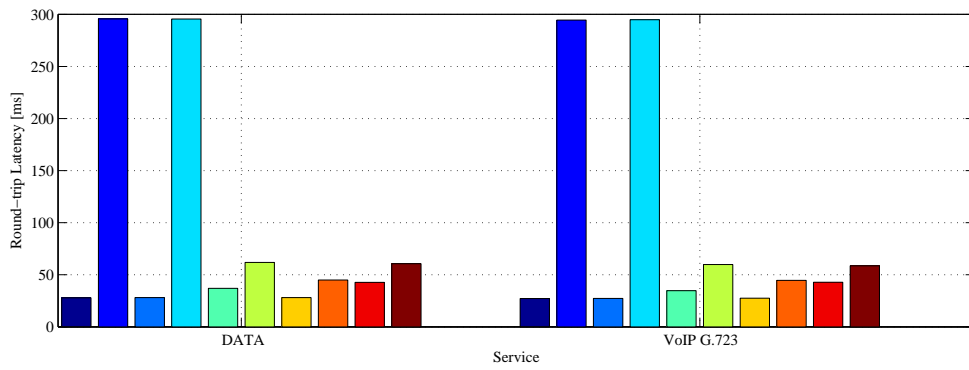


Figure 153: EtherSAM - EPON/ADSL2+ - Round-trip Latency - Full results

## D Results of ITU-T Y.1564 EtherSAM test - EPON/VDSL2

Figures below show the full results of ITU-T Y.1564 EtherSAM applied on EPON/VDSL2 network. Figures show that the length of metallic wire has a great impact on services and under these conditions, not even one service fulfills the demands on quality of services. From figures can be also seen that the differences between the tested profiles are minimum.



Figure 154: Legend for EPON/VDSL2

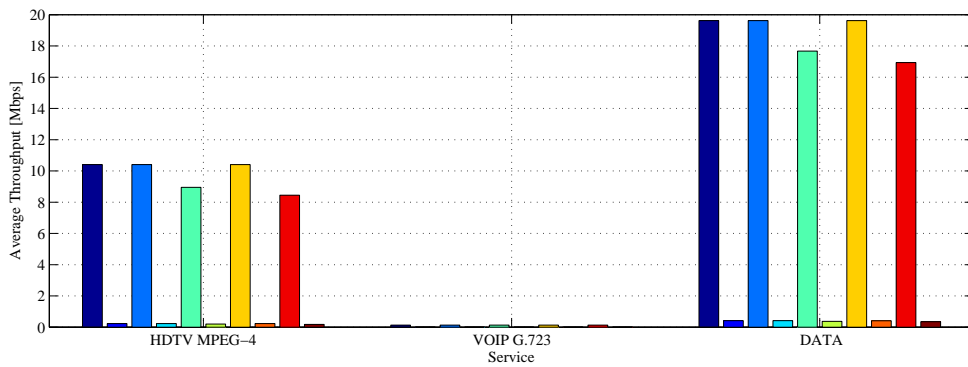


Figure 155: EtherSAM - EPON/VDSL2 - Average Throughput - Full results - profile A

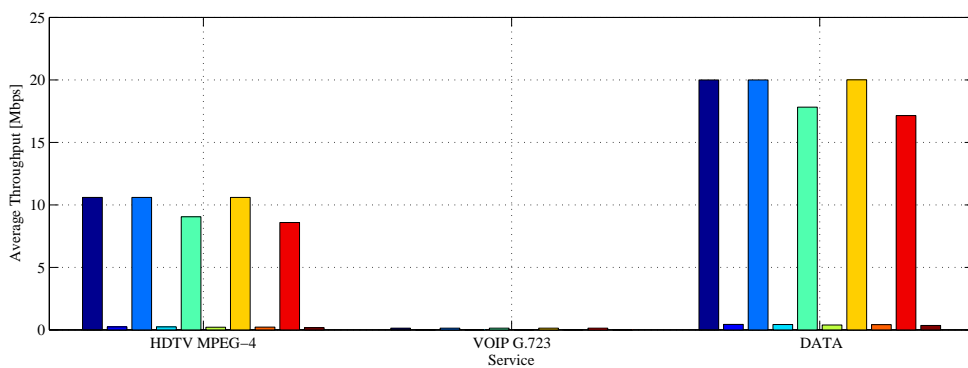


Figure 156: EtherSAM - EPON/VDSL2 - Average Throughput - Full results - profile B

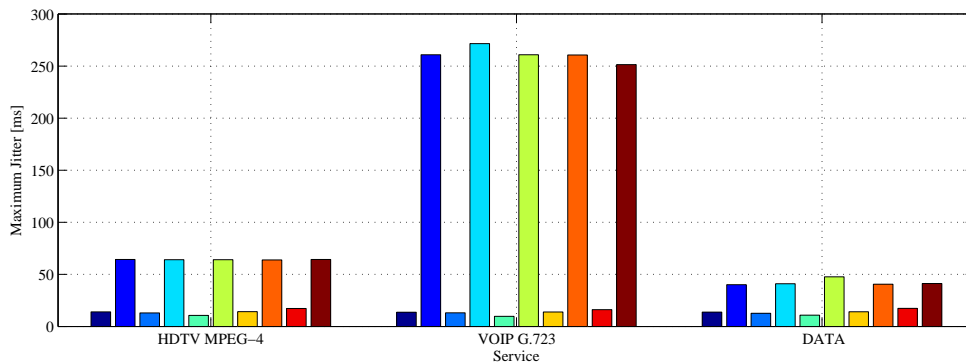


Figure 157: EtherSAM - EPON/VDSL2 - Maximum Jitter - Full results - profile A

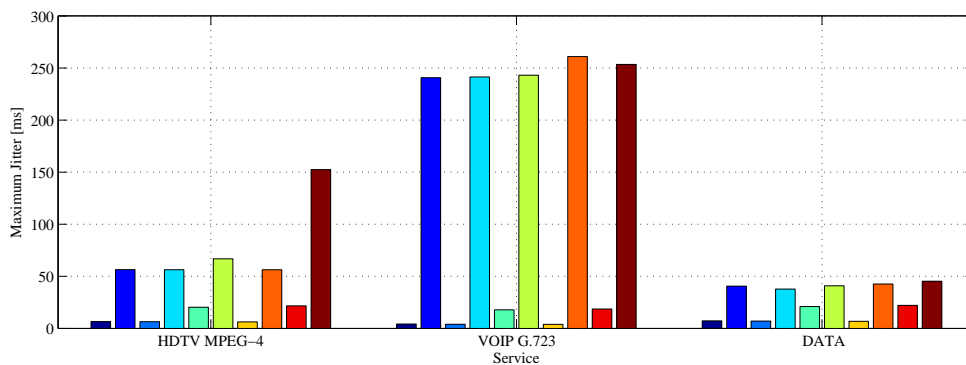


Figure 158: EtherSAM - EPON/VDSL2 - Maximum Jitter - Full results - profile B

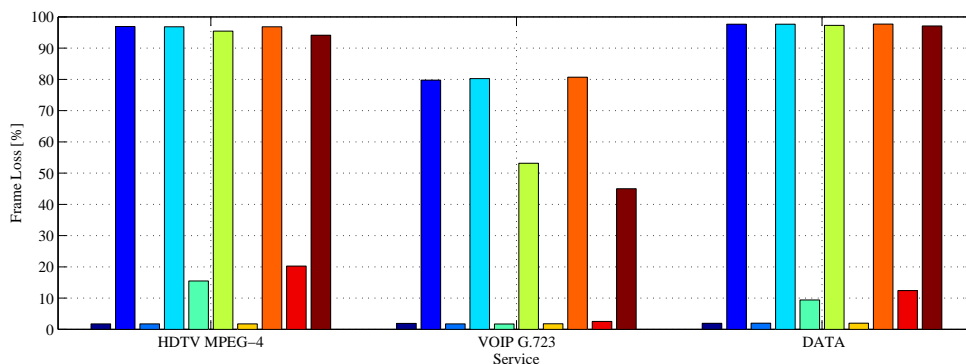


Figure 159: EtherSAM - EPON/VDSL2 - Frame Loss - Full results - profile A



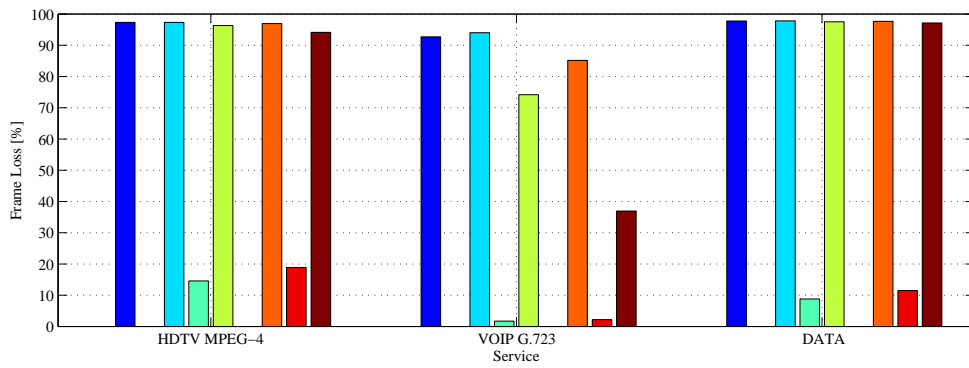


Figure 160: EtherSAM - EPON/VDSL2 - Frame Loss - Full results - profile B

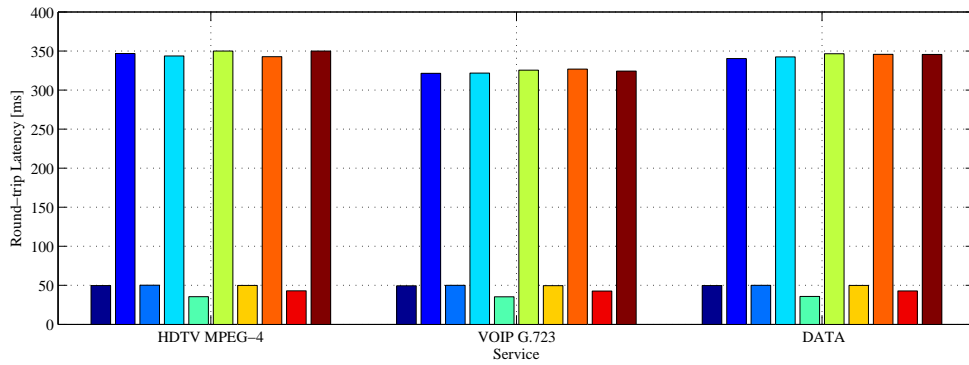


Figure 161: EtherSAM - EPON/VDSL2 - Round-trip Latency - Full results - profile A

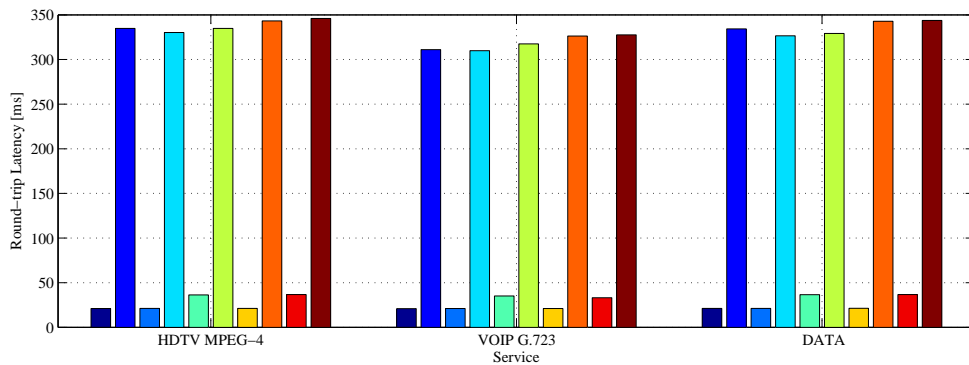


Figure 162: EtherSAM - EPON/VDSL2 - Round-trip Latency - Full results - profile B